การออปติไมซ์และควบคุมเครื่องปฏิกรณ์แบบเพอร์เวเพอเรทีฟเมมเบรน

นางสาวอรลัดดา มูลศาสตรสาทร

OPTIMIZATION AND CONTROL OF PERVAPORATIVE MEMBRANE REACTOR

Miss Orladda Moolasartsatorn

A Thesis Submitted in Partial Fulfillment of the Requirements
for the Degree of Master of Engineering in Chemical Engineering
Department of Chemical Engineering
Faculty of Engineering
Chulalongkorn University
Academic Year 2002
ISBN 974-17-0902-1

Thesis Title   Optimization and Control of Pervaporative Membrane Reactor

By   Miss Orladda Moolasartsatorn

Field of Study   Chemical Engineering

Thesis Advisor   Associate Professor Paisan Kittisupakorn, Ph. D.

Accepted by the Faculty of Engineering, Chulalongkorn University in Partial Fulfillment of the Requirements for the Master 's Degree

…………………………………………… Dean of Faculty of Engineering

(Professor Somsak Panyakeow, Dr. Eng.)

THESIS COMMITTEE

…………………………………………… Chairman

(Professor Piyasan Praserthdam, Dr. Ing.)

…………………………………………… Thesis Advisor

(Associate Professor Paisan Kittisupakorn, Ph. D.)

…………………………………………… Member

(Montree Wongsri, D. Sc.)

…………………………………………… Member

(Associate Professor Tawatchai Charinpanitkul, Dr. Ing.)

อรลัดดา มูลศาสตรสาทร : การออปติไมซ์และควบคุมเครื่องปฏิกรณ์แบบเพอร์เวเพอเรทีฟเมมเบรน (OPTIMIZATION AND CONTROL OF PERVAPORATIVE MEMBRANE REACTOR) อ. ที่ปรึกษา : รศ.ดร. ไพศาล กิตติศุภกร, 132 หน้า. ISBN 974-17-0902-1

ปัจจุบันเครื่องปฏิกรณ์แบบเมมเบรน ซึ่งเป็นการรวมกระบวนการแยกสารแบบเมมเบรนเข้ากับเครื่องปฏิกรณ์แบบดั้งเดิม เพื่อพัฒนาให้เครื่องปฏิกรณ์มีประสิทธิภาพมากยิ่งขึ้นได้รับความสนใจเป็นอย่างมาก ระบบที่นำมาศึกษาในงานวิจัยนี้คือปฏิกิริยาเอสเทอร์ริฟิเคชั่นของกรดอะซิติกกับบิวทานอล ภายในเครื่องปฏิกรณ์แบบเพอร์เวเพอเรทีฟเมมเบรน ซึ่งมีการดึงน้ำออกจากสารละลายผสมมีผลทำให้สมดุลของระบบถูกรบกวนและทำให้เกิดปฏิกิริยาไปข้างหน้าได้มากขึ้น จึงเกิดผลิตภัณฑ์ที่ต้องการได้มากขึ้น

จากแบบจำลองทางคณิตศาสตร์จะเห็นว่าอุณหภูมิเป็นปัจจัยหลักที่ส่งผลต่อประสิทธิภาพของระบบ โดยส่งผลต่อทั้งอัตราการเกิดปฏิกิริยา และอัตราการแพร่ของสารผ่านเมมเบรน ดังนั้นเพื่อให้การดำเนินการของเครื่องปฏิกรณ์แบบเพอร์เวเพอเรทีฟเมมเบรนเป็นไปอย่างมีประสิทธิภาพจึงทำการออปติไมซ์เพื่อหาอุณหภูมิที่เหมาะสม โดยมีออปเจกทีฟฟังก์ชันคือให้เกิดผลิตภัณฑ์ที่ต้องการมากที่สุด และอุณหภูมิที่คำนวณได้จะถูกนำมาใช้เป็นเซ็ทพอยท์ในการควบคุมระบบ ตัวควบคุมแบบเจเนอริกโมเดลร่วมกับตัวประมาณค่าสเตทและพารามิเตอร์แบบคาลมานฟิลเตอร์แบบยืดขยายถูกออกแบบเพื่อควบคุมอุณหภูมิของเครื่องปฏิกรณ์แบบเพอร์เวเพอเรทีฟให้อยู่ที่ค่าเซ็ทพอยท์ที่ต้องการ จากผลที่ได้จะเห็นว่าตัวควบคุมแบบเจเนอริกโมเดลร่วมกับคาลมานฟิลเตอร์แบบยืดขยายให้ผลการควบคุมที่ดีและมีความทนทานในสภาวะที่มีความผิดพลาดของแบบจำลองกระบวนการ

ภาควิชาวิศวกรรมเคมี   ลายมือชื่อนิสิต…………………………………..

สาขาวิชาวิศวกรรมเคมี   ลายมือชื่ออาจารย์ที่ปรึกษา………………………..

ปีการศึกษา 2545

ORLADDA MOOLASARTSATORN : OPTIMIZATION AND CONTROL OF PERVAPORATIVE MEMBRANE REACTOR. THESIS ADVISOR : ASSOC. PROF. PAISAN KITTISUPAKORN, Ph.D., 132 pp. ISBN 974-17-0902-1

The hybrid process integrating chemical reaction with membrane separation has been increasingly received much interest. In this work, a pervaporation-based reactor has been studied for esterification of acetic acid and butanol. The combination of pervaporation with a conventional esterification process can shift the chemical equilibrium of esterification by removing water from the reaction mixture and, therefore, increases the yield of desired product. The effect of operating parameters on thermodynamic equilibrium of esterification is taken into account in the reactor model. Since a reactor temperature is one of key factors, which influences both the reaction and pervaporation process through the reaction rates and membrane permeability, in order to operate the pervaporative membrane reactor efficiently, optimization framework is formulated to determine the optimal temperature policy. The maximization of the desired product is considered as an objective function in the optimization problem formulation subject to other process constraints, which is solved by the sequential optimization approach. A generic model control (GMC) coupled with an extended Kalman filter is implemented to track both optimal temperature set point and optimal temperature profile obtained in the off-line optimization. Application of these control strategies to control the pervaporative membrane reactor shows that the proposed control strategy provides good control performances in a nominal case. The GMC coupled with Kalman filter has been found to be effective and robust with respect to changes in process parameters.

Department Chemical Engineering   Student's signature…………………………

Field of Chemical Engineering   Advisor's signature…………………………

Academic Year 2002

ACKNOWLEDGEMENTS

CONTENT

CONTENT (Continued)

LIST OF TABLES

LIST OF FIGURES

LIST OF FIGURES (Continued)

LIST OF FIGURES (Continued)

LIST OF FIGURES (Continued)

NOMENCLATURES

A	=	heat transfer area, m^2
b	=	*pseudo* reaction rate constant
C_{cat}	=	catalyst concentration, g/l
C_i	=	concentration of component i, mol/l
$C_{i,0}$	=	initial concentration of component i, mol/l
C_{pi}	=	molar heat capacity of component i, J/mol K
C_{pj}	=	mass heat capacity of the jacket, J/g K
C_{pr}	=	molar heat capacity of the reactor contents, J/mol K
$e(t)$	=	error
E	=	activation energy of reaction
E_a	=	activation energy of permeation
$\mathbf{g(x)}$	=	vector of inequalities of dimension m_2
$\mathbf{h(x)}$	=	vector of equations of dimension m_1
H_k	=	Hessian matrix of the Lagrangian function
J_i	=	permeation flux of component i, mol/m^2 hr
k_0	=	pre-exponential factor of reaction
k_1	=	rate constant for forward reaction
K_1	=	tuning constant of GMC controller
k_2	=	rate constant for reverse reaction
K_2	=	tuning constant of GMC controller
K_c	=	proportional gain of PID controller
M_i	=	molar mass of species i, g/mol
M_r	=	mole of the reactor contents, mole
M_w	=	molar mass of water, g/mol
P	=	estimation error covariance matrix
$p(t)$	=	controller output
P_0	=	pre-exponential factor of permeation
Q	=	process noise covariance matrix
Q_r	=	heat released by the reaction, J/hr
Q_{re}	=	estimated heat released by the reaction, J/hr
R_g	=	gas constant

NOMENCLATURES (Continued)

R =   measurement noise covariance matrix

r_i =   rate of reaction

S =   membrane area for permeation, cm^2

T =   absolute temperature, K

t_f =   final time, hr

T_j =   jacket temperature, K

T_{jsp} =   jacket temperature set point, K

T_r =   reactor temperature, K

u =   manipulated input variable

U =   heat-transfer coefficient, J/m^2 hr K

V =   volume of reaction mixtures, liter

V_j =   jacket volume, liter

$\mathbf{x}$ =   vector of n decision variables $(x_1, x_2, \ldots, x_n)$

y =   output of the process model

Greek Letters

τ =   time constant

τ_D =   derivative time constant

τ_I =   integral time constant

τ_j =   time constant of jacket

ΔH =   heat of reaction, J/mol

ρ_i =   density of species i, g/l

ρ_j =   density of jacket, g/l

ρ_w =   density of water, g/l

α_k =   step length parameter

ξ =   damping constant

NOMENCLATURES (Continued)

Subscript

A	=	acetic acid
B	=	butanol
E	=	butyl acetate
W	=	water
j	=	jacket
0	=	initial
r	=	reactor
sp	=	set point

CHAPTER I

INTRODUCTION

Nowadays membrane technology plays an important role in chemical industries and has been used in a broad range of applications. A multitude of potential applications is identified and a several billion-dollar market is predicted for the membrane-based industry by the turn of this century. With the development of new membranes, the improved transport properties and better chemical and thermal stability in recent years, a large number of new potential applications have been described and the membrane-based industry responds to the market needs by rapidly exploiting these applications on an industrial scale.

The key property is the ability of a membrane to control the permeation rate of a chemical species through the membrane. Membranes and membrane processes are used in four main areas: the separation of molecular and particulate mixtures, the controlled release of active agents, the membrane reactors and the artificial organs, and the energy storage and the conversion systems. In these applications, a large variety of processes, membrane structures, and membrane materials has been used (Ho and Sircar, 1992)

There is currently a great deal of interest in the development and use of alternative non-conventional techniques that allow both the separation and purification of the compounds obtained during a process and the use of systems that combine reaction and separation into a single process unit to improve process performance. In recent years, membrane technology has emerged as one of the viable unit operations in separation processes. The potential applications of membrane technology in reaction engineering are being recognized (Waldburger and Widmer, 1996; Xuehui and Lefu, 2001; Liu et al., 2001). Since separation membranes permit selective permeation of a component from a mixture, membrane reactors can enhance the conversion of thermodynamically or kinetically limited reactions through controlled removal of one or more reactant or product species from the reaction mixture (Feng and Huang, 1996).

Esterification is one of the most important chemical processes in organic chemical industry and is a typically reversible process in which conversion is limited by equilibrium conditions. The integration of pervaporation into the conventional esterification process, therefore, offers the opportunity to shift the chemical equilibrium by removing water from the reaction mixture directly or by a side loop of the reactor. Due to the effect of the operating temperature, which influences the reactor performance through its influences on reaction rate and membrane permeability, it is necessary to optimize the process to operate in the most favorable conditions to achieve a desired objective.

As batch processes require different control strategies from those continuous processes do. This is due to the fact that they are operated dynamically. From an engineering point of view, the objectives of control of batch chemical reactors are divided into two categories: optimization of yield and control of product quality (Kravaris et al., 1989). To achieve the desired control objective, the performance of a proposed control strategy is generally set to force the system output to track optimal or reference trajectories efficiently. In summary, to achieve the desired successful control of batch processes, the system depends on the integration of three important ingredients: an optimal operating trajectory, a suitable control law, and a suitable design of the control configuration (Chang and Hseih, 1995).

In this work, a batch reactor integrated with pervaporation developed by Liu et al. (2001) is considered. The study is aimed at exothermic, reversible esterification reaction. A jacket is used to control the operating temperature at its desired trajectory. First, an off-line optimal control problem is solved with fixed batch time to find an optimal temperature that maximizes the final concentration of ester. A generic model control (GMC) coupled with an extended Kalman filter (EKF) is implemented to track an optimal operating temperature.

1.1 Research Objectives

The objectives of this research are:

1. To develop a suitable model for a pervaporative membrane reactor,
2. To determine an optimal operating temperature for a pervaporative membrane reactor to maximize a final concentration of ester,
3. To design a control configuration for a pervaporative membrane reactor to track the obtained optimal operating temperature.

1.2 Scope of Research

1. A batch reactor integrated with pervaporation is considered. The study is aimed at exothermic, reversible esterification reactions. A jacket is used to maintain the temperature of a pervaporative membrane reactor.
2. An ideal case where the membrane is perfectly permselective to water is investigated to show the maximum improvement in reactor performance achievable by the use of membrane pervaporation.
3. A mathematical model of a pervaporative membrane reactor is studied.
4. An off-line optimal control problem is solved with fixed batch time to find the optimal temperature that maximizes the final concentration of ester. A nonlinear programming problem (NLP) is solved using a successive quadratic programming (SQP) based optimization technique.
5. An extended Kalman filter is used to estimate the amount of heat released by the reaction.
6. A generic model control (GMC) coupled with the extended Kalman filter (EKF) is implemented to track an optimal operating temperature.
7. Programs written to simulate and control the reactor are based on Matlab Program and Matlab Toolbox.

1.3 Contribution of Research

1. Mathematical model of a pervaporative membrane reactor has been developed.

2. A computer program simulation has been developed to study the behavior of a pervaporative membrane reactor.

3. Unmeasurable state variable of a pervaporative membrane reactor has been estimated.

4. A pervaporative membrane reactor has been optimized and controlled to achieve a desire objective.

1.4 Activity Plan

1. Relevant information regarding membrane process and membrane reactor are reviewed.

2. Mathematical model of a pervaporative membrane reactor is developed.

3. Relevant information regarding optimization and control are reviewed.

4. Kalman filter is applied to estimate uncertain parameters.

5. An optimal operating temperature of a pervaporative membrane reactor is determined to achieve the desired objective.

6. A suitable control law is designed to track the obtained optimal operating temperature.

7. Simulation results are collected and summarized.

This thesis is divided into five chapters.

Chapter I is an introduction to this research. This chapter consists of research objective, scope of research, contribution of research, and activity plan.

Chapter II reviews the work carried out on pervaporative membrane reactor, optimization, GMC controller, and Kalman filter

Chapter III covers some background information of membrane process (membrane separation, membrane reactor, pervaporation process, and pervaporative membrane reactor), optimization, Generic model control (GMC), and Kalman filter.

Chapter IV describes the mathematical model of a pervaporative membrane reactor, optimization formulation, and control configuration. Simulation results obtained by simulating the optimization formulation and the formulation of a GMC controller are detailed in each section.

Chapter V presents the conclusions of this research and makes the recommendations for future work.

This is follow by:

References

Appendix A: Permeability Coefficient Determination,

Appendix B: Numerical Method,

Appendix C: Integral Error Criteria,

Appendix D: Introlduction to Matlab,

Appendix E: Program Verification,

Appendix F: Tuning of GMC Controller,

Appendix G: Simulation Results.

CHAPTER II

LITERATURE REVIEW

2.1 Pervaporative membrane reactor

The majority of published work on membrane reactor to date is in the field of biotechnology. The membranes used are typically microporous, and the function of membranes is mainly for immobilizing enzymes, eliminating product inhibition, recycling enzymes and other biocatalysts, and manipulating substrates and nutrients. Recently, extensive studies have been carried out on membrane reactors applied to catalytic dehydrogenation, hydrogenation, and decomposition reactions. However, relatively little work has been done on liquid-phase reversible reactions due to lack of suitable membranes with good permselectivity and solvent resistance. Ultrafiltration membranes are too porous to effect efficient separation of small liquid molecules, while reverse osmosis membranes are likely to require an inconveniently high operation pressure due to osmotic pressure of the reaction mixtures. Pervaporation, an emerging membrane process specially used for organic-water and organic-organic separations (Huang, 1991), seems to be an appropriate choice (Feng and Huang, 1996). In this process, the mass transport through the membrane is induced by maintaining a low vapor pressure on the downstream side, thereby eliminating the effect of osmotic pressure.

The concept of using pervaporation to remove by-product species from reaction mixtures was proposed in the early stage of pervaporation research by Jennings and Binning (1960), but the interest in pervaporative membrane reactors was only rekindled recently when pervaporation has been proven to be a viable separation technique in the chemical industry. Presently, pervaporation is best applied to dehydration of organic solvents, and the dehydration membranes normally work best when water content in feed mixture is not high. Thus, reversible reactions that produce by-product water are a niche of pervaporation for reaction enhancement.

Esterification represented a significant group of the reactions commonly found in the chemical industry. The use of pervaporative membrane reactor for esterification was different from the combination of reactive distillation and pervaporation in which water was externally removed from the top or bottom stream. In the pervaporative membrane reactor, the product water was simultaneously removed from the reaction zone while the reaction took place. A number of reactions have been tested in this reactor.

Pervaporative membrane reactor for esterification of oleic acid and ethanol to produce ethyl oleate was studied using *p*-toluenesulfonic acid as a catalyst (Kita et al., 1987-88; Okamoto et al., 1993). Polyimide, chitosan, nafion, polyetherimide and perfluorated ion-exchange were used as membranes. Among these membranes, polyimide showed the highest selectivity. Complete conversion could be achieved at about 6 hours when ethanol was in excess.

Bitterlich et al. (1991) proposed an alternative hybrid process combining a reactor and a pervaporation unit for esterification of butanol and acetic acid to produce butyl acetate. In the conventional process, an acid catalyst (sulfuric acid) was used which had to be removed from the product after the reaction by neutralization with sodium hydroxide. The by-product water was removed by distillation. The alternative process layout used a fixed bed of immobilized acid in an ion exchange resin to replace the sulfuric acid. Hence, no neutralization was required. Furthermore, the distillation for the dehydration was replaced by a pervaporation unit with hydrophilic membranes (Sulzer Chemtech/ GFT and University of Cologne). The hybrid process, therefore, overcame the problems inherent with the use of sulfuric acid, i.e. waste treatment and acidic corrosion problems. The use of pervaporation unit for the dehydration reduced the energy consumption and wastewater flow, and achieved an increased flexibility due to its modular design.

David et al. (1991) studied the esterification of 1-propanol and 2-propanol with propionic acid to produce propyl propionate and iso-propyl propionate. Pervaporation with PVA membranes was externally added to the reactor. It was revealed that the hybrid process was governed by four main parameters that influenced the conversion rate: in order of significance, these were temperature, initial molar ratio, membrane area to reaction volume ratio, and catalyst concentration.

Most of the models presented so far of pervaporative membrane reactor describe both the kinetics and membrane permeation in term of concentrations of the reacting species.

For thermodynamically nonideal mixtures, however, activities are needed in the description of transport (pervaporation) by a solution-diffusion mechanism through the membrane. For nonideal reacting mixtures, furthermore, expressing the reaction rates in terms of concentration results in reaction rates constants, which often depend on concentrations since the latter do not completely, take into account the interactions between molecules. The use of activities not only rectifies this problem but also provides a unified approach in treating both the thermodynamic equilibrium and the driving force in the rate equation. Several authors have made use of activities for the description of esterification reaction rates.

A pervaporation-based hybrid process was analyzed by Okamoto et al., 1993 for the esterification of oleic acid with ethanol using *p*-toluene sulphonic acid as catalyst to produce ethyl oleate. The reaction was carried out within the pervaporation unit using a process layout similar to the membrane reactor with asymmetric hydrophilic poly-etherimide (PEI), and 4,4'-oxydiphenylene pyromellitimide (POPMI) membranes. Though the application of this hybrid process a 98% conversion was achieved in experiments.

Keurentjes et al. (1994) studied the kinetic parameters for the esterification of tartaric acid with ethanol. Both concentration-based as well as activity-based reaction rate constants and equilibrium constants had been determined. The equilibrium composition could be shifted significantly towards the formation of the final product diethyltartrate when pervaporation was used to remove the water produced in this reaction.

Zhu et al. (1996) studied the esterification reaction between acetic acid and ethanol in a continuous flow pervaporation membrane reactor utilizing a polymeric/ceramic composite membrane. For a range of experimental conditions reactor conversions were observed which were higher than the corresponding calculated equilibrium values due to the ability of the membrane to remove water, a

product of the reaction. A developed model gave a reasonable fit of the experimental results.

Waldburger and Widmer (1996) presented a review on membrane reactors with special emphasis on membrane-assistance of esterification reactions and a continuous tube membrane reactor for the pervaporation-assistance of the esterification. The heterogeneously catalyzed esterification of ethanol and acetic acid to ethyl acetate and water was investigated as a typical chemical equilibrium reaction. The selective and simultaneous water separation from the reaction mixture of the esterification with polyvinyl alcohol pervaporation membranes was considered to be an interesting process alternative to the conventional distillation process. Compared to the distillation process, for the pervaporation-assisted process a decrease of the energy input of over 75% and of the investment and operating costs of over 50% each was calculated.

Krupicka and Koszorz (1999) studied in the same reaction. A comparison of the measured concentrations with those calculated according to the model showed sound agreement when the activities were used. The experiments were performed using a wide range of initial molar ratios with commercial hydrophilic PERVAP 1105 GFT membrane. The model was independent of the initial molar ratios due to the stability of thermodynamic and kinetic constants.

Due to simplicity of a concentration-based model, some researchers still explained the models in term of concentrations. In a parameter study, Feng and Huang (1996) revealed that reaction and conversion rate could be improved. It was discovered that a complete conversion could be achieved if one reactant was in excess. Membrane area and permeability as well as the volume of the mixture to be treated were identified as the important parameters of the process. Furthermore, it was shown that the operating temperature influenced both the reaction and membrane reactor for the esterification of acetic acid and benzyl alcohol by applying *p*-toluenesulfonic acid as a catalyst to form benzylacetate. In both cases concentration-based models were used to determine the kinetic parameters. A theoretical model was developed and satisfactorily agreed with the obtained experimental results.

Liu et al. (2001) developed a kinetic model for the coupling esterification of acetic acid with *n*-butanol catalyzed by $Zr(SO)_4 \cdot 4H_2O$ with pervaporation. Experiments were conducted to investigate the effects of several operating parameters, such as reaction temperature, initial molar ratio of acetic acid to n-butanol, ratio of the membrane area to the reacting mixture volume and catalyst concentration, on the coupling process.

There were a number of works on developing new processes to improve the etherification yield. Matouq et al. (1994) proposed a process layout combining an external pervaporation process using hydrophilic polyvinyl alcohol (PVA) membranes with reactive distillation for the production of MTBE. Two types of catalysts i.e. ion exchange resin Amberlyst 15 and heteropoly acid for the reaction of methanol and TBA to form MTBE were investigated. HPA showed higher selectivity than the ion exchange resin. It was found that the hybrid process using pervaporation might be effective in removing water.

Yang and Goto (1997) implemented the similar process for the production of ETBE from EtOH and TBA using Amberlyst 15 as a catalyst. Microporous hydrophilic hollow fiber membranes were employed in the pervaporation unit to dehydrate in the bottom product of the reactive distillation column. Shifting the reaction equilibrium led to almost doubling of the mole fraction of ETBE product in the top product.

Worapon (2001) investigated a pervaporative membrane reactor for the synthesis of ethyl *tert*-butyl ether (ETBE) from a liquid phase reaction between ethanol and *tert*-butyl alcohol. The study was divided into 3 parts: kinetic study of supported β-zeolite, study on permeation through polyvinyl alcohol (PVA) membrane and study on pervaporative membrane reactor. In the pervaporative membrane reactor studies, both experiment and simulation were carried out. An activity-based model was developed to investigate the performance of the pervaporative membrane reactor using parameters obtained from the independent experiments. Simulation results agreed well with experimental results.

2.2 Optimization and Control

Batch or semibatch processes require control strategies different from those for continuous processes because they are commonly not operated at steady states. From an engineering point of view, the objectives of control of batch or semibatch chemical reactors are divided into two categories: optimization of yield and control of product quality (Kravaris et al., 1989). To achieve the desired control objective, the performance of a proposed control strategy is generally set to force the system output to track some optimal or reference trajectories efficiently.

Tremblay and Luus (1989) proposed to present a computational procedure to enable one to examine benefits to be expected from non-steady-state operation of chemical reactors. Three examples showed that the proposed algorithm using dynamic programming can be used for a wide variety of problems, such as to maximize the yield, average rate of production or average concentration overtime. It was found that dynamic programming performed well even for a 6th order system. The optimum period, split of period and amplitude of the input could be obtained in a reasonable computation time when the optimal input signal was in fact periodic in nature.

Due to the important mechanical properties of polymers have been shown to depend strongly on the molecular weight distribution (MWD). Chang and Lai (1992) proposed a modified two-step calculation procedure for estimating the reactor temperature to give the desired average chain length and polydispersity of polymer at the desired final conversion in a polymerization batch reactor. The proposed method was accurate and effective. The adaptation of this calculation procedure to different mathematical models showed this procedure to be very flexible.

Soroush and Kravaris (1993) proposed a framework for integrated design and operation of single-stage batch or semibatch reactors. A systematic decoupling of optimization and design of reactor dynamics was proposed and applied successfully in an experimental demonstration (Soroush and Kravaris, 1992). One could obtain two subsystems with distinct characteristics. Notions of feasibility, flexibility, controllability, and safety of the design for batch processes were introduced for the first time and some criteria for their assessment were presented. The proposed framework included (a) mathematical modeling of the process dynamics, (b) dynamic

optimization (c) design of the heat exchange and/or feeding system(s) and investigation of process operability (feasibility, flexibility, controllability, and safety of the design), and (d) design of a control scheme for automatic startup and optimal operation of the reactor.

Chang and Hseih (1995) proposed an integrated method for optimization and control of semibatch reactors. Based on the desired control objective, dynamic programming was applied to obtain optimal operating trajectories. Yield optimization was assured for a real plant by tracking model-dependent optimal trajectories according to the proposed modified globally linearizing control (MGLC) structure. The behavior of the proposed MGLC structure was predictable and reliable, with tuning parameters based on the proposed tuning method if the manipulated variables were not constrained.

Garcia et al. (1995) converted the optimal control problem into a nonlinear programming problem solved by the generalized reduced gradient procedure coupled with the golden search method, for the search of the total batch time for fine chemical productions in batch reactors. The efficiency of the methodology was shown by its application to different formulations of the problem for different chemical reaction schemes and with stress laid on the influence of the constraints on the limitation of temperature variations and byproduct formation.

Chang et al. (1996) proposed an integrated method for optimization and control of batch reactors. Based on the desired performance index, the modified two-step method was applied to optimize an operating trajectory. Yield optimization was assured for a real plant by tracking the model-dependent optimized trajectory through the proposed modified globally linearizing control (MGLC) structure. Experimental results revealed that the proposed MGLC structure could be applied in tracking an operating trajectory determined on-line or off-line.

Rojnuckarin and Floudas (1996) applied an optimal control strategy to the problem of finding the flux profiles for the conversion of methane to ethylene and acetylene in a plug flow reactor. The optimal control approach implemented in the paper belonged to the class known as gradient methods in function space. The optimal control designs were performed with respect to the final mass fractions of ethylene

and acetylene in a plug flow reactor using heat, oxygen, and chlorine fluxes as controls.

Carrasco and Banga (1997) considered the dynamic optimization (optimal control) of chemical batch reactors. The solution of these types of problems was usually very difficult due to their highly nonlinear and multimodal nature. Two algorithms based on stochastic optimization were proposed as reliable alternatives. These stochastic algorithms were used to successfully solve four difficult case studies taken from the recent literature: the Denbign's system of reactions, the oil shale pyrolysis problem, the optimal fed-batch control of induced foreign protein production by recombinant bacteria, and the optimal drug scheduling of cancer chemotherapy. The advantages of these alternative techniques, including ease of implementation, global convergence properties, and good computational efficiency, were discussed.

Guntern et al. (1998) proposed a methodology for the optimization of semibatch reactors using dynamic programming. This included synthesis of a mathematical model, analysis of the performance of the process at its present state, definition of a set of decision variables, and optimization and simplification of this optimum toward feasibility. The methodology was applied to an industrial case study in the fine chemical industry using the lowest product cost as the objective function.

Luus and Okongwu (1999) determined the optimal flow rates of heating and cooling fluids instead of finding only the optimal temperature profile, so that the yield of a desired product in a batch reactor was maximized. The purpose of this paper was to investigate such an approach in the control of typical chemical reactors by considering two examples. By using iterative dynamic programming (IDP) in multi-pass fashion, the optimal policy could be readily obtained. Optimization as carried out on two typical batch reactor problems showed that if the heat transfer coefficient was reasonably chosen, then the optimal yield could be significantly larger than what could be expected from the best isothermal operation.

Faliks et al. (2000) applied an optimal control methodology to the problem of finding the heat, hydrogen, and oxygen flux profiles for the homogeneous gas-phase conversion of methane to ethylene in a plug flow reactor. The calculations used a

detailed reaction model for the oxidative pyrolysis of methane and a model for the growth of polycyclic aromatic hydrocarbons and soot particle nulceation and growth.

Recently developments in nonlinear systems theory combined with advances in control system hardware and software made the practical application of nonlinear process control strategies a reality. The review article (Bequette, 1991) surveyed nonlinear control system techniques ranging from ad hoc or process-specific strategies to predictive control approaches based on nonlinear programming. The capabilities of these techniques to handle the common problems associated with chemical processes, such as time delays, constraints, and model uncertainty were discussed.

Chang and Huang (1994) proposed a modified globally linearizing control (MGLC) structure and a nonlinear feedforward-feedback control (NFF/FB) structure to track trajectories of processes in a batch reactor. The MGLC structure performed trajectory tracking perfectly when the model inversion could be obtained by linearization of state feedback. Otherwise, the NFF/FB structure was recommended. The performance of the control laws was compared with other control laws designed with the same technique. The proposed control law based on the MGLC structure exhibited robust performance whereas that based on NFF/FB structure produced decreased sensitivity to process noise.

Chang et al. (1996) proposed an integrated method for optimization and control of batch reactors. Based on the desired performance index, the modified two-step method was applied to optimize an operating trajectory. Yield optimization was assured for a real plant by tracking the model-dependent optimized trajectory through the proposed modified globally linearizing control (MGLC) structure. Experimental results revealed that the proposed MGLC structure could be applied in tracking an operating trajectory determined on-line or off-line.

Ali et al. (1998) used a dynamic model describing and ethylene gas-phase polymerization reaction in a fluidized bed reactor to investigate the process static and dynamic behavior. The static analysis determined optimal operating condition at which the monomer conversion can be increased to 25% per pass. However, this optimal operating point was shown to be unstable, and thus any changes in the plant operation might lead to temperature runaway, degrading the reactor performance. In

addition, the reactor temperature must be kept within a narrow range between the gas dew point and the polymer melting point. For these reasons, two control algorithms, that was, proportional-integral (PI) and nonlinear model predictive control (NLMPC), were tested for the stabilization of the process during load changes.

2.3 Generic model control (GMC)

Lee and Sullivan (1988) presented a general framework for process controllers that relied upon a model to approximate plant behavior. By careful selection of a performance index and an approximate plant model, it was shown that single-loop PI control, feedforward and decoupling control, multivariable regulators, time horizon matrix controllers, internal model control and process model based control could all be derived. Furthermore, nonlinear process models could be imbedded directly into the controller without resorting to linearization. This unifying framework was illustrated with a number of examples to highlight the utility of such an approach.

Lee et al. (1989) summarized the use of a process model directly in a control algorithm. The process considered, a forced circulation single-stage evaporator, was a nonlinear interacting process. The control strategy employing a process model derived from fundamental mass and energy balances was shown to outperform single loop and predictive control strategies by a significant amount. The control structure was first presented in general form and then specifically applied to this process.

Cott and Macchietto (1989) presented a new model-based controller for the initial heat-up and subsequent temperature maintenance of exothermic batch reactors. The controller was developed by using the Generic Model Control framework of Lee and Sullivan, which provided a rigorous and effective way of incorporating a nonlinear energy balance model of the reactor and the heat-exchange apparatus into the controller. It also allowed the use of the same control algorithm for both heat-up and temperature maintenance, thereby eliminating the need to switch between two separate control algorithms as was the case with today' s more commonly used strategies. A deterministic on-line estimator was used to determine the amount and rate of heat released by the reaction. This information was, in turn, utilized to determine the change in jacket temperature setpoint in order to keep the reaction

temperature on its desired trajectory. The performance of the new GMC-based controller was compared to that of the commonly used dual-mode controller. Simulation studies showed the new controller to be as good as the dual-mode controller for a nominal case for which both controllers were well tuned. However, the new controller was shown to be much more robust with respect to changes in process parameters and to model mismatch.

Riggs and Rhinehart (1990) compared two nonlinear process-model based controllers (PMBC), nonlinear internal model control, IMC and generic model control, GMC. An idealized SISO CSTR and a SISO heat exchanger were considered. The simulation results showed that GMC and nonlinear IMC gave nearly the same performance throughout a wide range of process nonlinearity and process gain.

Control in the face of process constraints is of great practical importance in the processing industries. Lee et al. (1991) examined the use of GMC for controlling the level in a surge tank. In particular, it examined the effect of certain user-selectable parameters on the controlled response to changes in the inlet flowrate. In addition, the effects of model inaccuracies were considered. The overall algorithm was shown to be significantly lower in computational requirements than previously proposed algorithms for surge tank control. Implementation was straightforward and was suitable for even small-scale process control computing systems.

Barolo et al. (1993) proposed a new on-line control algorithm, based on GMC, for improving the automatic startup of a binary distillation column. A series of tests had been performed on an industrial-scale distillation column. The experimental results demonstrated the effectiveness and robustness of the proposed method with respect to process/model mismatch. The implementation of the algorithm was simple and could be accomplished with standard industrial instrumentation and a cheap personal computer.

When a process model differed from the true process, the closed-loop qualities of a model-based control algorithm such as GMC are in doubt. The conditions under which stability of the closed-loop GMC system was guaranteed (robust stability) and the performance of the closed loop system was guaranteed to meet predetermined performance objectives (robust performance) were given for the first time in terms of

the model and its uncertainty description (Signal and Lee, 1993). The GMC parameters, which gave the best performance, could be determined through a simple optimization procedure. The analytical techniques were illustrated through a simple example.

Kershenbaum and Kittisupakorn (1994) studied a temperature control of a batch reactor using GMC controller. The amount of heat released by the reactions had been estimated online using an extended Kalman filter, and incorporated into the GMC algorithm. Simulation results had shown that the Kalman filter gave an accurate estimate of the amount of heat released and together with the GMC controller, gave reliable robust control. An experimental extension of the work using the PARSEX reactor showed that the extended Kalman filter was rather more sensitive to plant/model mismatch than would have been predicted from simulations alone.

Costello (1994) investigated, by simulation, the ability to control the neutralization of an acid stream by a strong alkali stream using a model-based nonlinear transformation control technique to augment a PI controller. This approach was compared with a standard PI controller and GMC controller. The simulation results had shown that it is indeed possible to successfully control an acid-base neutralization process with a simple model-based nonlinear transformation applied to a PI controller, and that the more complex model-based control techniques, as represented by GMC control might not be appropriate for this problem.

Douglas et al. (1994) studied the problem of dual product composition control of an industrial high purity distillation column, a deisohexanizer (DIH), using a GMC framework. The performance of GMC incorporating different process models was studied. The different controllers were implemented and compared using a dynamic simulation of an industrial DIH to select the best candidate controller. A controller using a nonlinear process model emerged as the best controller and was implemented on the actual process, resulting in improved performance over the original controller.

Farrell and Tsai (1995) implemented a GMC algorithm for batch crystallization process. The resulting algorithm which was called batch GMC (BGMC) algorithm utilized a time variant reduced-order input-output model derived by correlating historical data of solubility vs. weight mean size. Control of the weight mean size trajectory in response to seed disturbances was demonstrated in this paper.

Vega et al. (1995) used a dynamic model of the evolution of the temperature of a batch cooling crystallizer for the development of a GMC system for the crystallizer. This servo-control system had been found experimentally to work adequately. The crystallizer had also been controlled with a conventional PI controller, and the process had been simulated with the model. Simulations were accurate enough to allow the model to be used for the design of control strategies for programmed cooling crystallizers. The methodology described could be adapted to the study of other systems or control algorithms.

Khandalekar and Riggs (1995) applied the nonlinear process model based control (PMBC) to the Amoco/Lehigh University Model IV FCC industrial challenge problem. In particular, PMBC was applied for the control of reactor temperature, regenerator temperature and the flue gas oxygen concentration. The GMC law was used for the nonlinear PMBC controller. Both the nonlinear PMBC and conventional PI controllers were tested first for the unconstrained control. Finally, the nonlinear PMBC constraint controllers were used for optimization studies to analyze the operation at the economic optimum in the face of variations in feed characteristics and variations in operative constraints.

A large number of applications of GMC had been published in the literature. However, an overview of the potential difficulties in implementation had not been provided. Dunia and Edgar (1996) evaluated the basic GMC algorithm when applied to SISO linear processes and provided insight regarding its limitation to ensure robust stability. The effect of sampling time on the reference trajectory for discrete systems was analyzed in order to avoid unstable responses for perfect models. Finally, a predictive GMC was developed to handle models with dead time in a reliable way.

Xie et al. (1999) proposed a new approach to Adaptive Generic Model Control (AGMC), based on the theory of Strong Tracking Filter (STF). Two AGMC schemes were developed. The first was a parameter-estimation-based AGMC, After introducing a new concept of Input Equivalent Disturbance (IED), another AGMC scheme called IED-estimation-based AGMC was further proposed. The unmeasurable disturbance and structural process/model mismatches could be effectively overcome

by the second AGMC scheme. The laboratory experimental results on a three-tank-system demonstrated the effectiveness of the proposed AGMC approach.

Nussara (1999) presented the application of GMC to control the temperature of a batch polyvinyl chloride polymerization reactor. In this work, heat released of reactions was needed in the GMC formulation but not available for measurement, on-line heat released estimator was used to estimate the heat released of the reactions. The GMC controller coupled with the estimator could give better control performance than the PID controller could. Furthermore, the GMC controller was more robust than the PID controller in the presence of plant/model mismatches.

Aziz et al. (2000) designed and implemented three different types of controllers namely PI, PID (both in DM strategy) and GMC controllers to track the optimal reactor temperature profiles using a complex reaction scheme in a batch reactor. Off-line optimal control problem had been formulated and solved to obtain the optimum temperature profiles (dynamic set point for controllers) to maximize the amount of the desired product while minimizing the waste by-product. Neural network technique was used as the on-line estimator the amount of heat released by the reaction within the GMC algorithm. The GMC controller coupled with a neural network was found to be more effective and robust than the PI and PID controllers in tracking the optimal temperature profiles to obtain the desired products on target.

Pijak (2002) applied GMC for a concentration control of continuous stirred tank reactor with first-order exothermic reaction, which was the process of relative degree two. This research used an internal controlled variable, the key component that made the control variable to be effected directly like the relative degree one processes. The results showed that the GMC with internal controlled variable could use the techniques that improved the robustness like a conventional GMC.

2.4 Kalman filter

In most industrial processes, the state variables are not all measurable or, not with sufficient accuracy for control purposes. Furthermore, measurements that are available often contain significant amounts of random noise and systematic errors. For these situations, an estimator has been applied to estimate state variables. In 1960,

Kalman published a famous paper describing a recursive solution to the discrete data linear filtering problem. The Kalman filter has been the subject of extensive research and application, particularly in the area of autonomous or assisted navigation.

Myers and Luecke (1991) described and illustrated an efficient new algorithm on process examples for solution of the extended Kalman filter equations for a continuous dynamic system with discrete measurements. Implicit simultaneous methods, which were powerful in terms of accuracy and efficiency, were utilized for numerical integration. At the internal integration step level, the new algorithm exploited the decoupled nature of the state estimate and error covariance equations along with the symmetry of the error covariance matrix. The error control strategy included both the state estimates and error covariance.

Tan et al. (1991) applied two estimation techniques, the extended Kalman filter (EKF) and the iterative extended Kalman filter (IEKF), to a nonlinear time-varying system that had non-measurable state variables. An iterative solution to a fed-batch fermentation process was reported using the EKF based on measurements of the oxygen and carbon dioxide concentrations. The results demonstrated that this estimation technique could be successfully applied to complex biological processes.

An adaptive control of input-output linearizable systems, together with an extended Kalman filter (EKF), was applied to a simulated batch polymerization reactor to realize the output (monomer conversion) tracking in the presence of model parameter uncertainties (Wang et al., 1993). Simulation results showed that this technique was robust and the output tracking performance could be ensured even in the presence of large model parameter errors and disturbances.

Gudi et al. (1995) presented the design and development of a multirate software sensor for use in the chemical process industry. The measurements of process outputs that arrived at different sampling rates were formally accommodated into the estimation strategy by using the multirate formulation of the iterated extended Kalman filter. Measurement delays associated with some of the process outputs were included in the system description by addition of delayed states. Observability issues associated with state and parameter estimation in a multirate framework were

discussed and modified measurement equations were proposed for systems with delayed measurements to ensure relatively strong system observability.

Ahao and Kummel (1995) presented an application of state and parameter estimation techniques in an altering activated sludge process with regard to biological phosphorus removal. A simplified model describing the phosphorus dynamics in an alternating activated sludge process was proposed based on insight into the process with a mechanistic activated sludge model. State and parameter estimation problems relating to the non-measurable dynamics of a most important limiting substrate poly-hydroxy-alkanoate (PHA) were formulated and discussed. Several schemes were presented which involved a state estimator designed with the extended Kalman filter algorithm, two specific parameter estimation procedures and an adaptive scheme for simultaneous state and parameter estimation.

Sarawut (1998) studied the temperature control of a batch reactor with exothermic reaction and compared the performance of MPC with GMC. In addition, since both MPC and GMC were the model based controllers and needed the measurement of all states as well as the value of process parameters Kalman Filter was used to estimate the heat released of chemical reactions.

State estimation methods, like the extended Kalman filter (EKF) were used for obtaining reliable estimates of the states from the available measurements in the presence of model uncertainties and unmeasured disturbances. The main open issue in applying EKF was the need to quantify the accuracy of the model in terms of the process noise covariance matrix, Q. Valappil and Georgakis (1999) proposed two methods that utilized the parametric model uncertainties to calculate the Q matrix of an EKF. The first approach was based on a Taylor series expansion of the nonlinear equations around the nominal parameter values. The second approach accounted for the nonlinear dependence of the system on the fitted parameters by use of Monte Carlo simulations that were easily be performed on-line. The value of the process noise covariance matrix obtained was not limited to a diagonal and constant matrix and was dependent on the current state of the dynamic system. The application of these techniques to an example process was discussed.

Russell et al. (2000) investigated a model-based inferential quality monitoring approach for a class of batch systems. First, an extended Kalman filter based fixed-point smoothing algorithm was presented and compared to a popular approach to estimating the initial conditions. Subsequently, a nonlinear optimization-based approach was introduced and analyzed. A sub-optimal on-line approximation to the optimization problem was developed and shown to be directly related to the extended Kalman filter based results. Finally, some practical implementation aspects were discussed, along with simulation results from and industrially relevant example application.

Nantana (2000) presented the implementation of Globally Linearizing Control (GLC) together with an extended Kalman filter to control pH of the wastewater treatment process that was a part of an electroplating plant. The extended Kalman filter had been applied to estimate unavailable or unknown states and parameters and these estimates were incorporated in the control action determination in the GLC algorithm.

Veerayut (2000) designed and developed two software programs based on Kalman filter. The first one, named kSTAPEN+, was a software component based on Kalman filter. In kSTAPEN+, users could define their own systems including states and parameters to be estimated. After running the program, estimation results are given. The estimates obtained from the kSTAPEN+ had been compared to those obtained from the program written on Matlab. Furthermore, the program had been tested with a heater, a stirred-tank reactor and a microfeeder. In kSTAPEN-C, the component had been developed by using Component Object Model (COM) technology. The estimates obtained from kSTAPEN-C had been compared to those obtained from kSTAPEN+. Results had shown that both kSTAPEN-C and kSTAPEN+ were equivalent.

CHAPTER III

THEORY

The variety of membrane separation processes, the novel characteristics of membrane structures, and the geometrical advantages offered by the membrane modules have been employed to enhance and assist reaction schemes to attain higher performance levels compared to conventional approaches. Membrane reactors have been investigated since the 1970s and have found utility in a broad range of applications including biochemical, chemical, environmental, and petrochemical systems.

This chapter provides some background information necessary for understanding membrane process, optimization, generic model control (GMC) and Kalman filter.

3.1 Membrane Process

The details on membrane separation, membrane reactor, pervaporation process, and pervaporative membrane reactor are provided in the following sections.

3.1.1 Membrane Separation

Membrane can be used to satisfy many of the separation requirements in the process industries. These separations can be put into two general areas; where materials are present as a number of phases and those where species are dissolved in a single phase.

A membrane is a permeable or semi-permeable phase, polymer, inorganic or metal, which restricts the motion of certain species. This membrane, or barrier, controls the relative rates of transport of various species through itself and thus, as with all separations gives one product depleted in certain components and a second

product concentrated in these components. The performance of a membrane is defined in terms of two simple factors, flux and retention or selectivity. Flux or permeation rate is the volumetric (mass or molar) flowrate of fluid passing through the membrane per unit area of membrane per unit time. Selectivity is a measure of the relative permeation rates of different components through the membrane. Retention is the fraction of solute in the feed retained by the membrane. Ideally a membrane with a high selectivity or retention and with a high flux or permeability is required, although typically attempts to maximize one factor are compromised by a reduction in the other.

Membranes are used for various separations; the separation of mixtures of gases and vapors, miscible liquids (organic mixtures and aqueous/organic mixtures) and solid/liquid and liquid/liquid dispersions and dissolved solids and solutes from liquids. The main uses of membrane separations in industry are in:

- The filtration of micron and submicron size particulates from liquid and gases (Microfiltration),

- The removal of macromolecules and colloids from liquids containing ionic species (Ultrafiltration),

- The separation of mixtures of miscible liquids (Pervaporation),

- The selective separation of mixtures of gases and vapor and gas mixtures (Gas Permeation and Vapor Permeation),

- The selective transport of only ionic species (Electrodialysis),

- The virtual complete removal of all material, suspended and dissolved, from water or other solvents (Reverse Osmosis).

The main feature, which distinguishes membrane separations from other separation techniques, is the use of another phase, the membrane. This phase, either solid, liquid or gaseous, introduces an interface(s) between the two bulk phases involved in the separation and can give advantages of efficiency and selectivity. The

membrane can be neutral or charged and porous or non-porous and acts as a permselective barrier.

Transport of selected species through the membrane is achieved by applying a driving force across the membrane. The processes in which membranes are used can be classified according to the driving force used in the process. The technically and commercially most relevant processes are:

- pressure-driven processes, such as reverse osmosis, ultrafiltration, microfiltration, or gas separation,

- concentration-gradient-driven processes, such as dialysis,

- partial-pressure-driven processes, such as pervaporation,

- electrical-potential-driven processes, such as electrolysis and electrodialysis.

Membranes are manufactured as flat sheets, hollow fibers, capillaries, or tubes, for practical applications membranes are installed in a suitable device, which is referred to as *membrane module*. The most commonly used devices are pleated cartridges, tubular and capillary membrane modules, plate-and-frame and spiral-wound modules, and hollow-fiber modules. There are several other module types used in special applications, such as the rotation cylinder and the transversal flow capillary module. The key properties of efficient membrane modules are high packing density, good control of concentration polarization and membrane fouling, low operating and maintenance costs, and cost-efficient production. For the efficiency of a membrane process in a certain application, the choice of the proper membrane module is of great importance.

3.1.2 Membrane Reactor

There has been an engineering effort to combine reaction and separation into a single process unit so as to improve process performance. Various functions of the membranes in a reactor can be categorized according to the essential role of the membranes. They can be employed to introduce/separate/purify reactant(s) and products, to provide the surface for reactions, to provide a structure for the reaction medium, or to retain specific catalysts. Within these broad contexts, the membranes can be catalytic/noncatalytic, polymeric/inorganic, and ionic/nonionic and have different physical/chemical structures and geometries. The functions of the membrane in a reaction can be enhanced or increased also by the use of multiple membrane-based schemes.

Figure 3.1 schematically identifies many of the major generic functions performed by a membrane in a reactor. One should not conclude from the figure that a given membrane in a given reactor is capable of all functions identified in the figure. However, a given membrane under appropriate circumstances can perform more than one generic function. The introduction of another membrane into the reactor can increase the number of generic membrane functions in the reactor or achieve the same generic membrane function vis-à-vis some other species. Figure 3.1 also indicates other activities concurrently taking place in the so-called nonreactor (or permeate) side of the membrane as well as in the reactor side of the membrane. A list of the generic membrane functions performed by a membrane or two in a reactor is provided next:

1. Separation of products from the reaction mixture,

2. Separation of a reactant from a mixed stream for introduction into the reactor,

3. Controlled addition of one reactant or two reactants,

4. Nondispersive phase contacting (with reaction at the phase interface or in the bulk phases),

5. Segregation of a catalyst (and cofactor) in a reactor,

6. Immobilization of a catalyst in (or on) a membrane,

7. Membrane is the catalyst,

8. Membrane is the reactor,

9. Solid-electrolyte membrane supports the electrodes, conducts ions, and achieves the reactions on its surfaces,

10. Transfer of heat,

11. Immobilizing the liquid reaction medium.
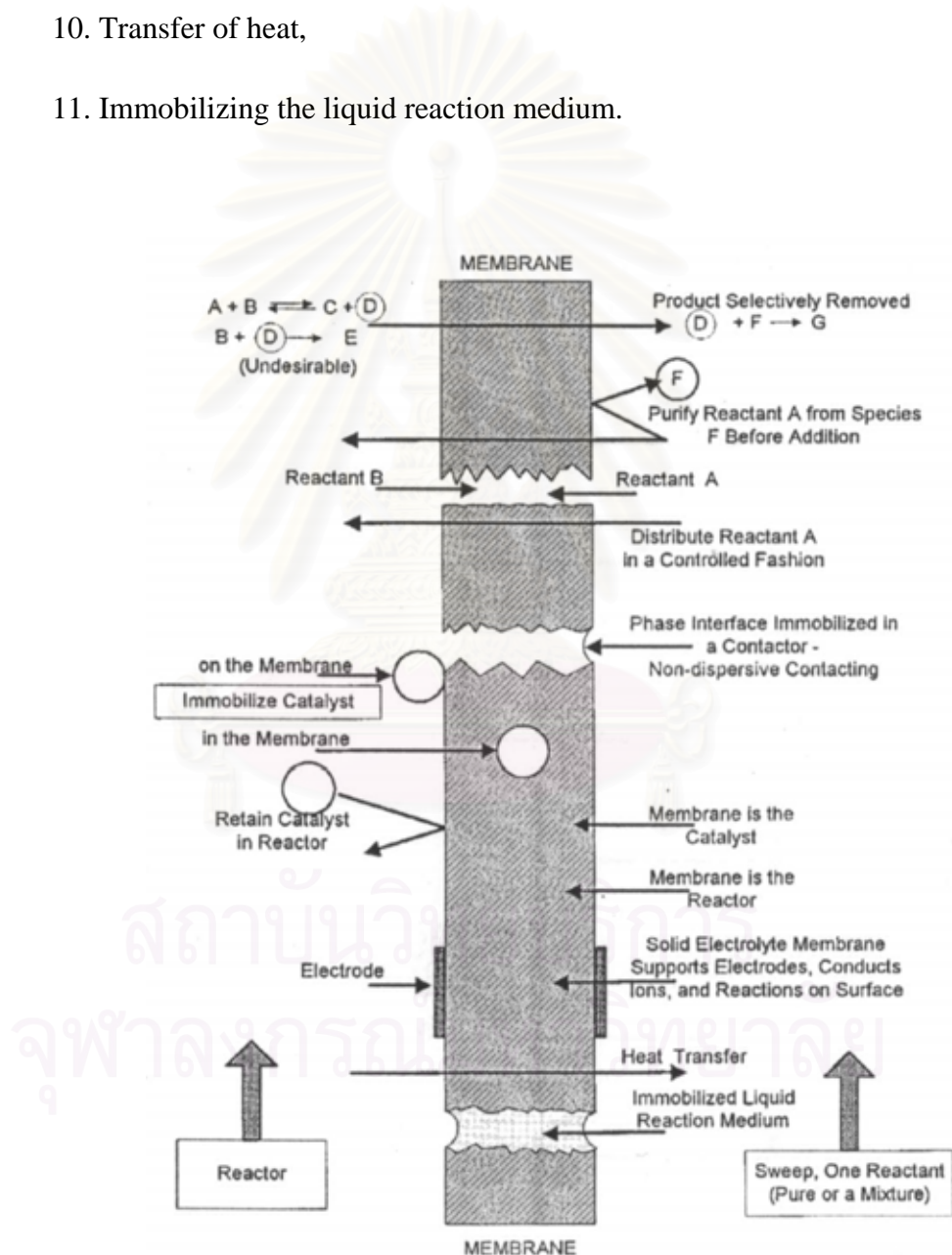
Figure 3.1 Schematic of possible functions of a membrane in a reactor

3.1.2.1 Separation of products from the reaction mixture

Separation of products from the reaction mixture is one of the most common functions of a membrane in a reactor and this work is mainly focused on this function. The separation may be purification, enrichment, or concentration. Consider the following elementary reversible reaction (see figure 3.1).

$$A + B \longleftrightarrow C + D \tag{3.1}$$

Where D is a product needed to be removed via the membrane to the permeate side. The separation process employed may produce a permeate side stream where the mole fraction of D is much higher than that in the reactor side.

Removal of D via the separation function of the membrane has the following effects on reaction (3.1) and the reactor performance:

- The equilibrium condition indicated in the reversible reaction (3.1) is shifted to the right, i.e., leading to higher equilibrium conversion of A and B to C and D.

- If there is an undesirable side reaction as shown below,

$$B + D \longleftrightarrow E \tag{3.2}$$

Taking place in the reactor (see figure 3.1), the separation of product D from the reaction mixture reduces the loss of reactant B to the side reaction, increasing the selectivity of conversion to product C (or D)

- In consecutive catalytic reactions,

$$A \longrightarrow B \tag{3.3a}$$

$$B \longrightarrow C \tag{3.3b}$$

Where B is the desired intermediate product, if the rate constant for reaction (3.3b) is significantly larger than the rate constant for reaction (3.3a), it is difficult to achieve a high selectivity to B using a conventional packed bed, plug flow reactor. By using an inert sweep gas on the outside of a permeable tube having the catalysts and the

reaction taking place inside the tube, the intermediate product B may be selectively removed from the reaction zone, leading to increased selectivity.

- In fermentation processes, one of the products may be inhibitory to the fermentation process. Removal of the product from the fermentation broth via a membrane can substantially reduce product inhibition and increase volumetric productivity of the fermentor. Further, one can use higher concentrations of the substrate in the feed (e.g., glucose for ethanol fermentation) since the product is being removed as it is being formed.

The separation of a reaction product(s) (C or D or both) can be implemented using a variety of membrane processes. The nature of the membrane process is obviously influenced by the phase of the reaction medium exposed to the membrane and the desired phase of the permeated product stream.

3.1.2.2 Separation of a reactant from a mixed stream for introduction into the reactor

Figure 3.1 identified a particular function of the membrane as "purify reactant A from species F before addition" to the reactor on the left-hand side. The effect of this separation on the reaction system is generally quite different from that of a reaction product from the reaction mixture. The purification may lead to pure A being introduced into the reactor; a direct effect of this is prevention of dilution of the reaction mixture. It can also lead to rejection of a class of compounds by the membrane while the membrane preferentially introduced reactant species (one or a class) into the reactor from the feed stream; the species rejected can inhibit the reaction. An additional possibility involves simultaneous operation of two different reactions on two sides of the membrane wherein the products of one reaction feed the other and vice versa; the latter could be in a coupled mode as well.

3.1.2.3 Controlled addition of one reactant or two reactants

Control of the reaction pathway is a major concern in reaction engineering. Partial oxidation reactions of hydrocarbons are especially relevant here. In particular cases, possibilities of thermal runaway and catalyst poisoning do exist. In biodegradation processes for toxic organics, microorganism growth may be affected by inhibition from the toxic organics unless their concentrations are controlled. In an aerobic wastewater treatment process, high O_2 utilization with minimum waste to the atmosphere requires controlled but efficient introduction of O_2 to the system. In processes using reactants having limited half-lives, e.g., ozonation of wastewater or for water purification, efficient and localized introduction of O_3 at a controlled rate can lead to higher O_3 utilization. Using a membrane to introduce a reactant or two in a controlled fashion in the reactor can facilitate achievement of the desired reaction conditions.

3.1.2.4 Nondispersive phase contacting (with reaction at the phase interface or in the bulk phases)

In many reactions, aqueous and organic phases are frequently used together. One phase is dispersed as drops in the other phase followed by coalescence after the process is over. This can be problematic if there are tendencies for emulsification. Microporous/porous membranes can be particularly useful here since the two immiscible phases can be kept on two sides of the membrane with their phase interfaces immobilized at the membrane pore mouths. Solvent extraction is conventionally used to isolate and concentrate dilute organic products obtained from whole cell-based fermentation processes. If the fermentation suffers from product inhibition, then extraction of the product(s) during fermentation increases the fermentor productivity. However, solvent dispersion can lead to a phase-level toxicity problem for the whole cells. Nondispersive phase contacting using microporous/porous membranes can resolve this problem.

In nondispersive phase contacting employing microporous/porous hydrophobic membranes, the organic phase wets the membrane pores; the aqueous phase is maintained outside the pores at a pressure equal to or higher than that of the organic phase. As long as this excess pressure does not exceed a breakthrough

pressure, the aqueous-organic interface remains immobilized on the aqueous side of the membrane with each phase flowing on a particular side of the membrane. For hydrophilic microporous/porous membranes, the aqueous phase is inside the pores; the organic phase is kept outside the pores at a pressure higher than that of the aqueous phase

3.1.2.5 Segregation of a catalyst (and cofactor) in a reactor

A membrane incorporated in a catalytic reaction system can perform, among others, a number of functions related to the catalyst. If the catalyst is mobile in the reaction fluid, the membrane can prevent its escape from the system. If the catalyst is to be immobilized with easy access to the reactants and convenient exit for the products, a porous/microporous membrane structure may have the catalyst immobilized on/within its structure (function 3.1.2.6). Alternately, the membrane material itself may act as the catalyst (function 3.1.2.7). We focus here on cases where the catalyst is mobile in the reaction fluid. Examples of such catalysts are enzymes (and cofactors where applicable), whole cells, and homogeneous catalysts (in organic synthesis). The segregation of particulate heterogeneous catalysts by filters is not under consideration.

3.1.2.6 Immobilization of a catalyst in (or on) a membrane

Four basic types of catalysts are relevant: (a) enzymes and (b) whole cells for biocatalysis; (c) oxides and (d) metals for nonbiological synthesis. Biocatalysts will be considered first since their immobilization in (or on) the membrane was explored much earlier. Five techniques have been studied in varying degrees. They are (1) enzyme contained in the spongy fiber matrix; (2) enzyme immobilized on the membrane surface by gel polarization; (3) enzyme adsorbed on the membrane surface; (4) enzyme immobilized in the membrane pore by covalent bonding; (5) enzyme immobilized in the membrane during membrane formation by the phase inversion process of membrane making.

3.1.2.7 Membrane is the catalyst

Most catalytic membrane reactors for higher temperature operations employ ceramic membranes in the pores/micropores of which catalysts were deposited. The base membranes, e.g., silica and alumina, are generally not catalysts for the reactions studied. There are, however, a number of membranes, which are inherently catalytic for particular reactions; no catalyst needs to be deposited on or in the membrane. Particular examples are cation-exchange membranes, Nafion membranes, palladium membranes, and zeolite membranes

3.1.2.8 Membrane is the reactor

In a membrane reactor, catalysts are used frequently. The membrane may physically segregate the catalyst in the reactor (function 3.1.2.5) or have the catalyst immobilized in the porous/microporous structure or on the membrane surface (function 3.1.2.6). The membrane having the catalyst-immobilized in/on it functions almost in the same way as a catalyst particle in a reactor does except separation of the product(s) (function 3.1.2.1) takes place, in addition, through the membrane to the permeate side. All such configurations involve the bulk flow of the reaction mixture along the reactor length while diffusion of the reactants/products takes place generally in a perpendicular direction to/from the porous/microporous catalyst.

3.1.2.9 Solid-electrolyte membrane supports the electrodes, conducts ions, and achieves the reactions on its surfaces

Solid electrolytes are solid-state materials possessing ionic conductivity. The two ions of the greatest relevance are H^+ and O^{2-}, although other ions, Cl^-, F^-, Ag^+, etc., have been found to be conducted as well. Solid polymer electrolytes such as perfluorinated ionomer membranes (e.g., Nafion) allow transport of H^+ ions in the presence of water and are often called proton-exchange membranes. Solid solutions of oxides of di- or trivalent cations (e.g., Y_2O_3) in oxides of tetravalent metals such as ArO_2 can conduct O^{2-} over a wide temperature range. Nonporous disks of such a solid

electrolyte can act as membranes for such ionic species and are quite useful for fuel cells and as O^{2-} conductors.

3.1.2.10 Transfer of heat

The most recent studies of membrane reactors have been in the context of the petrochemical industry. They take place at higher temperatures ($>200\ ^{o}C$) and there likely is a need for considerable heat transfer because the reaction may be exothermic or endothermic. Dehydrogenation reactions studied frequently are endothermic. The membrane, if inert, is in a catalytic reactor, packed bed, or fluidized bed. Thus, the membrane may have to participate in heat transfer.

In actual practice, there will be one particular reaction going on and heat is going to be supplied from a fired heater, molten salt baths, or thermal fluid jackets. Therefore, the membrane is most likely going to be decoupled from the heat transfer process. A common configuration of some interest in a packed bed membrane reactor consists of multiple membrane tubes inside tubular catalyst beds, placed in turn, in another enclosure for heat exchange. Thermal expansion properties of the membrane tube, sealing at the header, and protection from abrasional damage from catalyst particles are of much greater importance.

3.1.2.11 Immobilizing the liquid reaction medium

Many reactions are carried out in an organic solvent. These include two-phase reactions, e.g., those encountered in phase transfer catalysis, gas-liquid reactions, etc. A porous/microporous membrane can immobilize an appropriate reaction medium in the pores. The two different phases containing reactants can be brought to the two sides of the membrane. As long as the two feed phases are immiscible with the reaction medium, reactants can partition into the reaction medium and react and then the products can partition back into the flowing phases on opposite sides of the membrane. Unfortunately, such a configuration, usually termed as the supported liquid membrane (SLM), has limited stability because of a variety of reasons

including a finite solubility of the reaction medium in the two different reactant-containing phases.

3.1.3 Pervaporation

Pervaporation is a relatively new membrane separation process that has elements in common with reverse osmosis and membrane gas separation. In pervaporation, the liquid mixture to be separated (feed) is placed in contact with one side of a membrane and the permeated product (permeate) is removed as a low-pressure vapor from the other side (Figure 3.2). The permeate vapor can be condensed and collected or released as desired. The chemical potential gradient across the membrane is the driving force for the mass transport. The driving force can be created by applying either a vacuum pump or and inert purge (normally air or steam) on the permeate side to maintain the permeate vapor pressure lower than the partial pressure of the feed liquid.

Vacuum pervaporation, which is customarily referred to as the standard pervaporation, is the most widely utilized mode of operation, while inert purge pervaporation is normally of interest if the permeate can be discharged without condensation. Besides these two modes of operation, there are several other process variants, including thermal pervaporation, perstraction or osmotic distillation, saturated vapor permeation, and pressure-driven pervaporation (Franken et al., 1990; Neel, 1991; Goncalves et al., 1990). Some of them are really process hybrids rather than process variants. Recently, electrically induced pervaporation has also been attempted by Timsahev et al. (1994).

(a)

(b)
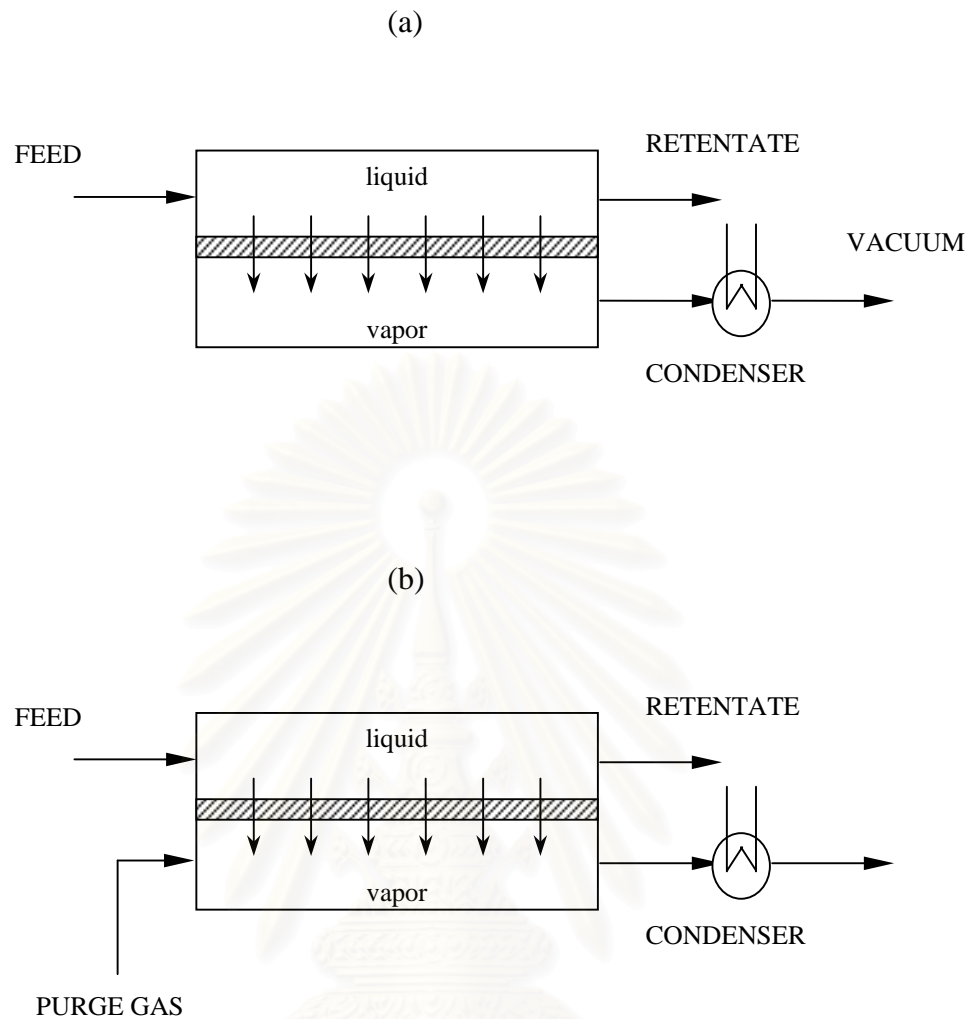
Figure 3.2 Schematic diagram of the pervaporation process. (a) Vacuum pervaporation, (b) purge gas pervaporation

The mass transport in non-porous pervaporation membranes can be described by the solution-diffusion-mechanism (see figure 3.3):

- Sorption of the permeating components in the membrane polymer on the retentate side of the membrane,

- Diffusion of the sorbed components through the polymer membrane,

- Desorption of the permeated components by evaporation into a vacuum chamber or a sweep gas stream on the permeate side of the membrane.

Membrane
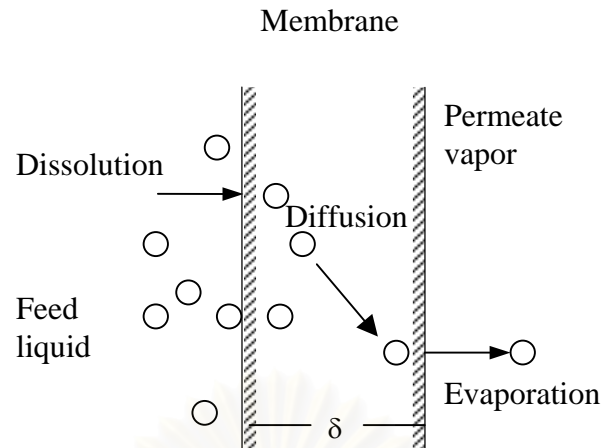
Figure 3.3 Schematic representation of the pervaporation transport mechanism: solution-diffusion model.

The separation of liquid mixtures by using pervaporation method can be classified into three fields:

1) Solvent dehydration,

2) Separation of dissolved organics from water,

3) Separation of organic mixtures.

3.1.3.1 Solvent dehydration

Most of the early solvent dehydration systems were installed for ethanol dehydration. This is a particularly favorable application for pervaporation because ethanol forms an azeotrope with water at 95 percent and a 99.5 percent pure product is needed. Essentially all pervaporation dehydration systems installed to date have been equipped with poly(vinyl alcohol) membrane. Because an ethanol/water azeotrope forms at 95% ethanol, the concentration of ethanol from fermentation feeds to high degrees of purity requires rectification with a benzene entrainer, some kind of molecular-sieve drying process, or a liquid-liquid extraction process. All these processes are expensive. However, the availability of extremely water-selective pervaporation membranes allows pervaporation systems to produce almost pure ethanol (>99.9 percent ethanol from a 90 percent ethanol feed). Reliable capital and operation cost comparisons between pervaporation and distillation are not available.

Pervaporation is less capital and energy-intensive than distillation or adsorption processes for small plants treating less than 5000 L/h of feed solution. However, because of the modular nature of the process, the costs of pervaporation are not as sensitive to economies of scale as are the costs of distillation and adsorption processes. Distillation costs, however, scale at a rete proportional to 0.6 to 0.7 times the power consumption. Thus, distillation remains the most economical process for large plants.

More recently pervaporation has been applied to dehydration of other solvents, particularly isopropanol used as a cleaning solvent. Dehydration of other solvents, including glycols, acetone, and methylene chloride, has been considered. A final interesting application of dehydration membranes is to shift the equilibrium of chemical reactions. For example, esterification reactions are usually performed in batch reactors, and the degree of conversion is limited by buildup of water in the reactor. By continuously removing the water, the equilibrium reaction can be forced to the right. In principle, almost complete conversion can be achieved.

3.1.3.2 Separation of dissolved organics from water

A number of applications exist for pervaporation to remove or recover volatile organic compounds from water. If the aqueous stream is very dilute, pollution control is the principal economic driving force. However, if the stream contains more than 1 to 2 percent VOC, recovery for eventual reuse can enhance the process economics.

Several types of membrane have been used to separate VOCs from water. Usually the membranes are made from rubbery polymers such as silicone rubber, polybutadiene, natural rubber, and polyamide-polyether copolymers. Rubbery pervaporation membranes are remarkably effective at separating hydrophobic organic solutes from dilute aqueous solutions. The concentration of VOCs such as toluene or trichloroethylene (TCE) in the condensed permeate is typically more than 1000 times that in the feed solution.

3.1.3.3 Separation of organic mixtures

The third application area for pervaporation is the separation of organic/organic mixtures. The competitive technology is generally distillation, a well-established and familiar technology. However, a number of azeotropic and close-boiling organic mixtures cannot be efficiently separated by distillation; pervaporation can be used to separate these mixtures. It would be unusual for a pervaporation process to perform an entire organic/organic separation. Rather, pervaporation will be most efficient when combined with distillation in a hybrid process. The two main applications of pervaporation-distillation in hybrid processes are likely to be in breaking azeotrope and in removing a single-component, high-purity side stream from a multicomponent distillation separation.

The principal problem hindering the development of commercial systems for organic/organic separations is the lack of membranes and modules able to withstand long-term exposure to organic compounds at the elevated temperatures required for pervaporation.

The performance of the pervaporation process depends not only upon the physicochemical properties of the polymeric materials and the structure of membrane but also upon the operating conditions, e.g. temperature, downstream pressure and composition of mixture. The followings summarize the effects of various factors on the performance of the pervaporation process.

- *Physico-chemical properties*

The permeation of solvents through a non-porous membrane usually can be described in terms of sorption and molecular diffusion. The extent of sorption (also called swelling) as well as the sorption selectivity are therefore determined by chemical nature of polymer and that of the solvents.

- *Operating temperature*

The variation of permeation rate follows from the operating temperature can be correlated with the Arrhenius' equation.

$$Jp \;=\; Jo \exp(-Ep/RgT) \tag{3.4}$$

Where Jp is the permeation rate, Jo is the pre-exponential factor, Ep is the apparent activation energy of permeation, and Rg and T are the gas constant and temperature, respectively.

- *Feed composition*

A change in feed composition directly affects the sorption phenomena at the liquid-membrane interface. The sorption selectivity depends obviously on the power of interaction between components. The extent of swelling as well as the sorption selectivity depends on the structure of polymer network. The lower affinity to the membrane can penetrate into the swollen system, and contribute to better swelling.

- *Feed concentration*

According to Fick's law, the permeation is proportional to the activity gradient across the membrane. Since the feed concentration directly affects the membrane activity, the increased feed concentration increased the driving force and the permeation flux through the membrane.

- *Downstream pressure*

Pervaporation process controls downstream pressure by pumping the permeate from downstream interface in the vapor form to provide the driving force. The decreased vapor pressure in downstream compartment is equivalent to and increased driving force for component transportation.

The values of partial vapor pressure, which directly control the transport of solvents, result from a dynamic equilibrium between the transport flux of the permeates and the pumping rate.

3.1.4 Pervaporative Membrane Reactor

A pervaporative membrane reactor is one of the membrane reactors for yield-enhancement of equilibrium-limited reactions. The concept was firstly proposed by Jenning and Binnings in 1960. While a reaction takes place in liquid phase, a by-product (usually water) is removed through a polymeric membrane in the permeate stream. The downstream pressure is kept below the vapor pressure of permeating species. The downstream side is evacuated by a vacuum pump or at least using an inert purge gas as illustrated in Figure 3.4

Pervaporative membrane reactors are expected to provide a promising alternative due to the following considerations: (1) pervaporation is a rate-controlled separation process, and the separation efficiency is not limited by relative volatility as in distillation, (2) in pervaporation only a fraction of feed that is permeated by membrane undergoes the liquid-to vapor-phase change, and thus energy consumption is generally low as compared to distillation, (3) with an appropriate membrane, pervaporation can be operated at a temperature that matches the optimal temperature for reaction.

The most common reaction system studied for the application of pervaporative membrane reactor is an esterification reaction between an alcohol and an acid in the presence of a highly acidic catalyst:

$$R_1COOH + R_2OH \longleftrightarrow R_1COOR_2 + H_2O \qquad (3.5)$$

The esterification represents an important class of chemical reactions. As esterification is equilibrium reaction (3.5), high yields can be obtained by adding an excess of one reactant or by constant removal of the produced water from the reaction mixture in order to shift the reaction to the product side.

Application of pervaporation processes to selectively separate water from the reacting mixture forms an interesting alternative to conventional distillation, especially in the case of azeotrope formation and low boiling reactants.
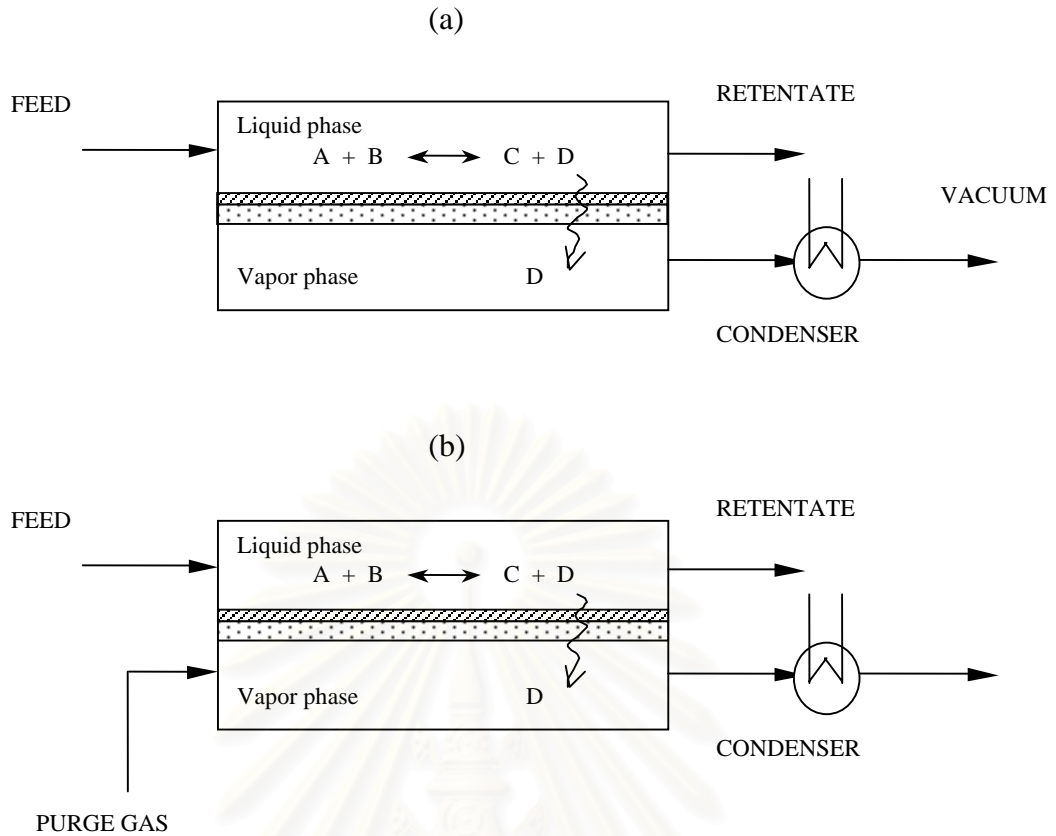
(a)

(b)

Figure 3.4 Schematic of a typical pervaporative membrane reactor (a) using vacuum pump, (b) using purge gas
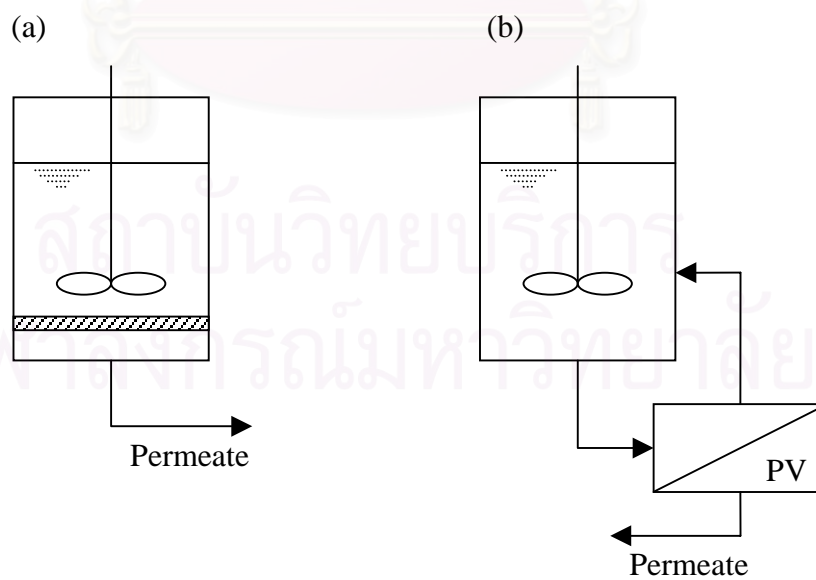

Figure 3.5 Configuration of a pervaporation reactor with an internal pervaporation unit (a) and with an external pervaporation unit (b)

Both polymer and ceramic membranes are applied in pervaporation-based reactors, for which Figure 3.5 shows the two basic configurations. Table 3.1 shows some examples of membrane-assisted esterification reactions. In addition to these low molecular weight esters, pervaporation can also be used for the production of polycondensation esters (resins).

Table 3.1 Overview of pervaporation-assisted esterification

Reaction	Membrane material	Membrane type	Membrane Area (m^2)	Temp. (^oC)
methanol + acetic acid $\leftrightarrow$ acetate + water	Nafion	Tube	5×10^{-3}	25
ethanol + acetic acid $\leftrightarrow$ ethyl acetate + water	Polyvinyl alcohol	Flat cell	1.2	90
ethanol + acetic acid $\leftrightarrow$ ethyl acetate + water	Nafion 117	Flat cell	1.2	90
ethanol + oleic acid $\leftrightarrow$ oleic acid ethyl ester + water	Polyether imide	Flat cell	1.9	60
1-propanol + propionic acid $\leftrightarrow$ propionic acid propyl ester + water	Polyvinyl alcohol	Flat cell	2.0	50
1-propanol + propionic acid $\leftrightarrow$ propionic acid propyl ester + water	Polyvinyl alcohol	Flat cell	2.0	50
1-propanol + propionic acid $\leftrightarrow$ propionic acid propyl ester + water	PSSH-polyvinyl alcohol	Flat cell	2.0	50
2-propanol + propionic acid $\leftrightarrow$ propionic acid propyl ester + water	Polyvinyl alcohol	Flat cell	2.0	55
1-butanol + acetic acid $\leftrightarrow$ butyl acetate + water	Polyvinyl acetate	Channel reactor	-	155
1-butanol + acetic acid $\leftrightarrow$ butyl acetate + water	Nafion	Tube	5.0	25

The influence of four different operating parameters on the conversion are evaluated, which can be divided into three group:

- Factors, which influence directly the esterification reaction (the catalyst concentration and initial molar ratio),

- Factors, which influence the pervaporation kinetics directly (the ratio of membrane area to reactor volume),

- Factors, which influence simultaneously the esterification as well as the pervaporation kinetics (the temperature).

For a rapid conversion of lab-scale results into an economically viable reaction-pervaporation system, an optimum value can be determined for each parameter. Based on experimental results as well as a model describing the kinetics of the system, it has been found that the temperature has the strongest influence on the performance of the system as it affects both the kinetics of esterification and of pervaporation. The rate of reaction increases with temperature according to Arrhenius law, whereas an increased temperature accelerates the pervaporation also. Consequently, the water content fluctuates much faster at a higher temperature. The second important parameter is the initial molar ratio. It has to be noted that a deviation in the initial molar ratio from the stoichiometric value requires a rather expensive separation step to recovery the unreacted component afterwards. The third factor is the ratio of membrane area to reaction volume, at least in the case of a batch reactor. For continuous operation, the flowrate should be considered as the determining factor for the contact time of the mixture with the membrane and subsequently the permeation flux. The catalyst concentration exhibits the weakest influence on the pervaporation-esterification system. The reaction rate increases linearly with the catalyst concentration.

3.2 Optimization

Optimization is the use of specific methods to determine the most effective and efficient solution to a problem or design for a process. This technique is one of the major quantitative tools in industrial decision making. A wide variety of problem in the design, construction, operation, and analysis of chemical plants (as well as many other industrial processes) can be resolved by optimization (Edgar et al., 2001).

3.2.1 The Essential Features of Optimization Problems

The essential elements of the optimization problems are:

1. Objective function,
2. Decision variable,
3. Constraint.

The objective function is a mathematical function that, for the best values of the decision variables, reaches a minimum (or maximum). Thus, the objective function is the measure of value or goodness for the optimization problem. There may be more than one objective function for a given optimization problem. There are different types of objective function depending on the needs and uses. The typical objective functions for reactors stated in terms of the adjustable variables are:

- Maximize conversion (yield) per volume with respect to time,

- Maximize production per batch,

- Minimize production time for a fixed yield,

- Minimize total production costs per average production costs with respect to time per fraction conversion,

- Maximize yield per number of moles of component per concentration with respect to time or operating conditions,

- Design the optimal temperature sequence with respect to time per reactor length to obtain (a) a given fraction conversion, (b) a maximum rate of reaction, or (c) the minimum residence time,

- Adjust the temperature profile to specification with respect to the independent variables,

- Minimize volume of the reactor(s) with respect to certain concentration(s),

- Change the temperature from T_o to T_f in minimum time subject to heat transfer rate constraints,

- Maximize profit with respect to volume,

- Maximize profit with respect to fraction conversion to get optimal recycle,

- Optimize profit per volume per yield with respect to boundary per initial conditions in time,

- Minimize consumption of energy with respect to operating conditions.

The decision variables are those independent variables over which the engineer has some control. These can be continuous variables such as temperature or discrete (integer) variables such as number of stages in a column.

Constraints are values that indicate the ability and limit of the feasible path of the process. Constraints can be classified into two types as follow:

1. Equality constraints are constraints that indicate the limits of the process or its product such as the purity of the products, mass and energy balance.

2. Inequality constraints are constraints that indicate the limit due to design and other limits

Constraints in optimization arise because a process must describe the physical bounds on the variables, empirical relations, and physical laws that apply to a specific problem. Examples of equality and inequality constraints follow:

- Production limitations,

- Raw material limitations (e.g., limitation of feedstock supplies),

- Safety or operability restrictions (e.g., temperature, pressure),

- Environmental limitations (e.g., production of toxic material),

- Physical property specifications on products.

The optimization models represent problem choices as decision variables and seek values that maximize or minimize objective functions of the decision variables subject to constraints on variable values expressing the limits on possible decision choices. The optimization model description is stated as:

	$f(\mathbf{x})$	objective function	
Subject to:	$\mathbf{h(x)} = \mathbf{0}$	equality constraints	(3.6)
	$\mathbf{g(x)} \geq \mathbf{0}$	inequality constraints	

where $\mathbf{x}$ is a vector of n decision variables ($x_1, x_2, \ldots, x_n$),

         $\mathbf{h(x)}$ is a vector of equations of dimension m_1,

         $\mathbf{g(x)}$ is a vector of inequalities of dimension m_2.

An efficient and accurate solution to this problem is not only dependent on the size of the problem in terms of the number of constraints and decision variables but also on characteristics of the objective function and constraints.

From equation (3.6), it is unconstrained problem if there are no constraint functions and no bounds on the x_i. Linear Programming (LP) refer to problems in which both the objective function and the constraints are linear. More difficult to solve is the Nonlinear Programming (NLP) problem in which the objective functions and constraints may be nonlinear functions of the decision variables.

3.2.2 Successive Quadratic Programming (SQP)

SQP methods represent state-of-the-art in nonlinear programming methods. Schittowski (1985), for example, has implemented and tested a version that out performs every other tested method in terms of efficiency, accuracy, and percentage of successful solutions. At each major iteration, an approximation is made of the Hessian of the Lagrangian function using a quasi-Newton updating method. This is then used to generate a QP subproblem whose solution is used to form a search direction for a line search procedure (Grace, 1999).

Given the problem description in equation (3.6) the principal idea is the formulation of a QP subproblem based on a quadratic approximation of the Lagrangian function.

$$L(x, \lambda) = f(x) + \sum_{i=1}^{m} \lambda_i \cdot g_i(x) \tag{3.7}$$

Here equation (3.6) is simplified by assuming that bound constraints have been expressed as inequality constraints. The QP subproblem is obtained by linearizing the nonlinear constraints.

3.2.2.1 Quadratic Programming (QP) Subproblem

$$\text{minimize} \ \ \frac{1}{2}d^T H_k d + \nabla f(x_k)^T d$$

$$\nabla g_i(x_k)^T d + g_i(x_k) = 0 \qquad i = 1, \dots m_e \qquad (3.8)$$

$$\nabla g_i(x_k)^T d + g_i(x_k) \leq 0 \qquad i = m_e + 1, \dots m$$

This subproblem can be solved using any QP algorithm. The solution is used to form a new iterate

$$x_{k+1} = x_k + \alpha_k d_k$$

The step length parameter α_k is determined by an appropriate line search procedure so that a sufficient decrease in a merit function is obtained. The matrix H_k is a positive definite approximation of the Hessian matrix of the Lagrangian function. H_k can be updated by any of the quasi-Newton methods.

A nonlinearly constrained problem can often be solved in fewer iterations than an unconstrained problem using SQP. One of the reasons for this is that, because of limits on the feasible area, the optimizer can make well-informed decisions regarding directions of search and step length.

3.2.2.2 SQP Implementation

The MATLAB SQP implementation consists of three main stages, which are discussed briefly in the following subsections:

- Updating of the Hessian matrix of the Lagrangian function,
- Quadratic programming problem solution,
- Line search and merit function calculation.

Updating the Hessian Matrix

At each major iteration a positive definite quasi-Newton approximation of the Hessian of the Lagrangian function, H, is calculated using the BFGS (Broyden, Flectcher, Goldfarb, and Shanno) method where $\lambda_i (i = 1,...,m)$ is an estimate of the Lagrange multipliers.

$$H_{k+1} = H_k + \frac{q_k q_k^T}{q_k^T s_k} - \frac{H_k^T H_k}{s_k^T H_k s_k}$$

where

$$s_k = x_{k+1} - x_k \qquad\qquad (3.9)$$

$$q_k = \nabla f(x_{k+1}) + \sum_{i=1}^{n} \lambda_i \cdot \nabla g_i(x_{k+1}) - \left(\nabla f(x_k) + \sum_{i=1}^{n} \lambda_i \cdot \nabla g_i(x_k) \right)$$

A positive definite Hessian is maintained providing $q_k^T s_k$ is positive at each update and that H is initialized with a positive definite matrix. When $q_k^T s_k$ is not positive, q_k is modified on an element by element basis so that $q_k^T s_k > 0$. The general aim of this modification is to distort the elements of q_k, which contribute to a positive definite update, as little as possible. Therefore, in the initial phase of the modification, the most negative element of $q_k^T s_k$ is repeatedly halved. This procedure is continued until $q_k^T s_k$ is greater than or equal to 10^{-5}. If after this procedure, $q_k^T s_k$ is still not positive, q_k is modified by adding a vector v multiplied by a constant scalar w, that is,

$$q_k = q_k + wv \qquad\qquad (3.10)$$

where

$$v_i = \nabla g_i(x_{k+1}) \cdot g_i(x_{k+1}) - \nabla g_i(x_k) \cdot g_i(x_k)$$

if

$$(q_k)_i \cdot w < 0$$

and

$$(q_k)_i \cdot (s_k)_i < 0 \qquad\qquad (i = 1,...m)$$

otherwise

$$v_i = 0$$

and w is systematically increased until $q_k^T s_k$ becomes positive.

Quadratic Programming Solution

At each major iteration of the SQP method a QP problem is solved of the form where A_i refers to the ith row of the m x n matrix A.

$$\text{minimize} \quad q(d) = \frac{1}{2} d^T H d + c^T d$$

$$A_i d = b_i \qquad\qquad i = 1, ..., m_e \qquad\qquad (3.11)$$

$$A_i d \leq b_i \qquad\qquad i = m_e + 1, ..., m$$

The solution procedure involves two phases: the first phase involves the calculation of a feasible point, the second phase involves the generation of a iterative sequence of feasible points that converge to the solution. In this method an active set is maintained, $\overline{A}_k$, which is an estimate of the active constraints (i.e., which are on the constraint boundaries) at the solution point.

$\overline{A}_k$ is updated at each iteration, k, and this is used to form a basis for a search direction $\hat{d}_k$. Equality constraints always remain in the active set, $\overline{A}_k$. The notation for the variable, $\hat{d}_k$, is used here to distinguish it from d_k in the major iterations of the SQP method. The search direction $\hat{d}_k$, is calculated and minimizes the objective function while remaining on any active constraint boundaries. The feasible subspace for $\hat{d}_k$ is formed from a basis, Z_k whose columns are orthogonal to the estimate of the active set $\overline{A}_k$ (i.e., $\overline{A}_k Z_k = 0$). Thus a search direction, which is formed from a linear summation of any combination of the columns of Z_k, is guaranteed to remain on the boundaries of the active constraints.

Line Search and Merit Function

The solution to the QP subproblem produces a vector d_k, which is used to form a new iterate

$$x_{k+1} = x_k + \alpha d_k \qquad\qquad (3.12)$$

The step length parameter α_k is determined in order to produce a sufficient decrease in a merit function. The merit function used by Han (1977) and Powell (1978) of the form below has been used in this implementation.

$$\Psi(x) = f(x) + \sum_{i=1}^{m_e} r_i \cdot g_i(x) + \sum_{i=m_e+1}^{m} r_i \cdot \max\{0, g_i(x)\} \qquad (3.13)$$

3.3 Generic Model Control (GMC)

Lee and Sullivan (1988) have generalized many of the model-based techniques into a generic structure called the generic model control, which allows the incorporation of nonlinear process models directly in the control algorithm. Consider a process described by:

$$\dot{x} = f(x,u,t) \qquad (3.14)$$
$$y = g(x) \qquad (3.15)$$

where $\dot{x}$ is a state variable,

       u is the manipulated input variable,

       y is the output of the process model.

In general, f and g are nonlinear functions. From equations (3.14) and (3.15), $\dot{y}$ can be written as

$$\dot{y} = G_x f(x,u,t)$$

where

$$G_x = \frac{\partial g}{\partial x} \qquad (3.16)$$

In a classical optimal control, the trajectory of y is usually compared against a nominal trajectory, $y^*(t)$, as a measure of system performance. As an alternative, consider the performance of the system to be such that:

$$(\dot{y})^*(t) = r^*(y) \qquad (3.17)$$

where r^* represents some arbitrary function to be specified.

When the process is away from its desired steady state y^*, the rate of change of y, y^*, is selected to be such that the process moves towards steady state, i.e.

$$\dot{y} = K_1(t)(y^* - y) \tag{3.18}$$

where $K_1(t)$ is some diagonal matrix.

The process is selected to have zero offset, i.e.

$$\dot{y} = K_2(t)\int(y^* - y)dt \tag{3.19}$$

where $K_2(t)$ is some diagonal matrix.

$K_1(t)$ and $K_2(t)$ are constant with respect to time. Good control performance will be given by some combination of these objectives, i.e.

$$(\dot{y})^* = K_1(y^* - y) + K_2\int(y^* - y)dt \tag{3.20}$$

It can be seen that by different choices of K_1 and K_2 the performance specification can be altered for each variable separately. One can use these values to select any "reasonable" desired response for the system. "Reasonable" implies that the parameters are chosen in relation to the system's natural dynamic response. How well the system matches this performance index is governed by how closely the chosen model matches the plant behavior.

Taking Laplace transform of the equation (3.20), transfer function of this equation becomes:

$$\frac{y}{y^*} = \frac{2\tau\xi s + 1}{\tau^2 s^2 + 2\tau\xi s + 1} \tag{3.21}$$

where

$$\tau = \frac{1}{\sqrt{K_2}} \quad \text{and} \quad \xi = \frac{K_1}{2\sqrt{K_2}}$$

This system does not yield the same response as a classical second-order system (Stephanopoulos, 1984). However, similar plots to the classical second-order response showing the normalized response of the system y/y^* vs. normalized time t/τ with ξ as a parameter can be produced and is shown in Figure 3.6. The design procedure can be specified as follows:

1.Choose ξ from Fig. 3.6 to give desired shape of response,

2.Choose τ from Fig. 3.6 to give "appropriate" timing of response in relation to known or estimated plant speed of response,

3.Calculate K_1 and K_2 using the following equations:

$$K_1 = \frac{2\xi}{\tau} \tag{3.22}$$

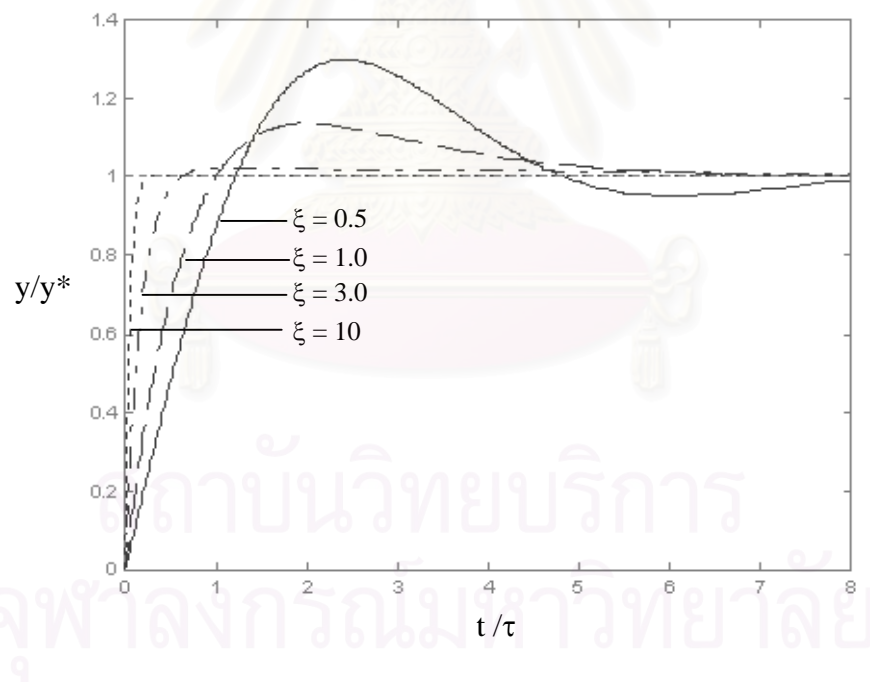$$K_2 = \frac{1}{\tau^2} \tag{3.23}$$

Figure 3.6 Generalized GMC profile specification

GMC has several advantages that make it a good framework for developing reactor controllers:

1. The process model appears directly in the control algorithm.

2. The process model does not need to be linearized before use, allowing for the inherent nonlinearity of exothermic batch reactor operation to be taken into account.

3. By design, GMC provides feedback control of the rate of change of the controlled variable. This suggests that the rate of temperature change, which as mentioned above is very important in heat-up operations, can be used directly as a control variable.

4. The relationship between feedforward and feedback control is explicitly stated in the GMC algorithm.

5. Finally and importantly, the GMC framework permits for developing a control algorithm that can be used for both heat-up and temperature maintenance and therefore eliminates the need for a switching criterion between different algorithms; this should result in a much more robust control strategy.

3.4 Kalman Filter

The Kalman filter is a set of mathematical equations that provides an efficient computational (recursive) solution of the least-squares method. The filter is very powerful in several aspects: it supports estimations of past, present, and even future states, and it can do so even when the precise nature of the model system is unknown.

3.4.1 The discrete Kalman filter

The Kalman filter addresses the general problem of trying to estimate the state $x \in \Re^n$ of a discrete-time controlled process that is governed by the linear stochastic difference equation

$$x_k = Ax_{k-1} + Bu_k + w_{k-1} \tag{3.24}$$

with a measurement $z \in \Re^m$ that is

$$z_k \;=\; Hx_k \;+\; v_k \tag{3.25}$$

The random variables w_k and v_k represent the process and measurement noise (respectively) and assume to be independent (of each other), white, and with normal probability distributions

$$p(w) \;\sim\; N(0,Q) \tag{3.26}$$
$$p(v) \;\sim\; N(0,R) \tag{3.27}$$

In practice, the process noise covariance Q and measurement noise covariance R matrices might change with each time step or measurement, however here they are assumed to be constant.

The n x n matrix A in the difference equation (3.24) relates the state at the previous time step k-1 to the state at the current step k, in the absence of either a driving function or process noise. Note that in practice A might change with each time step, but here it is assumed to be constant. The n x l matrix B relates the optional control input $u \in \Re^l$ to the state x. The m x n matrix H in the measurement equation (3.25) relates the state to the measurement z_k. In practice H might change with each time step or measurement, but here it is assumed to be constant.

3.4.1.1 The computational origins of the filter

Define $\hat{x}_k^- \in \Re^n$ to be *a priori* state estimate at step k given knowledge of the process prior to step k, and $\hat{x}_k \in \Re^n$ to be *a posteriori* state estimate at step k given measurement z_k. *A priori* and *a posteriori* estimate errors can be defined as

$$e_k^- \equiv x_k - \hat{x}_k^-$$

and
$$e_k \equiv x_k - \hat{x}_k$$

The *a priori* estimate error covariance is then

$$P_k^- = E[e_k^- e_k^{-T}] \tag{3.28}$$

and the *a posteriori* estimate error covariance is

$$P_k = E[e_k e_k^T] \tag{3.29}$$

An *a posteriori* state estimate $\hat{x}_k$ is computed as a linear combination of an *a priori* estimate $\hat{x}_k^-$ and a weighted difference between an actual measurement z_k and a measurement prediction $H\hat{x}_k^-$ as shown below in equation (3.30). Some justification for equation (3.30) is given in "The Probabilistic Origins of the Filter" found below.

$$\hat{x}_k = \hat{x}_k^- + K(z_k - H\hat{x}_k^-) \tag{3.30}$$

The difference $(z_k - H\hat{x}_k^-)$ in equation (3.30) is called the measurement *innovation*, or the *residual*. The residual reflects the discrepancy between the predicted measurement $H\hat{x}_k^-$ and the actual measurement z_k. A residual of zero means that the two are in complete agreement.

The *n* x *m* matrix *K* in equation (3.30) is chosen to be the *gain* or *blending factor* that minimizes the *a posteriori* error covariance equation (3.29). This minimization can be accomplished by first substituting equation (3.30) into the above definition for e_k, substituting that into equation (3.29), performing the indicated expectations, taking the derivative of the trace of the result with respect to *K*, setting that result equal to zero, and then solving for *K*. One form of the resulting *K* that minimizes equation (3.29) is given by:

$$\begin{aligned} K_k &= P_k^- H^T (H P_k^- H^T + R)^{-1} \\ &= \frac{P_k^- H^T}{H P_k^- H^T + R} \end{aligned} \tag{3.31}$$

From equation (3.31) as the measurement error covariance *R* approaches zero, the gain K weights the residual more heavily.

$$\lim_{R_k \to 0} K_k = H^{-1}$$

Another way of thinking about the weighting by *K* is that as the measurement error covariance *R* approaches zero, the actual measurement z_k is trusted more and more, while the predicted measurement $H\hat{x}_k^-$ is trusted less and less. On the other hand, as

the a priori estimate error covariance P_k^- approaches zero the actual measurement z_k is trusted less and less, while the predicted measurement $H\hat{x}_k^-$ is trusted more and more.

3.4.1.2 The discrete Kalman filter algorithm

The Kalman filter estimates a process by using a form of feedback control: the filter estimates the process state at some time and then obtains feedback in the form of (noisy) measurements. As such, the equations for the Kalman filter fall into two groups: *time update* equations and *measurement update* equations. The time update equations are responsible for projecting forward (in time) the current state and error covariance estimates to obtain the *a priori* estimates for the next time step. The measurement update equations are responsible for the feedback–i.e. for incorporating a new measurement into the *a priori* estimate to obtain an improved *a posteriori* estimate.

The specific equations for the time and measurement updates are presented below:

Time Update ("Predict") equations:

- Project the state ahead

$$\hat{x}_k^- = A\hat{x}_{k-1} + Bu_k$$

- Project the error covariance ahead

$$P_k^- = AP_{k-1}A^T + Q$$

Measurement Update ("Correct") equations:

- Compute the Kalman gain

$$K_k = P_k^- H^T (HP_k^- H^T + R)^{-1}$$

- Update estimate with measurement z_k

$$\hat{x}_k = \hat{x}_k^- + K_k(z_k - H\hat{x}_k^-)$$

- Update the error covariance

$$P_k = (I - K_k H)P_k^-$$

The time update equations can also be thought of as predictor equations, while the measurement update equations can be thought of as corrector equations. Indeed the final estimation algorithm resembles that of a predictor-corrector algorithm for solving numerical problems as shown in Figure 3.7
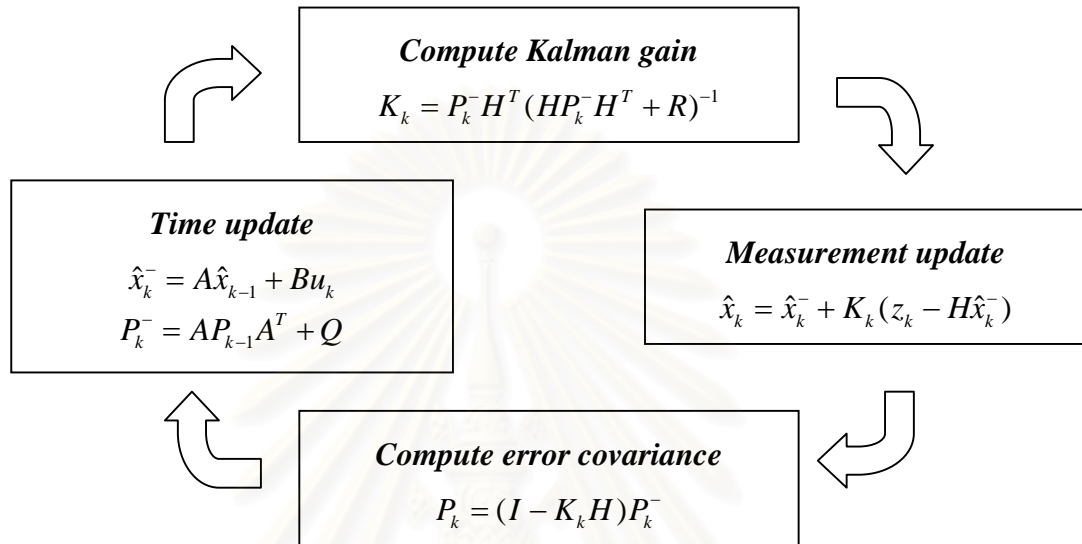
Compute Kalman gain

$$K_k = P_k^- H^T (HP_k^- H^T + R)^{-1}$$

Time update

$$\hat{x}_k^- = A\hat{x}_{k-1} + Bu_k$$

$$P_k^- = AP_{k-1}A^T + Q$$

Measurement update

$$\hat{x}_k = \hat{x}_k^- + K_k(z_k - H\hat{x}_k^-)$$

Compute error covariance

$$P_k = (I - K_k H)P_k^-$$

Figure 3.7 The discrete Kalman filter loop

3.4.1.3 Filter parameters and tuning

In the actual implementation of the filter, the measurement noise covariance R is usually measured prior to operation of the filter. Measuring the measurement error covariance R is generally practical and is supposed to be able to measure the process anyway (while operating the filter).

The determination of the process noise covariance Q is generally more difficult because it does not have the ability to directly observe the estimating process. Sometimes a relatively simple (poor) process model can produce acceptable results if one injects enough uncertainty into the process via the selection of Q. Certainly in this case one would hope that the process measurements are reliable.

The tuning of the parameters Q and R is usually performed off-line, frequently with the help of another (distinct) Kalman filter in a process generally referred to as system identification. Under conditions where Q and R are in fact constant, both the estimation error covariance P_k and the Kalman gain K_k will stabilize quickly and then

remain constant. If this is the case, these parameters can be pre-computed by either running the filter off-line or for example by determining the steady-state value of P_k.

3.4.2 The extended Kalman filter (EKF)

As described above, the Kalman filter addresses the general problem of trying to estimate the state $x \in \Re^n$ of a discrete-time controlled process that is governed by the linear stochastic different equation. Some of the most interesting and successful applications of Kalman filtering have been such the process to be estimated and (or) the measurement relationship to the process is nonlinear. A Kalman filter that linearizes about the current mean and covariance is referred to as an extended Kalman filter or EKF.

Assuming the process has a state vector $x \in \Re^n$, but the process is now governed by the nonlinear stochastic difference equation

$$x_k = f(x_{k-1}, U_k, w_{k-1}) \tag{3.32}$$

With a measurement $z \in \Re^m$ that is

$$z_k = h(x_k, v_k) \tag{3.33}$$

where the random variables w_k and v_k represent the process and measurement noise. In this case the nonlinear function f in the difference equation (3.32) relates the state at the previous time step k-1 to the state at the current time step k. It includes as parameters any driving function u_k and the zero-mean process noise w_k. The nonlinear function h in the measurement equation (3.33) relates the state x_k to the measurement z_k.

In practice of course one does not know the in individual values of the noise w_k and v_k at each time step. However, one can approximate the state and measurement vector as:

$$\tilde{x}_k = f(\widehat{x}_{k-1}, u_k, 0) \tag{3.34}$$

and
$$\tilde{z}_k = h(\tilde{x}_k, 0) \tag{3.35}$$

where $\tilde{x}_k$ is some *a posteriori* estimate of the state (from a previous time step k).

To estimate a process with nonlinear difference and measurement relationships, begin by writing new governing equations that linearize and estimate equation (3.34) and (3.35),

$$x_k \approx \tilde{x}_k + A(x_{k-1} - \hat{x}_{k-1}) + Ww_{k-1} \qquad (3.36)$$

$$z_k \approx \tilde{z}_k + H(x_k - \tilde{x}_k) + Vv_k \qquad (3.37)$$

where x_k and z_k are the actual state and measurement vectors,

$\tilde{x}_k$ and $\tilde{z}_k$ are the approximate state and measurement vectors from equation (3.34) and (3.35),

$\hat{x}_k$ is an *a posteriori* estimate of the state at step k,

A is the Jacobian matrix of partial derivatives of f with respect to x,

$$A_{[i,j]} = \frac{\partial f_{[i]}}{\partial x_{[j]}}(\hat{x}_{k-1}, u_k, 0)$$

W is the Jacobian matrix of partial derivatives of f with respect to w,

$$W_{[i,j]} = \frac{\partial f_{[i]}}{\partial w_{[j]}}(\hat{x}_{k-1}, u_k, 0)$$

H is the Jacobian matrix of partial derivatives of h with respect to x,

$$H_{[i,j]} = \frac{\partial h_{[i]}}{\partial x_{[j]}}(\tilde{x}_k, 0)$$

V is the Jacobian matrix of partial derivatives of h with respect to v,

$$V_{[i,j]} = \frac{\partial h_{[i]}}{\partial v_{[j]}}(\tilde{x}_k, 0)$$

Define a new notation for the prediction error

$$\tilde{e}_{x_k} \equiv x_k - \tilde{x}_k \qquad (3.38)$$

and the measurement residual

$$\tilde{e}_{z_k} \equiv z_k - \tilde{z}_k \qquad (3.39)$$

Using equation (3.38) and (3.39) an error process can be written as:

$$\tilde{e}_{x_k} \approx A(x_{k-1} - \hat{x}_{k-1}) + \varepsilon_k \tag{3.40}$$

$$\tilde{e}_{z_k} \approx H\tilde{e}_{x_k} + \eta_k \tag{3.41}$$

where ε_k and η_k represent new independent random variables having zero mean and covariance matrices WQW^T and VRV^T.

The *a posteriori* state estimates for the original nonlinear process can be obtained by:

$$\hat{x}_k = \tilde{x}_k + \hat{e}_k \tag{3.42}$$

The random variables of equation (3.40) and (3.41) have approximately the following probability distributions:

$$p(\tilde{e}_{x_k}) \sim N(0, E[\tilde{e}_{x_k}\tilde{e}_{x_k}^T])$$

$$p(\varepsilon_k) \sim N(0, WQ_kW^T)$$

$$p(\eta_k) \sim N(0, VR_kV^T)$$

Given these approximations and letting the predicted value of $\hat{e}_k$ be zero, the Kalman filter equation used to estimate $\hat{e}_k$ is

$$\hat{e}_k = K_k\tilde{e}_{z_k} \tag{3.43}$$

Substituting (3.43) back into (3.42) and making use of (3.39) gives:

$$\hat{x}_k = \tilde{x}_k + K_k\tilde{e}_{z_k}$$
$$= \tilde{x}_k + K_k(z_k - \tilde{z}_k) \tag{3.44}$$

The specific equations for the time and measurement updates are presented below:

Time Update ("Predict") equations:

- Project the state ahead

$$\hat{x}_k^- = f(\hat{x}_{k-1}, u_k, 0)$$

- Project the error covariance ahead

$$P_k^- = A_k P_{k-1} A_k^T + W_k Q_{k-1} W_k^T$$

Measurement Update ("Correct") equations:

- Compute the Kalman gain

$$K_k = P_k^- H_k^T (H_k P_k^- H_k^T + V_k R_k V_k^T)^{-1}$$

- Update estimate with measurement z_k

$$\hat{x}_k = \hat{x}_k^- + K_k(z_k - h(\hat{x}_k^-, 0))$$

- Update the error covariance

$$P_k = (I - K_k H_k)P_k^-$$

Compute Kalman gain

$$K_k = P_k^- H_k^T (H_k P_k^- H_k^T + V_k R_k V_k^T)^{-1}$$

Time update

$$\hat{x}_k^- = f(\hat{x}_{k-1}, u_k, 0)$$
$$P_k^- = A_k P_{k-1} A_k^T + W_k Q_{k-1} W_k^T$$

Measurement update

$$\hat{x}_k = \hat{x}_k^- + K_k(z_k - h(\hat{x}_k^-, 0))$$

Compute error covariance

$$P_k = (I - K_k H_k)P_k^-$$
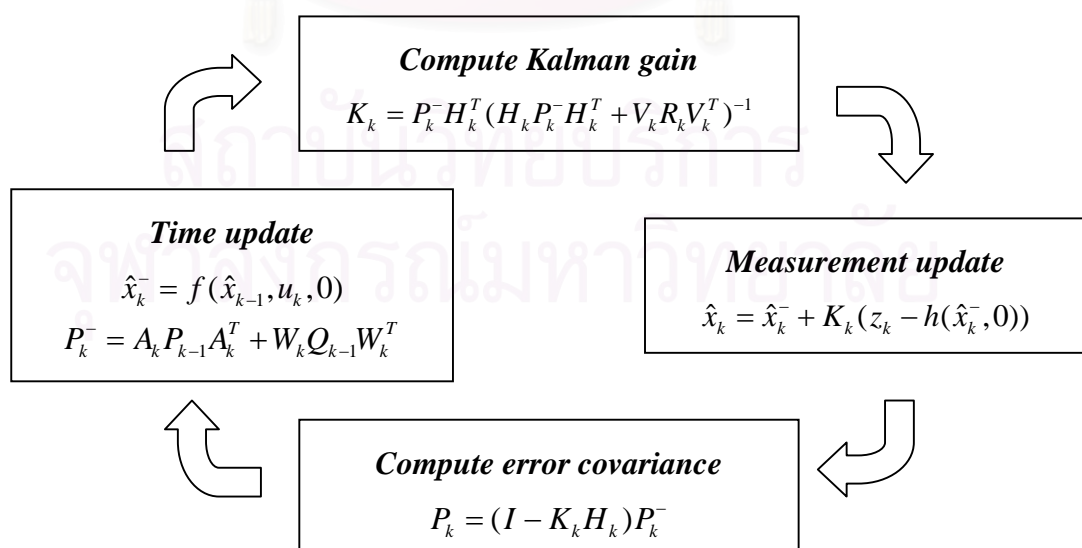
Figure 3.8 The extended Kalman filter loop

CHAPTER IV

PERVAPORATIVE MEMBRANE REACTOR

This chapter is divided into three sections: mathematical model of a pervaporative membrane reactor, optimization study, and control study. Simulation results obtained by simulating the optimization formulation and the formulation of a GMC controller are detailed in each section.

In this work, a batch reactor integrated with pervaporation developed by Liu et al. (2001) is considered. An ideal case where the membrane is perfectly permselective to water is investigated to show the maximum improvement in reactor performance achievable by the use of membrane pervaporation. The study is aimed at exothermic and reversible esterification reaction. A jacket is used to maintain the temperature of a pervaporative membrane reactor at a desired set point. The objectives of this work are: (1) to obtain optimum temperature that maximizes the final concentration of ester; (2) to track the optimum temperature obtained in (1) using GMC coupled with an extended Kalman filter.
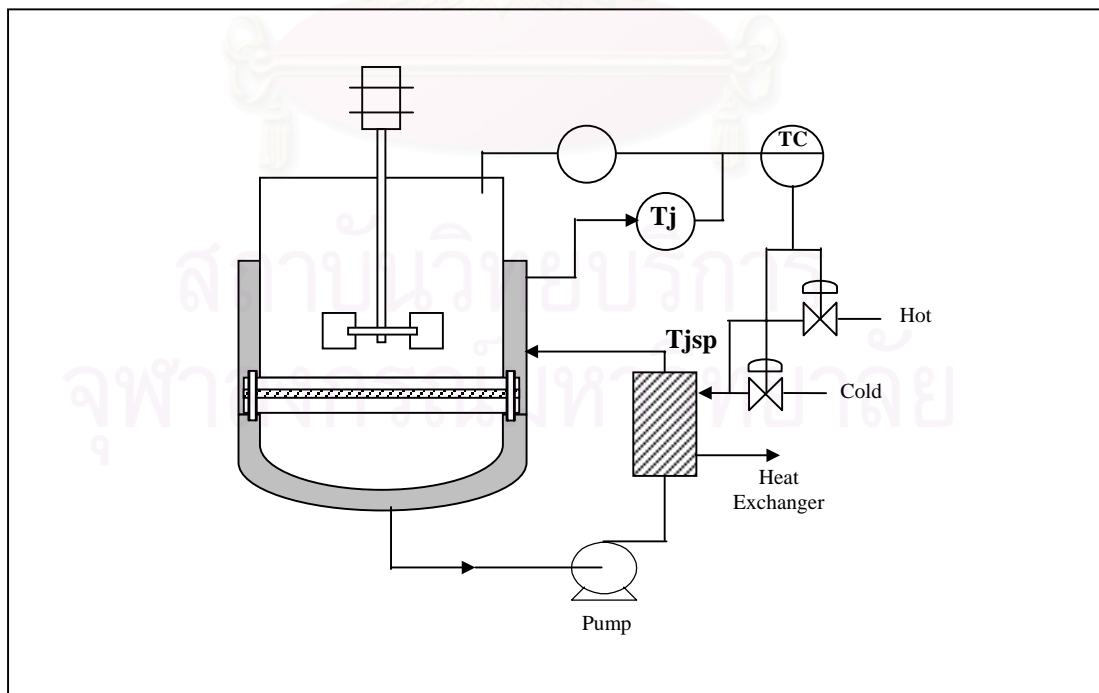
Figure 4.1 Membrane reactor schematic diagram

4.1 Mathematical Model

As shown in Fig. 4.1, an esterification of acetic acid and butanol studied by Liu et al. (2001) carried out in a batch reactor equipped with a pervaporation unit has been considered.

$$R_1COOH + R_2OH \longleftrightarrow R_1COOR_2 + H_2O \tag{4.1}$$

4.1.1 Material Balance

A pervaporation module consists of a hydrophilic membrane through which water permeates preferentially. Applying a material balance on any reactant or product species (Feng and Huang, 1996), the material balance of the pervaporative membrane reactor is given by:

$$\frac{d(C_iV)}{dt} = -r_iV - J_iS \tag{4.2}$$

where C_i is the concentration of component i (mol/l),

J_i is the permeation flux of component i (mol/m^2 hr),

V is the volume of reaction mixtures (liter),

S is the membrane area for permeation (cm^2),

r_i is the rate of disappearance of the species in the reactor due to chemical reaction; for product species, is the rate of formation and takes negative sign.

Since the stoichiometric coefficients for reactants and products are equal, the numerical values of reaction rate expressed with respect to any species i are equal. The reaction rate can be written by the following equation,

$$r = k_1C_AC_BC_{cat} - k_2C_EC_WC_{cat} \tag{4.3}$$

where C_A, C_B, C_E and C_W are concentration of alcohol, acid, ester and water, respectively (mol/l),

C_{cat} is the catalyst concentration (g/l),

k_1 and k_2 are rate constants for forward and reverse reactions, respectively.

According to the Arrhenius' equation, the rate of reaction depends on the temperature as shown in equation (4.4).

$$k = k_O \exp(-E/RT) \tag{4.4}$$

where k_0 is the pre-exponential factor,

E is the activation energy of reaction,

R is the gas constant,

T is the absolute temperature.

From Liu et al. (2001), the reaction rate constants for this reaction are described by the following equations.

$$k_1 = 4.531 \times 10^6 \exp\left(\frac{-6390}{T}\right) \tag{4.5}$$

$$k_2 = 4.376 \times 10^6 \exp\left(\frac{-7090}{T}\right) \tag{4.6}$$

From Feng and Huang (1996), the volume change of the reaction mixtures in the membrane reactor is given by:

$$\frac{dV}{dt} = -\sum_i \frac{J_i M_i}{\rho_i} S \tag{4.7}$$

where M_i is the molar mass of species i (g/mol),

ρ_i is the density of species i (g/l),

then equation (4.2)-(4.4) constitute the basic equations describing a batch-wise pervaporative membrane reactor. An ideal case where the membrane permeates only water is considered. Rewriting equation (4.7) gives

$$\frac{dV}{dt} = -\frac{J_w M_w}{\rho_w} S \tag{4.8}$$

The permeation flux through a pervaporation membrane is usually concentration dependent. To simplify the process model, it is assumed that the water flux is proportional to water concentration as seen in the following equation.

$$J_w = P_w C_w \tag{4.9}$$

where P_W is the permeability coefficient of water.

The relationship between the permeability coefficient and operating temperature can be expressed by Arrhenius' equation.

$$P = P_O \exp(-E_a / RT) \tag{4.10}$$

where P_0 is the pre-exponential factor,

E_a is the activation energy of permeation.

From Liu et al. (2001), a curve fitting method is employed to find the relationship between the permeability coefficient and the operating temperature as given in Appendix A, then

$$P_w = \exp\left(4.2934 - \frac{1039.24}{T}\right) \tag{4.11}$$

By substituting equation (4.8) into equation (4.2), the concentration of the components in the reaction can be determined:

$$C_i \frac{dV}{dt} + V \frac{dC_i}{dt} = -rV$$

$$-C_i \frac{J_w M_w}{\rho_w} S + V \frac{dC_i}{dt} = -rV$$

$$\frac{dC_i}{dt} = -r + C_i \frac{J_w M_w}{\rho_w} \frac{S}{V} \qquad (4.12)$$

where subscript i denotes A, B and E.

The concentration of water can be determined through the following equations:

$$C_W \frac{dV}{dt} + V \frac{dC_W}{dt} = -rV - J_w S$$

$$-C_W \frac{J_w M_w}{\rho_w} S + V \frac{dC_W}{dt} = -rV - J_w S$$

$$\frac{dC_W}{dt} = -r - \frac{S}{V} J_w + C_W \frac{J_w M_w}{\rho_w} \frac{S}{V} \qquad (4.13)$$

where the reaction rates of component E and W take negative sign.

4.1.2 Energy Balance

For temperature control of a batch reactor, a process model relating the reactor temperature, T_r, to the manipulated variable, the jacket temperature, T_j, is required. The energy balance around the reactor contents is given by the following equations:

$$Q_r = (-\Delta H) rV$$

$$\frac{dT_r}{dt} = \frac{Q_r + UA(T_j - T_r)}{M_r C_{pr}} \qquad (4.14)$$

$$M_r = (C_A + C_B + C_E + C_W) \cdot V \qquad (4.15)$$

and
$$C_{pr} = \frac{C_{pA} \cdot C_A + C_{pB} \cdot C_B + C_{pE} \cdot C_E + C_{pW} \cdot C_W}{C_A + C_B + C_E + C_W} \qquad (4.16)$$

where Q_r is the heat released by the reaction (J/hr),

U is the heat-transfer coefficient (J/m^2 hr K),

A is the heat transfer area (m^2),

ΔH is the heat of reaction (J/mol),

M_r is the mole of the reactor contents (mole),

C_{pr} is the molar heat capacity of the reactor contents (J/mol K).

The dynamic of the jacket is

$$\frac{dT_j}{dt} = \frac{q_j \rho_j C_{pj}(T_{jsp} - T_j) - UA(T_j - T_r)}{V_j \rho_j C_{pj}} \qquad (4.17)$$

It is reasonable to assume that the dynamics of the jacket temperature control are approximately first order (Liptak, 1986) with time constant τ_j and, hence, the $T_{jsp}(k)$, can be calculated by the following equation:

$$T_{jsp}(k) = T_j(k-1) + \frac{\tau_j}{\Delta t}\left(T_j(k) - T_j(k-1)\right) \qquad (4.18)$$

where $\tau_j = \frac{V_j}{q_j}$

q_j is the jacket flow rate (l/hr),

ρ_j is the jacket density (g/l),

V_j is the jacket volume (liter),

C_{pj} is the mass heat capacity of the jacket (J/g K).

All the parameters and constant values used in the model are given in Table 4.1

Table 4.1 The constant parameter values of the model

Variable	Value	Variable	Value
S	34 cm^2	C_{cat}	8.9 g/liter
V	150 ml	q_j	1 liter/hr
C_{pA}	124.265 J/mol K	V_j	50 ml
C_{pB}	177.025 J/mol K	U	50000 J/m^2 hr K
C_{pE}	255.5 J/mol K	A	45 cm^2
C_{pW}	75.4 J/mol K	ρ_w	1000 g/liter
C_{pj}	4.2 J/g K	ρ_j	1000 g/liter
M_W	18 g/mol	ΔH	-3.97x10^3 J/mol

Initial Conditions			
$C_{A,0}$	8.74 mol/l	$C_{E,0}$	0 mol/l
$C_{B,0}$	5.47 mol/l	$C_{W,0}$	0 mol/l
$T_{r,0}$	298 K	$T_{j,0}$	298 K

4.2 Optimization Study

The mathematical models of a pervaporative membrane reactor indicate that an operating temperature is one of key factors of the pervaporative membrane reactor, which influences both the reaction and pervaporation process through the reaction rates and membrane permeability. In order to operate the pervaporative membrane reactor efficiently, optimization framework is formulated to determine an optimal temperature of the esterification of acetic acid and butanol studied by Liu et al. (2001). An optimization goal is to determine an optimal operating temperature for the pervaporative membrane reactor to maximize a final concentration of ester with a fixed batch time.

In this work, a Matlab program is written to solve the optimization problem by using a successive quadratic programming (SQP) algorithm in Matlab Optimization Toolbox. The written program is tested to determine an optimal temperature of the exothermic batch reactor studied by Aziz et al. (2000) as detailed in Appendix E. The optimization results show that this program is effective and applicable to determine an optimal temperature of this work.

4.2.1 Optimization Formulation

The esterification of acetic acid and butanol studied by Liu et al. (2001) is considered. The reaction can be written as:

Acetic Acid (A) + Butanol (B) $\longleftrightarrow$ Butyl Acetate (E) + Water (W)
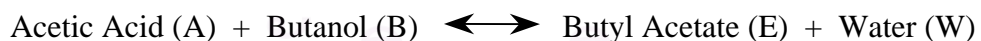
where butyl acetate is a desired product and water is permeated and removed from the reactor to shift the chemical equilibrium.

The objective function is to maximize the final concentration of butyl acetate at the specified final time. The objective function can be written as:

$$\max_{T} \quad C_E(t_f)$$

Subject to

$$\frac{dC_A}{dt} = -r + C_A \frac{J_W M_W}{\rho_W} \frac{S}{V}$$

$$\frac{dC_B}{dt} = -r + C_B \frac{J_W M_W}{\rho_W} \frac{S}{V}$$

$$\frac{dC_E}{dt} = r + C_E \frac{J_W M_W}{\rho_W} \frac{S}{V}$$

$$\frac{dC_W}{dt} = r - \frac{S}{V} J_W + C_W \frac{J_W M_W}{\rho_W} \frac{S}{V}$$

where

$$r = k_1 C_A C_B C_{cat} - k_2 C_E C_W C_{cat}$$

$$k_1 = 4.531 \times 10^6 \exp\left(\frac{-6390}{T}\right)$$

$$k_2 = 4.376 \times 10^6 \exp\left(\frac{-7090}{T}\right)$$

$$J_W = P_W C_W$$

$$P_W = \exp\left(4.2934 - \frac{1039.24}{T}\right)$$

and

$$298 \text{ K} \leq T \leq 363 \text{ K}$$

An initial state of $[C_A, C_B, C_E, C_W]$ used to solve an off-line optimization problem is given as

$$x(0) = [8.74, 5.47, 0, 0]^T$$

All parameters and constant values used in the model are given in Table 4.1. The batch time (t_f) is specified for 8 hour. The lower bound on the temperature is the initial temperature that operates at the ambient condition and the upper bound is dictated by the maximum temperature of the experimental data used by Liu et al. (2001) to build their models.

4.2.2 Optimization Results

An off-line optimal control is solved with fixed batch time to find the optimal temperature that maximizes the final concentration of butyl acetate. In this research, two runs of off-line optimal control are carried out:

Run 1: to determine an optimal temperature set point using one control interval (time),
Run 2: to determine an optimal temperature profile using four fixed control intervals.

As batch processes require different control strategies from those continuous processes do. This is due to the fact that they are operated dynamically. The purposes of this study are to compare the simulation results obtained by an optimal temperature set point and by an optimal temperature profile and to show the improvement of the final concentration of ester obtained by dynamic operation over steady state operation.

A Matlab program is written to simulate both a normal batch reactor without pervaporation and a pervaporative membrane reactor. The simulation results of both reactors are compared.

Case 1: a normal batch reactor without pervaporation,
Case 2: a pervaporative membrane reactor.

The optimization results are shown in Table 4.2 and Figure 4.2-4.3. Both optimal temperature set point and optimal temperature profile for the pervaporative membrane reactor obtained in this section are used as set point(s) in the control study of the pervaporative membrane reactor.

Table 4.2 The optimization results

Case	Condition	Off-line optimal temperature (K)				$C_E(t_f)^*$
		Switching time (hr)				
		0	2	4	6	
Batch Reactor	- Run 1	326.40	-	-	-	4.7976
	- Run 2	333.95	332.84	328.11	308.88	4.8169
Pervaporative Membrane Reactor	- Run 1	*363*	-	-	-	5.2560
	- Run 2	*363*	*363*	*363*	*340.83*	5.2669

$* C_E(t_f)$ is a final concentration of butyl acetate (mol/l)
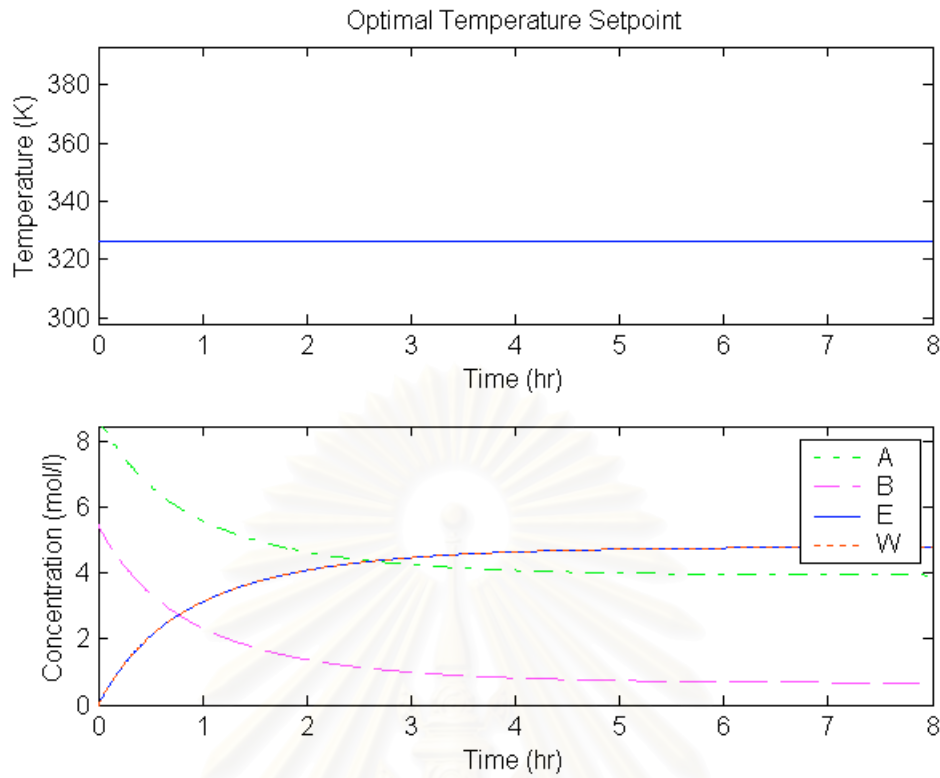
Figure 4.2 Optimal temperature set point and concentration profiles of a normal batch reactor
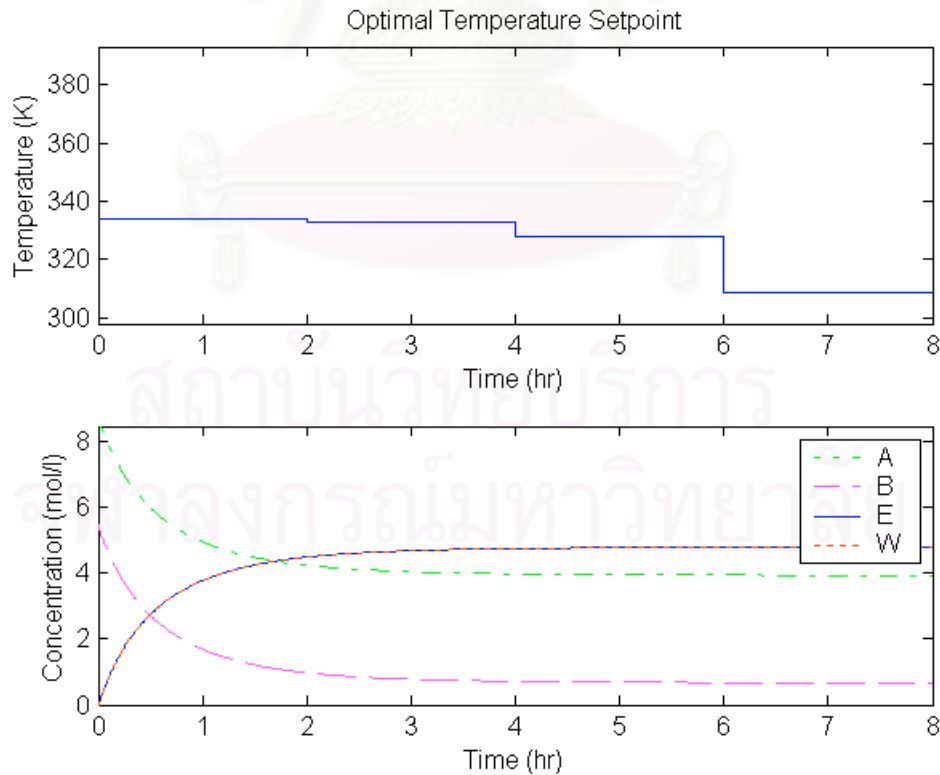
Figure 4.3 Optimal temperature profile and concentration profiles of a normal batch reactor
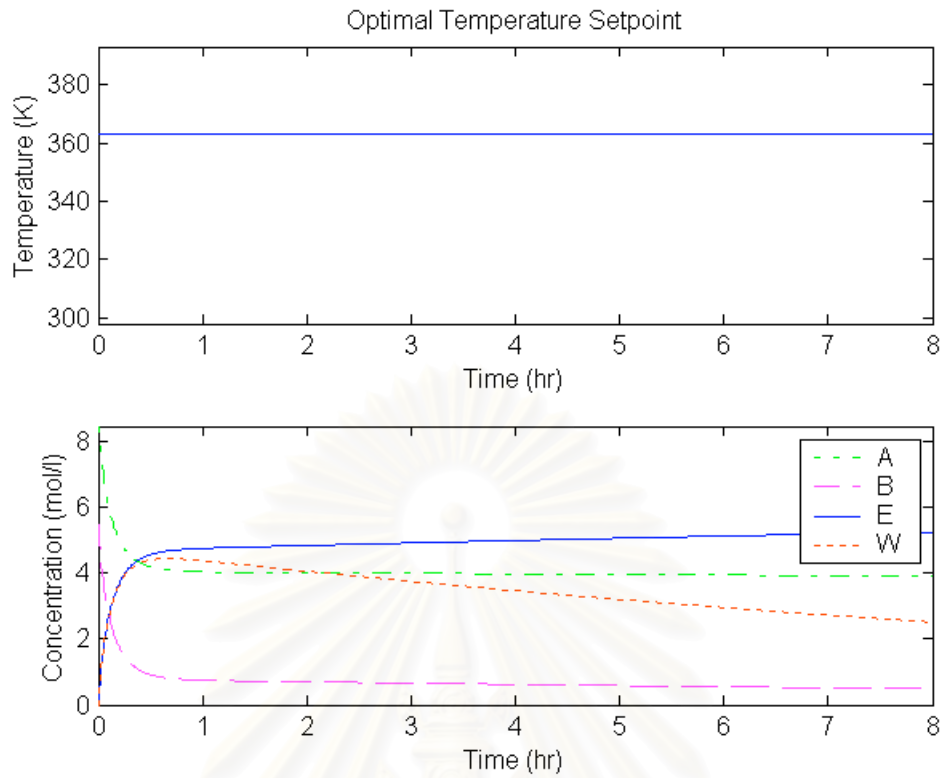
Figure 4.4 Optimal temperature set point and concentration profiles of a pervaporative membrane reactor
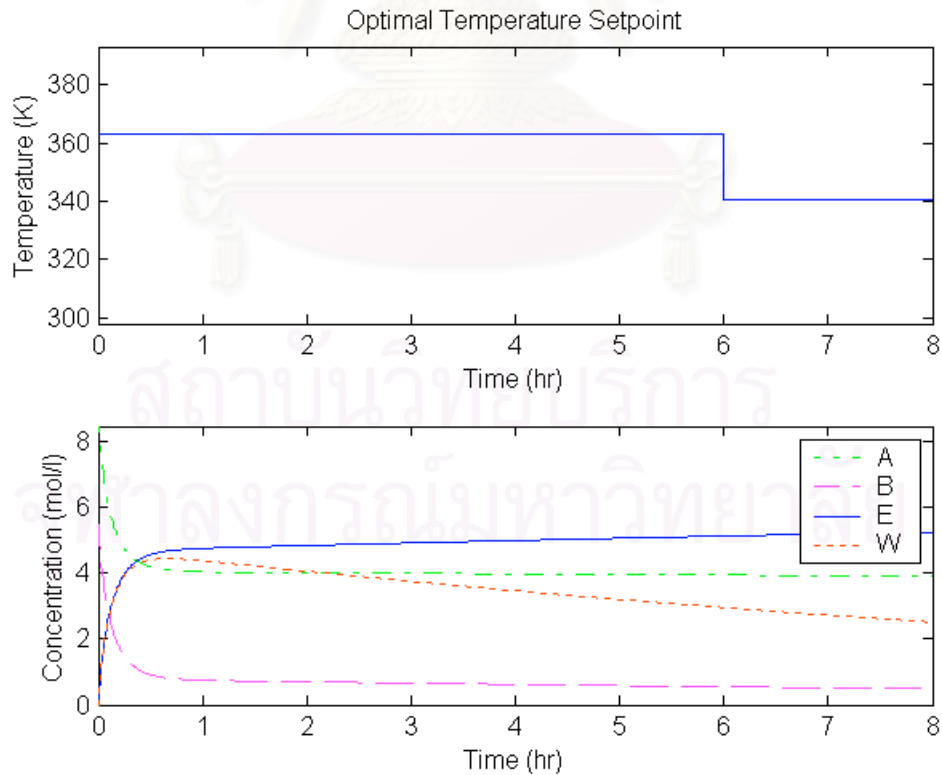
Figure 4.5 Optimal temperature profile and concentration profiles of a pervaporative membrane reactor

4.2.3 Discussion

The optimization results given in Table 5.1 indicate that:

- The batch reactor without pervaporation operated under the condition of an optimal temperature profile gives $C_E(t_f) = 4.8169$ mol/l which is 0.4% higher than the concentration $C_E(t_f) = 4.7976$ mol/l obtained by operating under the condition of an optimal temperature set point.

- The pervaporative membrane reactor operated under the condition of an optimal temperature profile gives $C_E(t_f) = 5.2669$ mol/l which is 0.2% higher than the concentration $C_E(t_f) = 5.2560$ mol/l obtained by operating under the condition of an optimal temperature set point.

It can be concluded that the operation of reactors by an optimal temperature profile gives an increase in the concentration of the desired product rather than using an optimal temperature set point.

- In comparison between the batch reactor without pervaporation and the pervaporative membrane reactor, simulation results show that the pervaporative membrane reactor gives 8.72% improvement for an optimal temperature set point and 8.54% improvement for an optimal temperature profile higher than the concentration obtained by the batch reactor without pervaporation.

From the above results, it can be concluded that the pervaporative membrane reactor can enhance the conversion of thermodynamically or kinetically limited reactions by the removal of the produced water from the reaction mixture. Then the performance of the pervaporative membrane reactor is superior to the conventional reactor.

4.3 Control Study

The purpose of this study is to design a control configuration for a pervaporative membrane reactor to track an optimal operating temperature. In this research, a generic model control (GMC) coupled with an extended Kalman filter (EKF) is implemented to track an optimal operating temperature. Either optimal temperature set point or optimal temperature profile obtained in section 4.2 is used as set point(s) of a pervaporative membrane reactor in this section.

The operating temperature is used as the controlled variable and is bounded between 298 K and 363 K. A jacket is used to control the reactor temperature at its desired trajectory. Due to the heat-exchanger capacities, the jacket temperature is assumed to be limited to the range 298-393 K. The reaction mixture is assumed to be at 298 K at the starting point. A generic model control (GMC) coupled with an extended Kalman filter (EKF) is implemented to track either optimal temperature set point or optimal temperature profile shown in Figure 4.4 and 4.5.

- *Controlled variable*: Reactor temperature, (T_r)
- *Manipulated variable*: Jacket temperature, (T_j)
- *Unmeasured variable*: Heat released by the reaction, (Q_r)

For the simulation studies, equations (4.3), (4.5), (4.6), (4.9), and (4.11)-(4.18) from the section 4.1 are solved to simulate the behavior of the reactor. The parameters and constant values used in the model are listed in Table 4.1.

4.3.1 Generic Model Control (GMC) Configuration

GMC is a model-based controller developed by Lee and Sullivan (1988). There are several advantages that make GMC a good control algorithm. The main advantage of the GMC is that the nonlinear process model does not need to be linearized because it directly inserts nonlinear process model into the controller itself. The generic model control diagram is shown in figure 4.6.
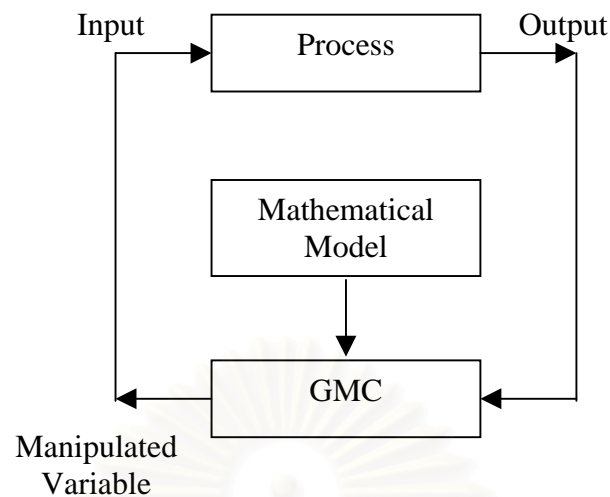
Figure 4.6 The generic model control diagram

The general form of the GMC control algorithm can be written as:

$$\frac{dy}{dt} = K_1(y_{sp} - y) + K_2 \int (y_{sp} - y)dt \tag{3.20}$$

where y is the current value of controlled variable,

   y_{sp} is a desired value of controlled variable,

   K_1 and K_2 are tuning constants.

The desired response can be obtained by incorporating two tuning parameters. The GMC defines the performance objective in terms of the time derivatives of the process output, i.e. minimizing the difference between the desired derivative of the process output and the actual derivative.

For temperature control of a pervaporative membrane reactor, the manipulated input of this tracking system is the jacket temperature, T_j and the tracked variable is the reactor temperature, T_r. It is assumed that the amount of heat retained in the walls of the reactor is small compared with the heat transferred in the reactor, an energy balance around the reactor contents gives:

$$\frac{dT_r}{dt} = \frac{Q_r + UA(T_j - T_r)}{M_r C_p} \tag{4.14}$$

Substituting T_r for y and T_{rsp} for y_{sp} in equation (3.20), combing equation (3.20) and (4.14), and finally solving for the manipulated variable, T_j, the control formulation is given by:

$$T_j = T_r + \frac{M_r C_p}{UA}\left\{ K_1(T_{rsp} - T_r) + K_2 \int (T_{rsp} - T_r)dt \right\} - \frac{Q_r}{UA} \qquad (4.23)$$

The discrete form of Eq. (4.23) for the kth time interval is given by:

$$T_j(k) = T_r(k) + \frac{M_r C_p}{UA}\left\{ K_1[T_{rsp} - T_r(k)] + K_2 \sum_0^k [T_{rsp} - T_r(k)]\Delta t \right\} - \frac{Q_r}{UA} \quad (4.24)$$

where Δt is the sampling time of the controller.

Equation (4.24) gives the actual jacket temperature, $T_j(k)$ that is not the jacket temperature set point, $T_{jsp}(k)$, needed to control the reactor temperature at its set point, T_{rsp}. However, it is reasonable to assume that the dynamics of the jacket temperature control are approximately first order (Liptak, 1986) with time constant τ_j and hence the $T_{jsp}(k)$ can be calculated by equation (4.18):

$$T_{jsp}(k) = T_j(k-1) + \tau_j \frac{[T_j(k) - T_j(k-1)]}{\Delta t} \qquad (4.18)$$

4.3.2 GMC with Extended Kalman Filter

As several model-based controllers, GMC requires the measurement or the estimation of the states of an appropriate process model. However, in most industrial, the state variables are not all measurable or, not with sufficient accuracy for control purposes. To succeed these difficulties, the estimation techniques have been used together with simplified process models. The flowchart of GMC with extended Kalman filter is shown in figure 4.7

As seen in equation (4.24), the success of the GMC controller is largely depended on the ability to measure, estimate, or predict the heat released, Q_r at any given period of time. In this work, it is assumed that users have some knowledge.
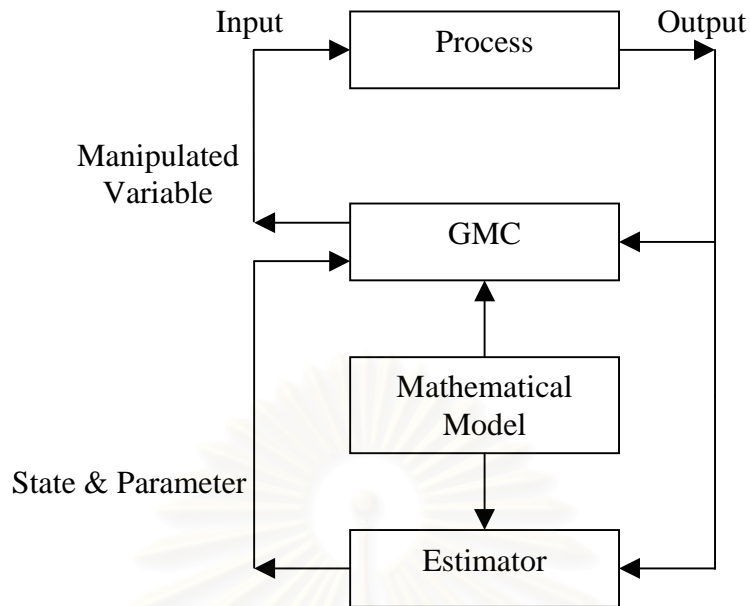
Figure 4.7 Flowchart of GMC with extended Kalman filter

(perhaps, mistaken) of the physical parameters in the system: M_r, C_p, U, A. The extended Kalman filter is used to estimate Q_r by using the bilinear models (Kershenbaum and Kittisupakorn, 1994). Due to the sensitivity of the estimation of the heat released by reaction to the heat transfer coefficient change, the extended Kalman filter is used to estimate the heat transfer coefficient to compensate the mismatch.

A simple model, which attempts to reflect the basic chemical kinetics in the batch reactor, is assumed that the rate of reaction, R, varies with respect to the reactant concentration, M_r, and the reactor temperature, T_{rm}, as shown in the following equation:

$$\frac{dM_r}{dt} = -R = -bM_r T_{rm} \tag{4.25}$$

where b is a *pseudo* reaction rate constant.

The estimated heat released from the reaction is given by:

$$Q_r = (-\Delta H)VR = -bVM_r T_{rm}\Delta H \tag{4.26}$$

where ΔH is the of reaction.

Define

$$N \equiv -bVM_r\Delta H \tag{4.27}$$

From energy balances on the jacket and reactor, the state equations for purposed of estimation are:

$$\frac{dT_{jm}}{dt} = \frac{UA(T_{rm} - T_{jm})}{V_j\rho_jC_{pr}} + \frac{(T_{jsp} - T_{jm})}{\tau_j} \tag{4.28}$$

$$\frac{dT_{rm}}{dt} = \frac{Q_{re}}{M_rC_{pr}} + \frac{UA(T_{jm} - T_{rm})}{M_rC_{pr}} \tag{4.29}$$

$$\frac{dN}{dt} = -bNT_{rm} \tag{4.30}$$

$$\frac{dQ_{re}}{dt} = N\frac{dT_{rm}}{dt} + T_{rm}\frac{dN}{dt} \tag{4.31}$$

$$\frac{db}{dt} = 0 \tag{4.32}$$

$$\frac{dUA}{dt} = 0 \tag{4.33}$$

T_{jm} and T_{rm} are measurable and are used to estimate the entire state, $[T_{jm}, T_{rm}, N, Q_{re}, b]^T$, by an extended Kalman filter. The diagram of the estimation is shown in figure 4.8.
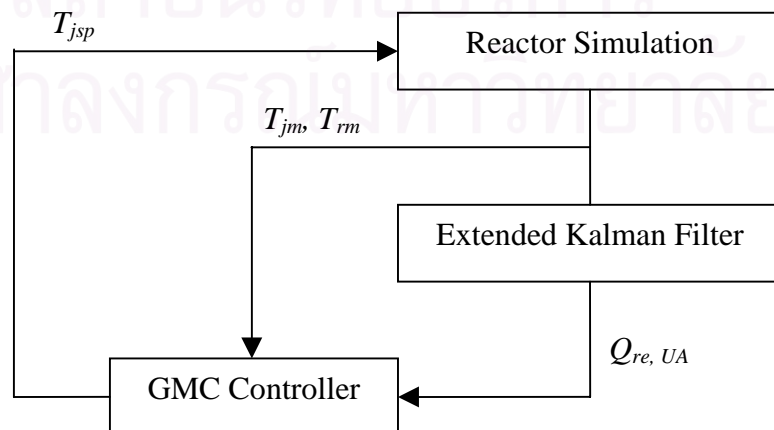
Figure 4.8 The estimation diagram of heat released from the reaction

4.3.3 Control Results

The simulation shown in figure 4.9 illustrates the open-loop response for the pervaporative membrane reactor operated under the ambient condition where the parameters and constant values used to simulate are given in Table 4.1. It has shown that the reactor temperature increases with time from 298 K to 333 K, which does not reach 363 K, the optimal temperature. Since the reactor temperature is one of the key factors, in order to operate the pervaporative membrane reactor efficiently, it is necessary to control the reactor temperature to the optimal operating temperature.

A generic model control (GMC) coupled with an extended Kalman filter (EKF) is implemented to track either optimal temperature set point or optimal temperature profile of a pervaporative membrane reactor as shown in Figure 4.4 and 4.5. The performance of GMC controller coupled with extended Kalman filter are simulated in nominal case, in which all model parameter used to simulate are specified correctly, and plant/model mismatch case, in which some parameters have changed from their nominal value.
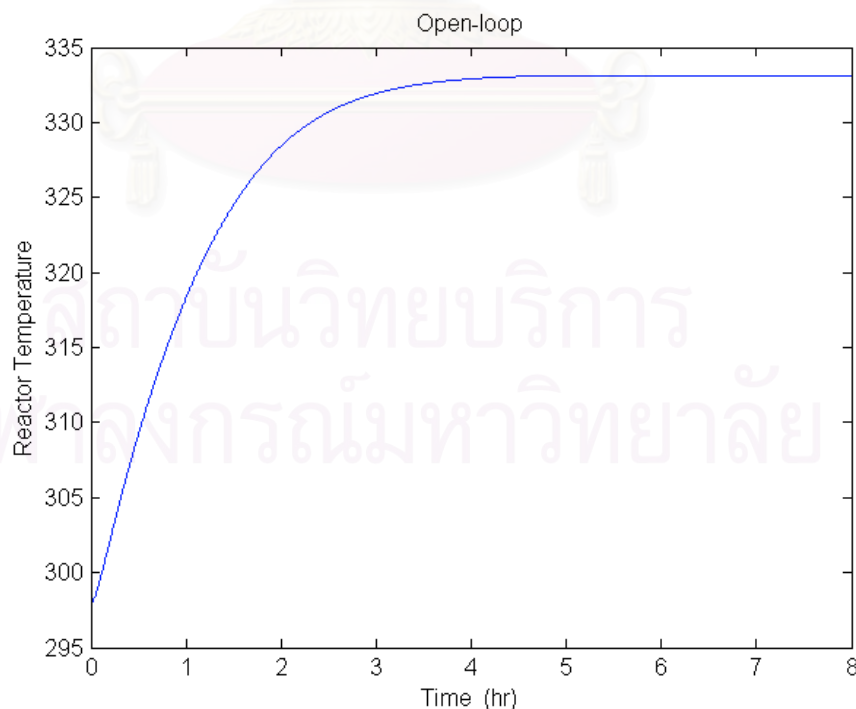
Figure 4.9 Open loop of pervaporative membrane reactor.

In this work, the appropriate values of the tuning parameters of GMC controller are K_1 = 5 hr^{-1} and K_2 = 0.0008 hr^{-2}. Two measurements (T_j and T_r) are available and are used to obtain estimates of the entire state, $[T_j, T_r, N, Q_{re}, b]^T$, using an extended Kalman filter. The values of Kalman filter parameters and initial state estimates are given in Table 4.3.

Table 4.3 Kalman filter parameters and initial state estimates for simulation

T_j^0 = 298 K	P(1,1) = 1	Q(1,1) = 1
T_r^0 = 298 K	P(2,2) = 1	Q(2,2) = 1
N^0 = 100	P(3,3) = 10^6	Q(3,3) = 10^6
Q_r^0 = 559 J/hr	P(4,4) = 2000	Q(4,4) = 2000
b^0 = 1.75 x 10^{-3}	P(5,5) = 100	Q(5,5) = 100
	P(6,6) = 10^6	Q(6,6) = 10^6
	R(1,1) = 0.001	R(2,2) = 0.001

Although the GMC controller coupled with the extended Kalman filter is effective to control the reactor temperature for the nominal case, it is important to examine the robustness aspects of both controllers with respect to changes in operating and process parameters and with respect to plant-model mismatch. The GMC controller coupled with the extended Kalman filter, tuned for the nominal case, is used to control an optimal operating temperature where some of the conditions have changed from their nominal value. The robustness test is divided into six cases as listed below:

- Rate constant, k_1, increase 30%,
- Rate constant, k_2, decrease 30%,
- Rate constants, k_1 increase 30% and k_2, decrease 30%,
- Heat of reaction, ΔH, increase 30%,
- Heat transfer coefficient, U, decrease 30%,
- k_1, ΔH increase 30% and k_2, U decrease 30%.

In this section, two cases of temperature control are carried out:

Case 1: tracking an optimal temperature set point

In this case, the control objective is to heat the reactor rapidly from a temperature of 298 K to 363 K and maintain the temperature at this value. The simulation results are shown in figure 4.10-4.23.

Table 4.4 The IAE and ISE comparison of T_r and Q_r (Case 1)

Condition	Reactor Temperature		Heat Released	
	IAE	ISE	IAE	ISE
Nominal case	45.089	1.864e+03	2.987	7.765
+30% k_1	44.640	1.839e+03	4.860	199.340
-30% k_2	45.032	1.863e+03	3.018	7.847
+30% k_1 and -30% k_2	44.574	1.838e+03	4.884	199.422
+30% ΔH	43.452	1.831e+03	4.832	198.903
-30% U	60.261	2.468e+03	7.426	1.711e+03
+30% k_1, ΔH and -30% k_2, U	56.774	2.333e+03	8.325	1.579e+03

Case 2: tracking an optimal temperature profile.

In this case, the control objective is to track an optimal temperature profile as shown in figure 4.3. The simulation results are shown in figure 4.24-4.37.

Table 4.5 The IAE and ISE comparison of T_r and Q_r (Case 2)

Condition	Reactor Temperature		Heat Released	
	IAE	ISE	IAE	ISE
Nominal case	53.310	1.981e+03	3.348	7.987
+30% k_1	52.853	1.956e+03	5.226	199.565
-30% k_2	53.248	1.980e+03	3.385	8.070
+30% k_1 and -30% k_2	52.782	1.955e+03	5.255	199.648
+30% ΔH	51.677	1.929e+03	5.196	199.129
-30% U	70.891	2.622e+03	7.745	1.711e+03
+30% k_1, ΔH and -30% k_2, U	67.389	2.487e+03	8.656	1.579e+03
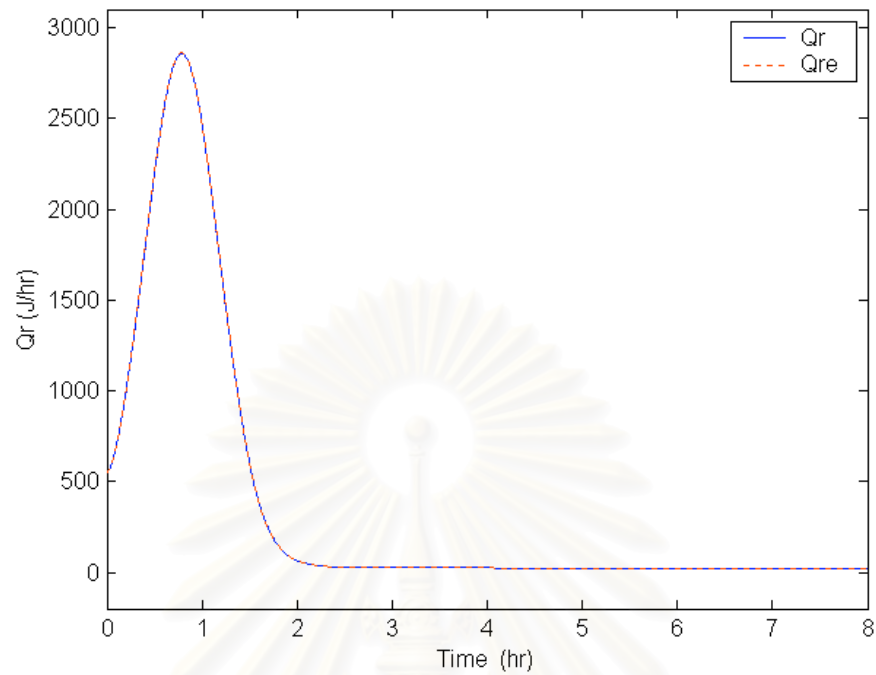
Figure 4.10 Estimates of heat released for nominal case (Case 1).
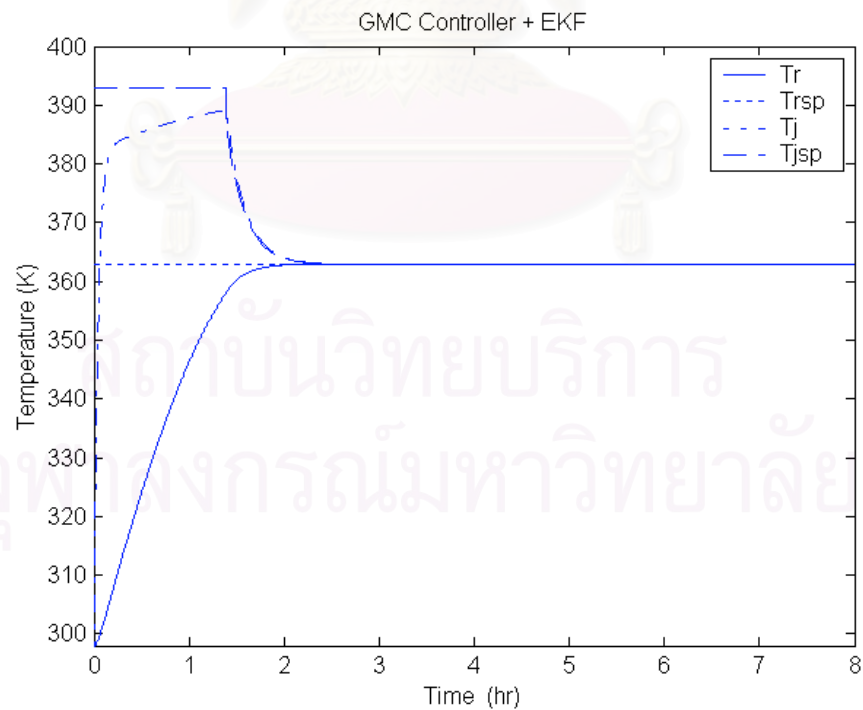
Figure 4.11 Response of pervaporative membrane reactor for nominal case (Case 1).
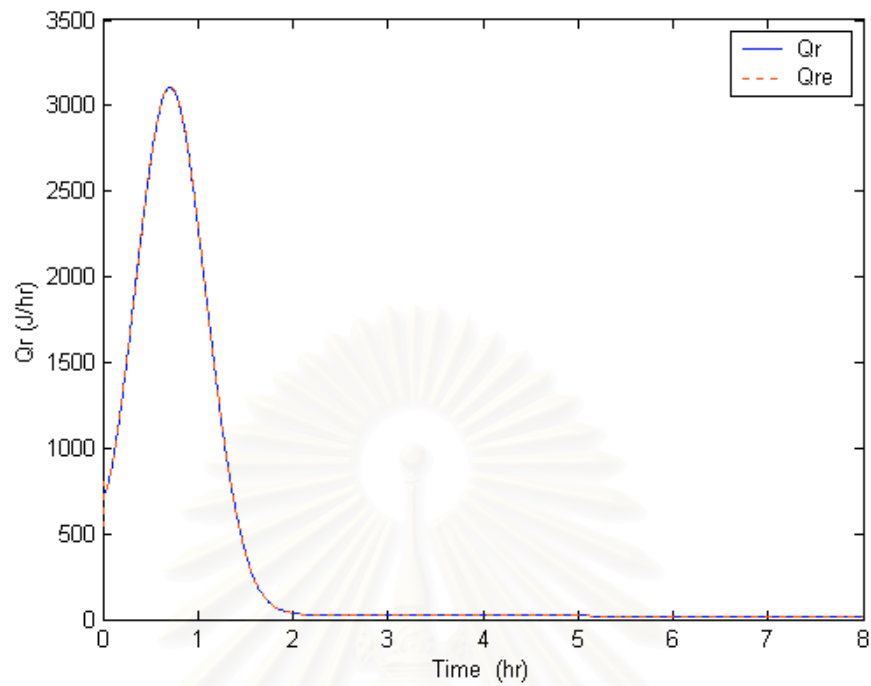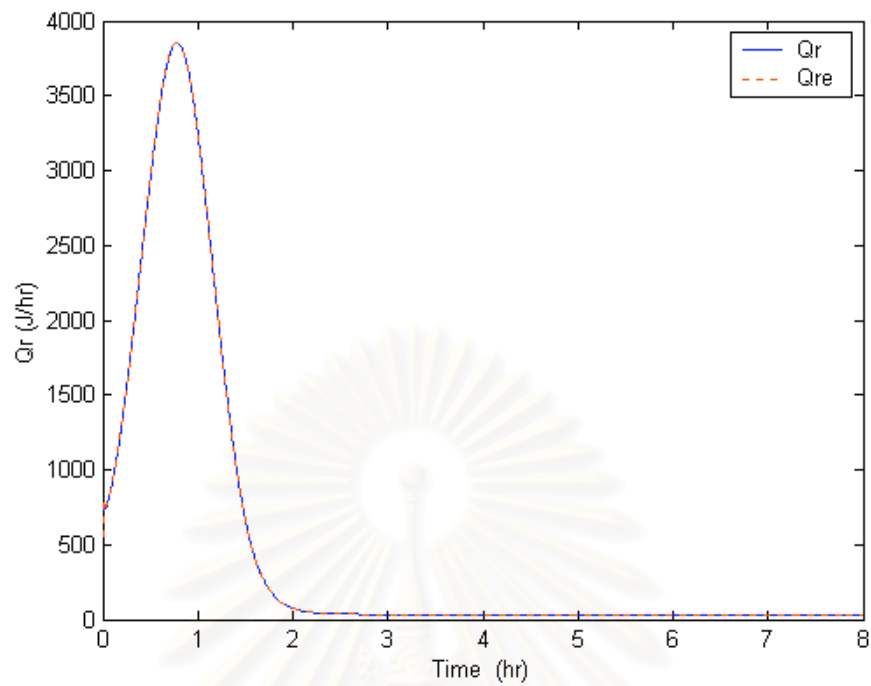
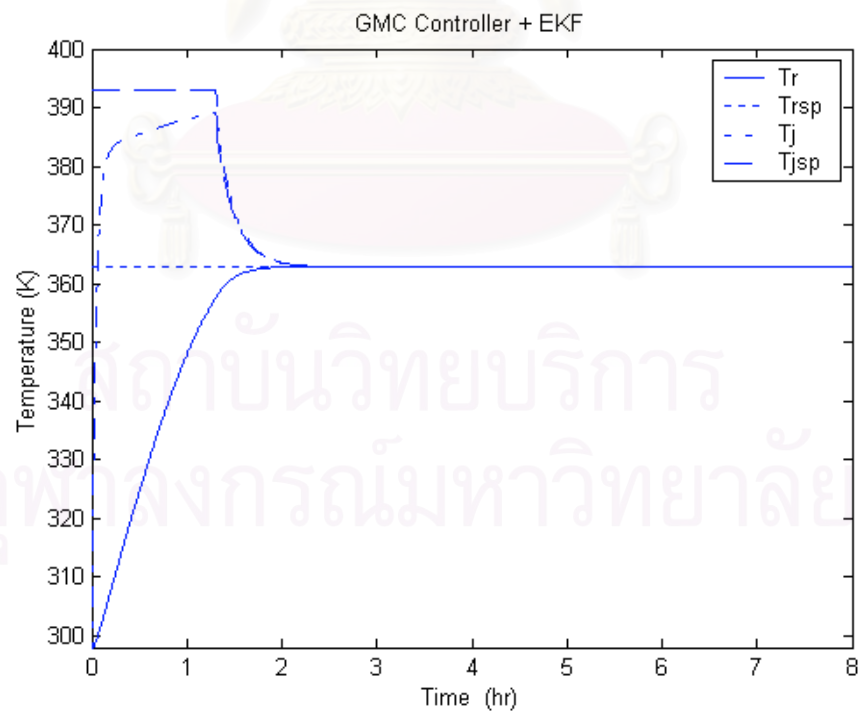**Figure 4.12** Estimates of heat released for +30% k_1 change (Case 1).
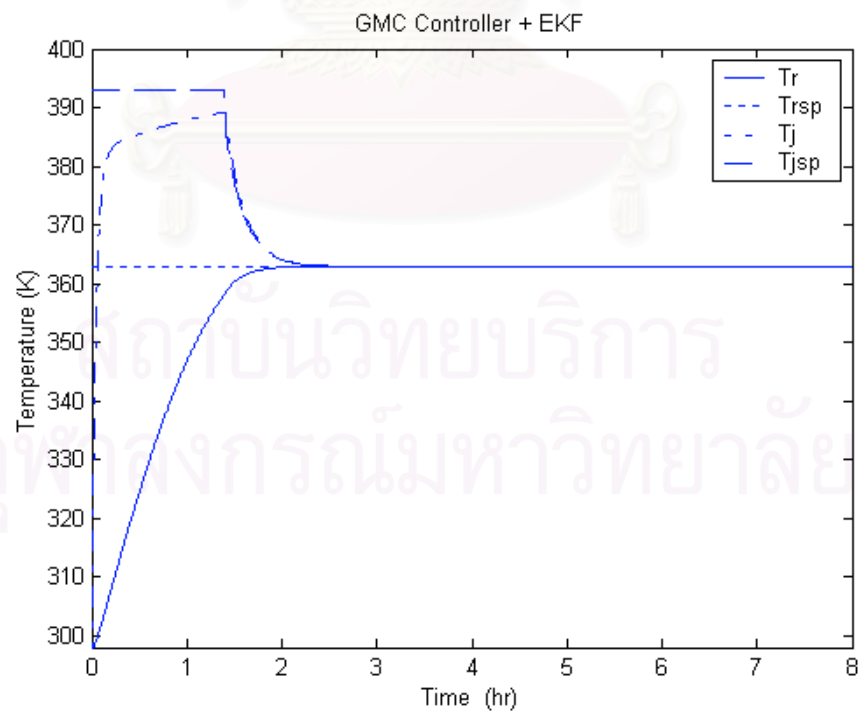
Figure 4.13 Response of pervaporative membrane reactor for +30% k_1 change (Case 1).
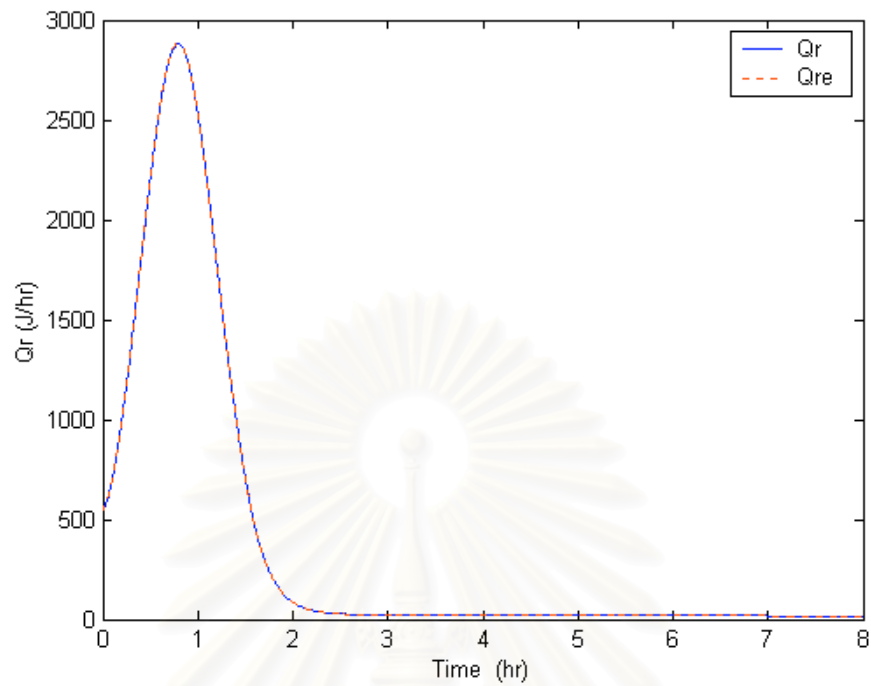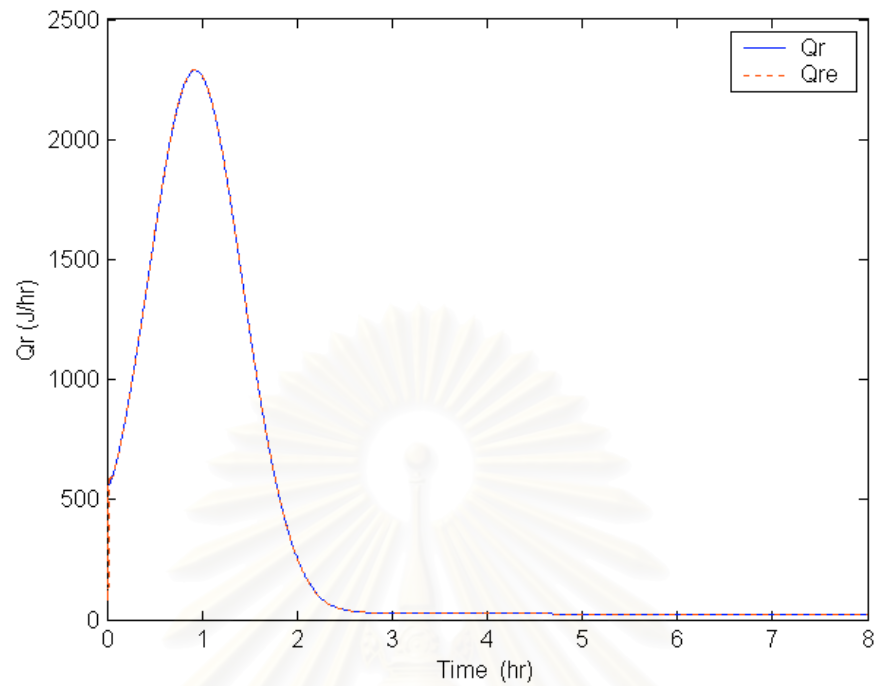
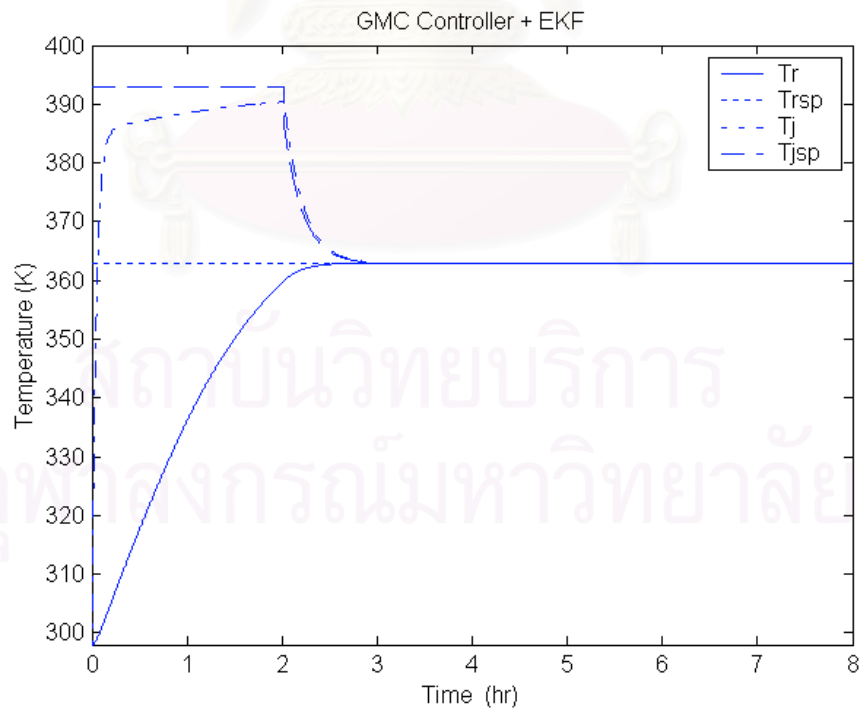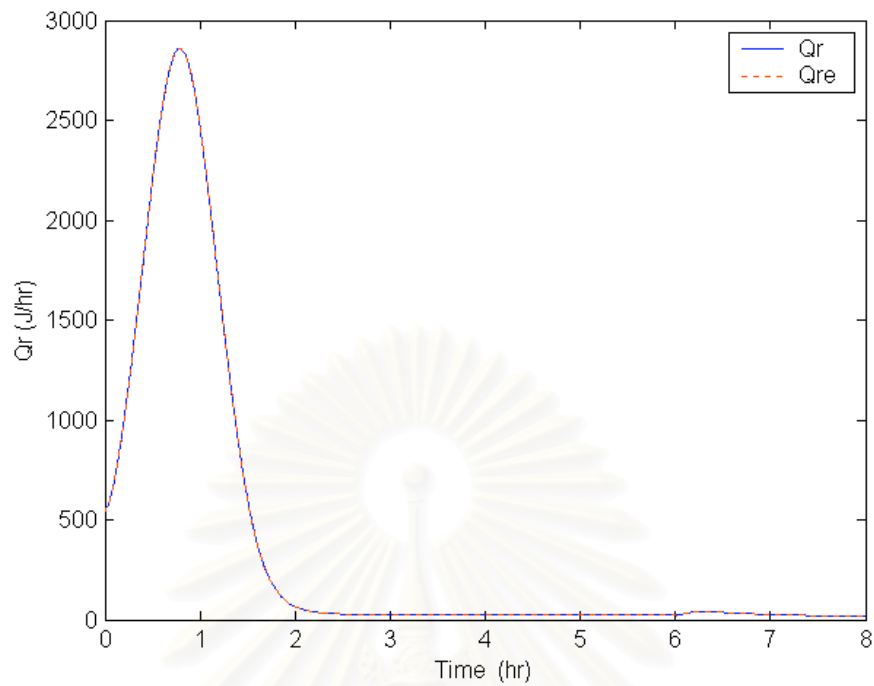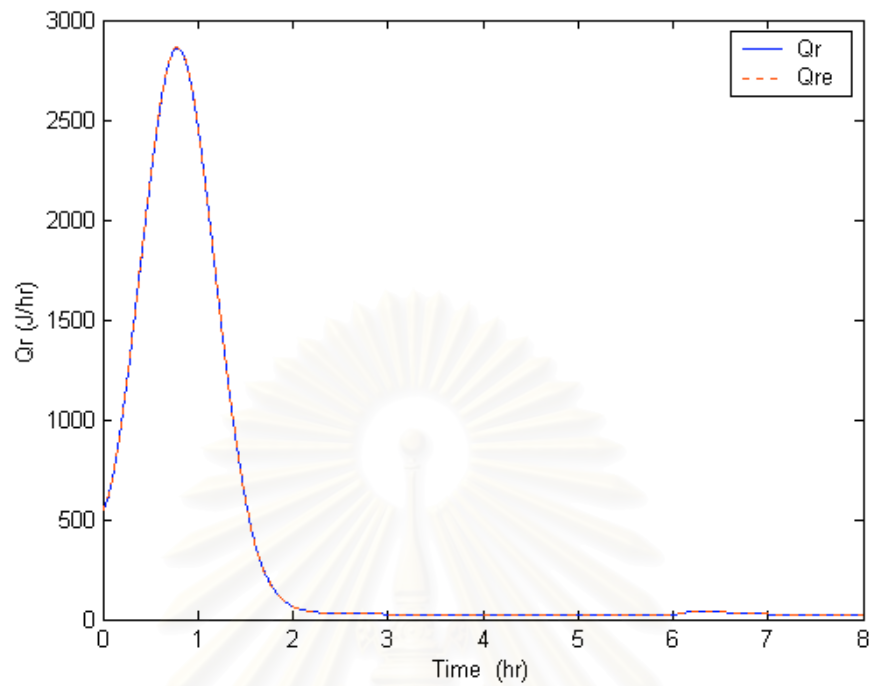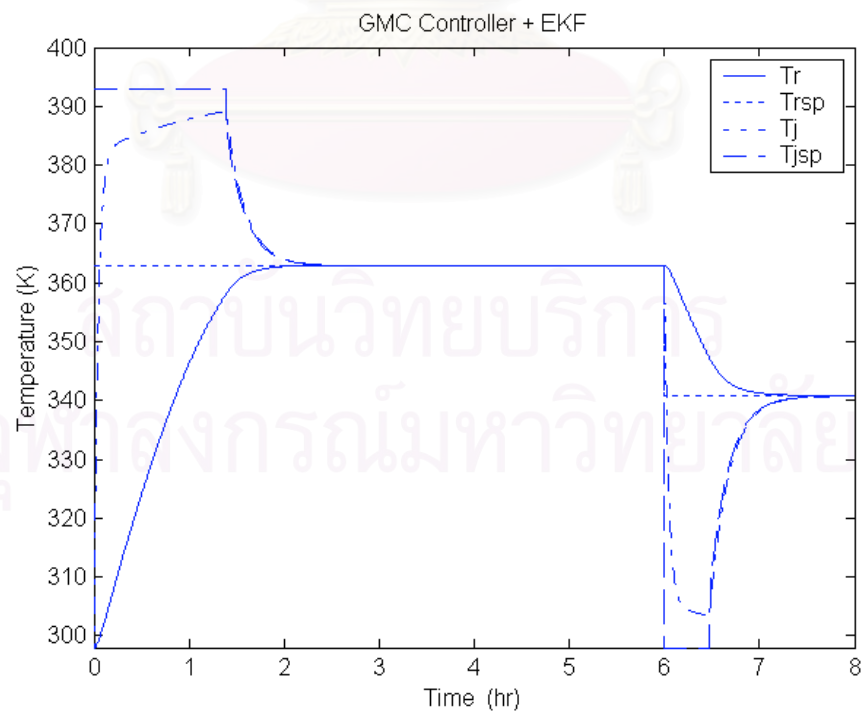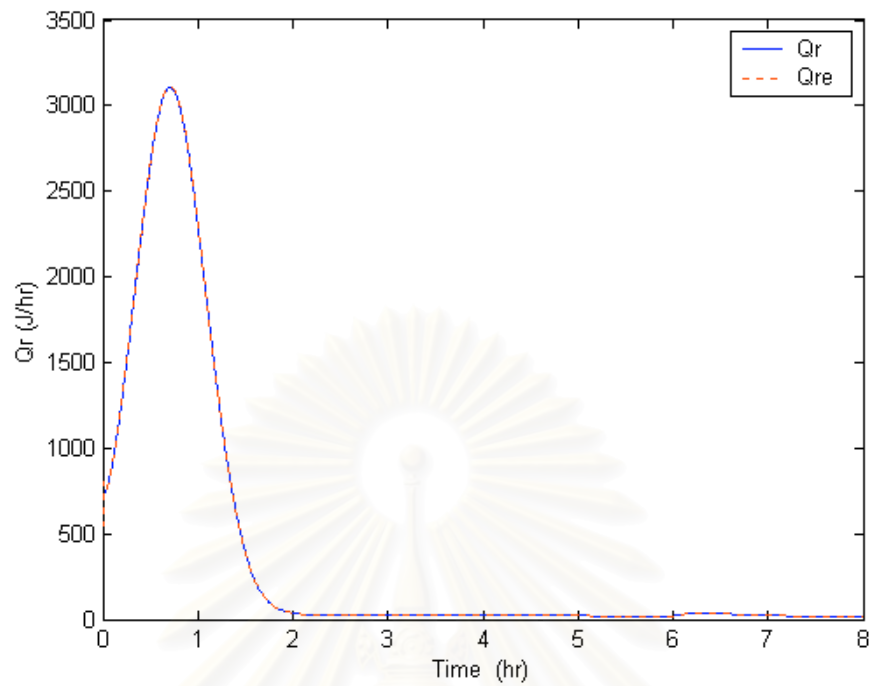**Figure 4.14** Estimates of heat released for -30% k_2 change (Case 1).
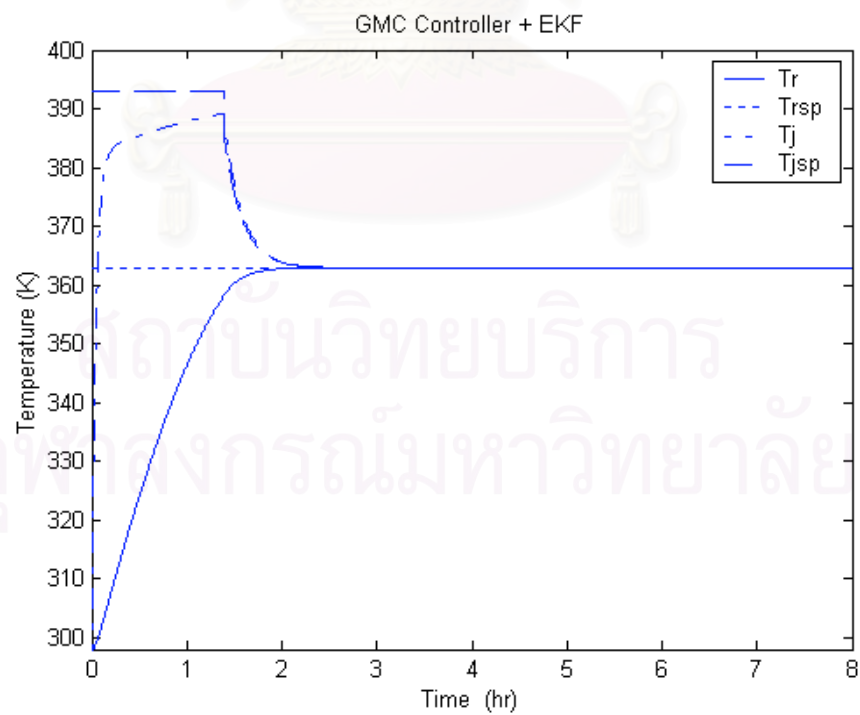
Figure 4.15 Response of pervaporative membrane reactor for -30% k_2 change (Case 1).
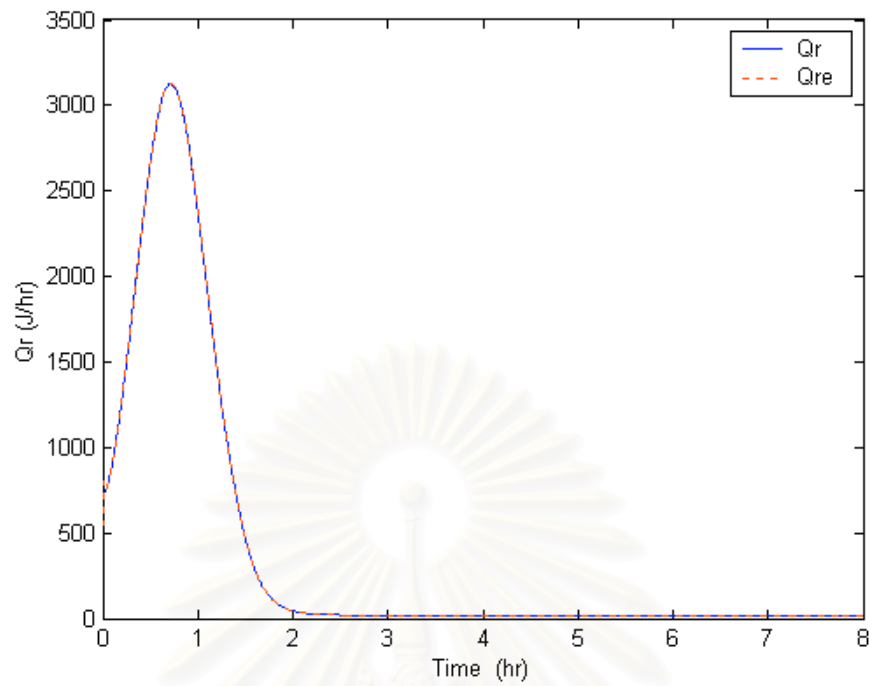
Figure 4.16 Estimates of heat released for +30%k_1 and -30%k_2 change (Case 1).
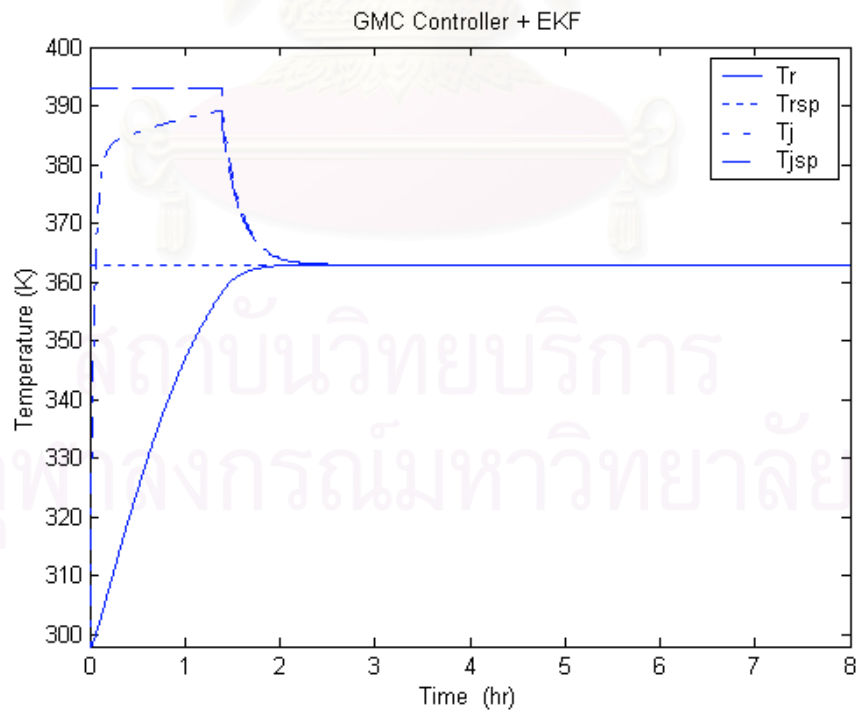
Figure 4.17 Response of pervaporative membrane reactor for +30%k_1 and -30%k_2 change (Case 1).

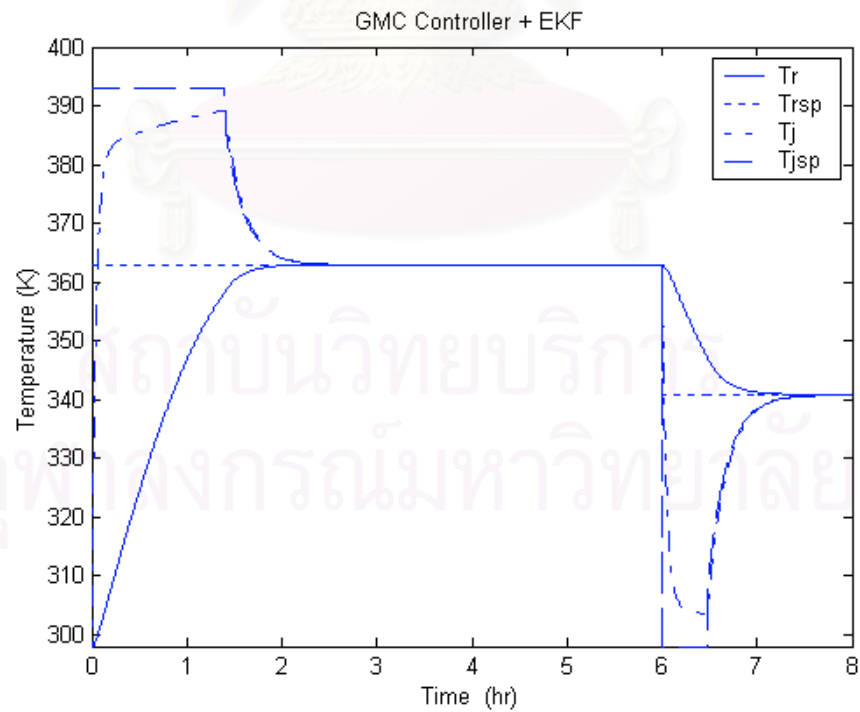**Figure 4.18** Estimates of heat released for +30% Δ*H* change (Case 1).

Figure 4.19 Response of pervaporative membrane reactor for +30%Δ*H* change
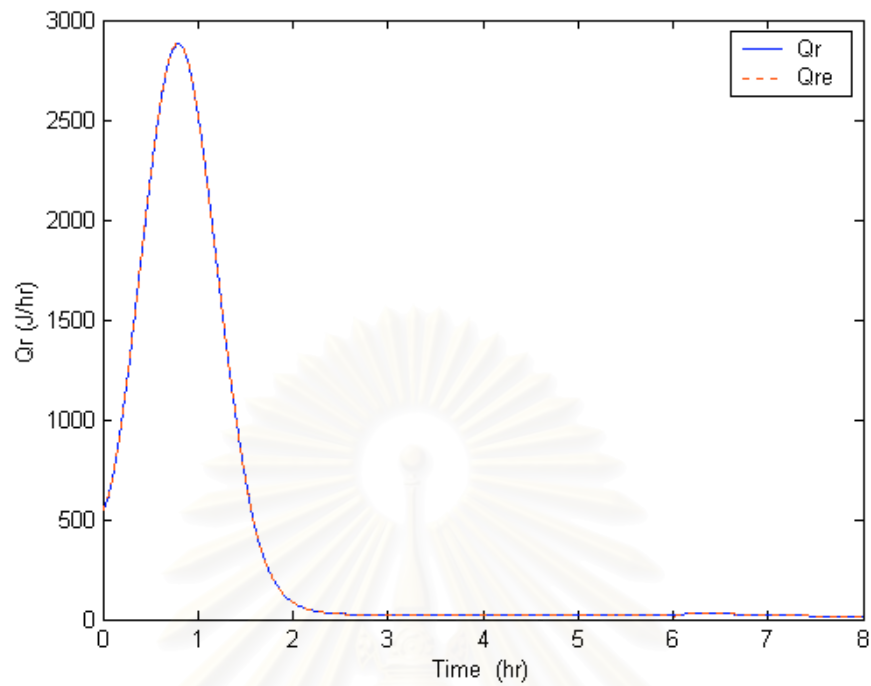(Case 1).

Figure 4.20 Estimates of heat released for -30% U change (Case 1).

Figure 4.21 Response of pervaporative membrane reactor for -30% U change (Case 1).

Figure 4.22 Estimates of heat released for $+30\%k_1$, $-30\%k_2$, $+30\%\Delta H$ and $-30\%U$ change (Case 1).
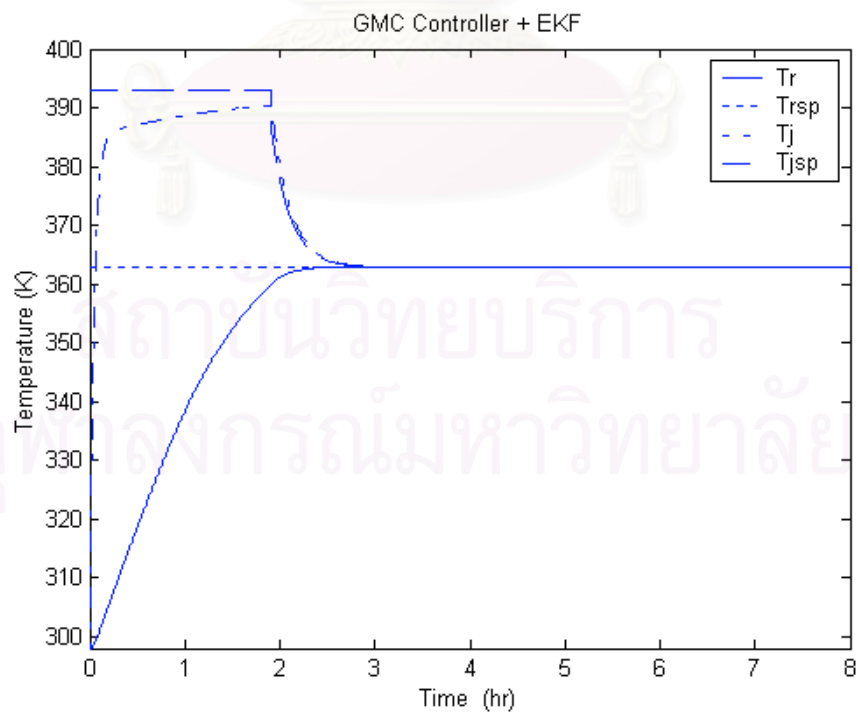
Figure 4.23 Response of pervaporative membrane reactor for $+30\%k_1$, $-30\%k_2$, $+30\%\Delta H$ and $-30\%U$ change (Case 1).

Figure 4.24 Estimates of heat released for nominal case (Case 2).

Figure 4.25 Response of pervaporative membrane reactor for nominal case (Case 2).

Figure 4.26 Estimates of heat released for +30% k_1 change (Case 2).

Figure 4.27 Response of pervaporative membrane reactor for +30% k_1 change (Case 2).

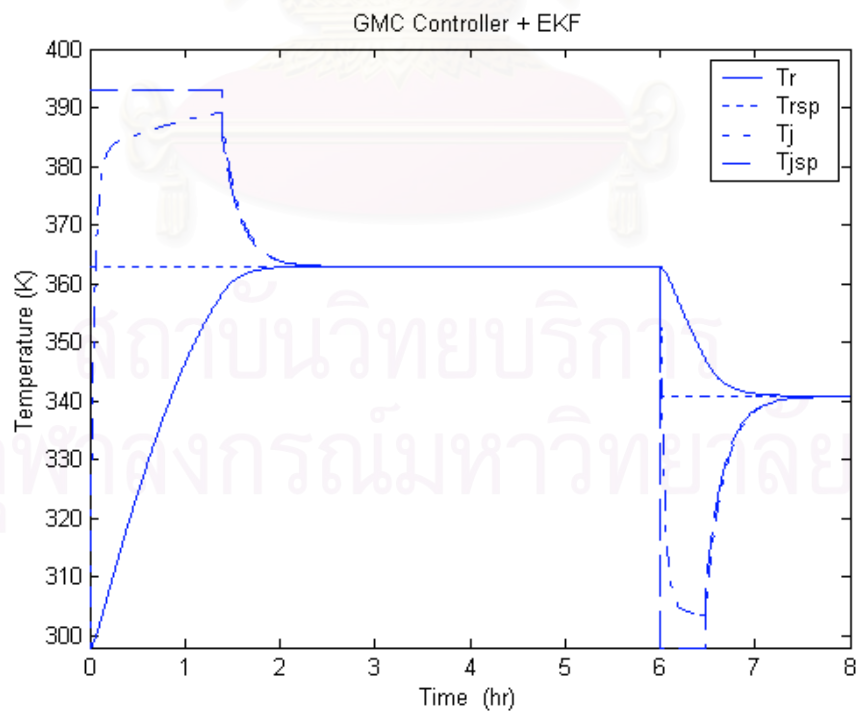**Figure 4.28** Estimates of heat released for -30% k_2 change (Case 2).

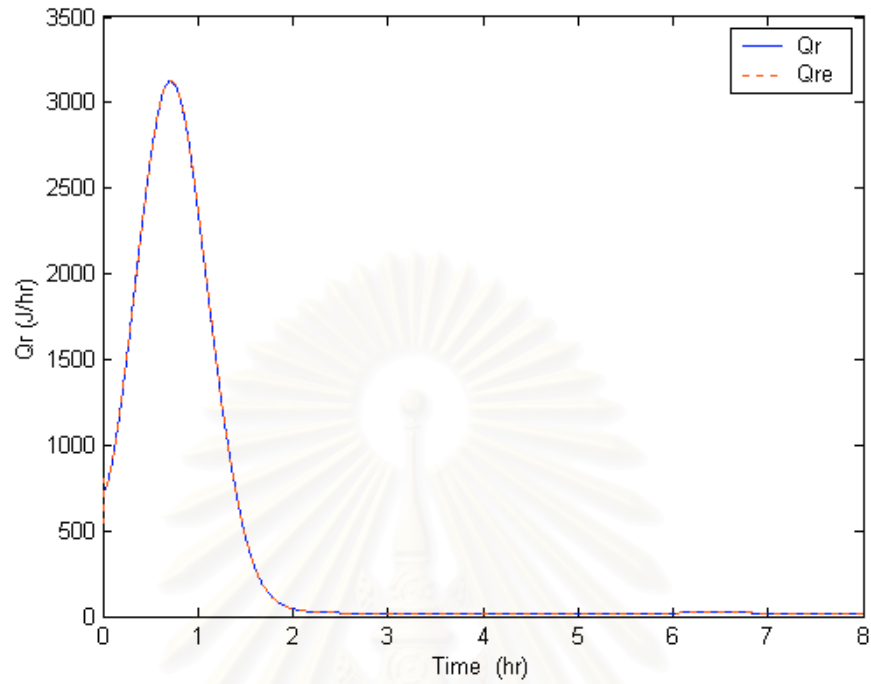**Figure 4.29** Response of pervaporative membrane reactor for -30% k_2 change (Case 2).

Figure 4.30 Estimates of heat released for +30%k_1 and -30%k_2 change (Case 2).
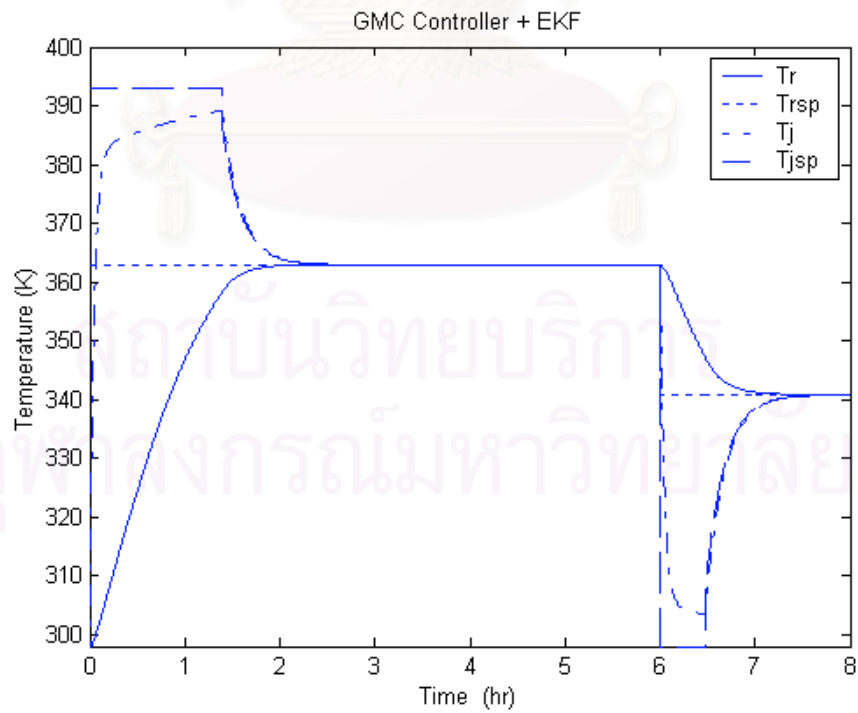

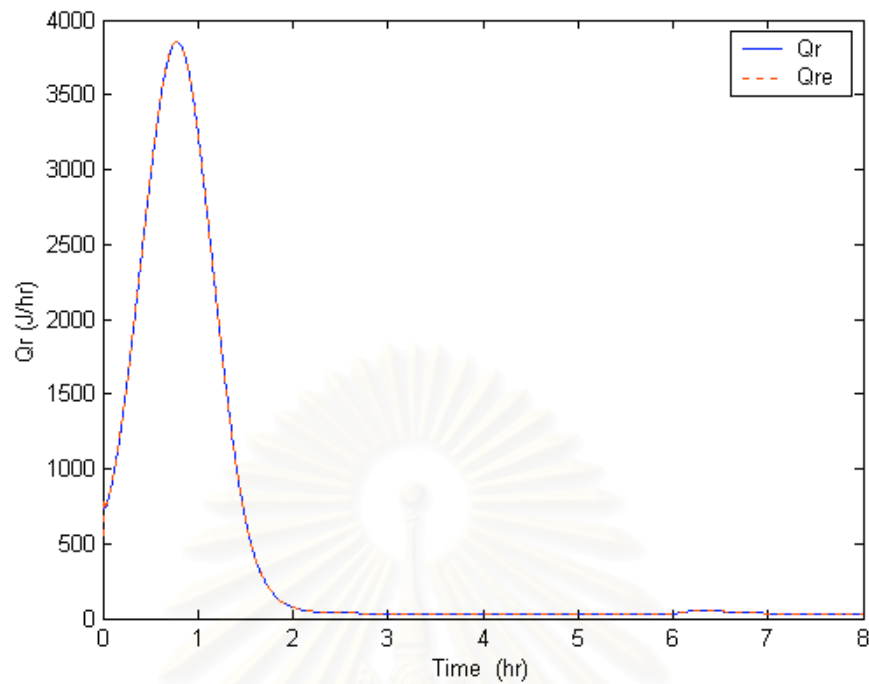**Figure 4.31** Response of pervaporative membrane reactor for +30%k_1 and -30%k_2 change (Case 2).

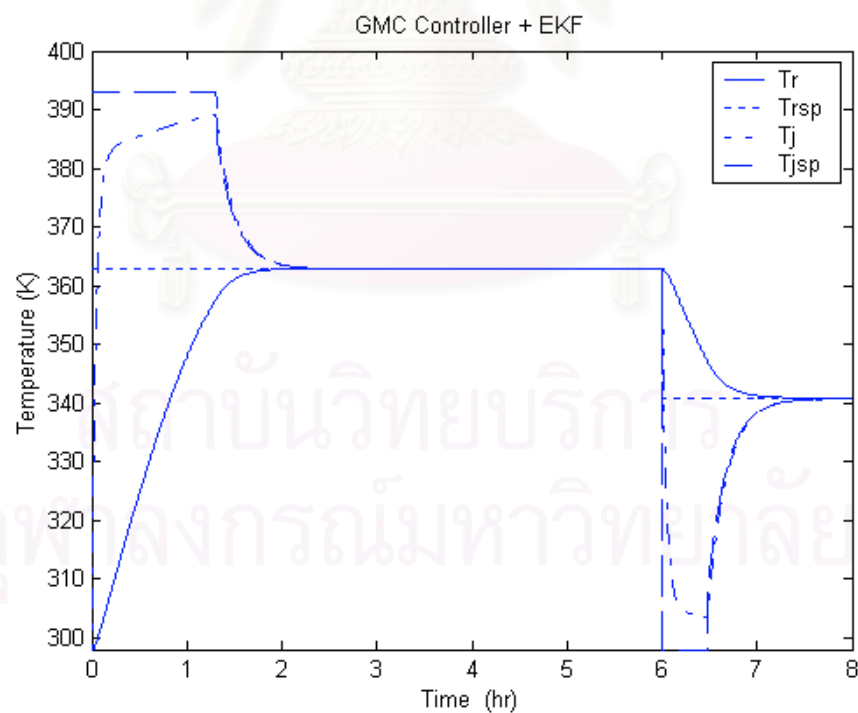**Figure 4.32** Estimates of heat released for +30% Δ*H* change (Case 2).

Figure 4.33 Response of pervaporative membrane reactor for +30%Δ*H* change
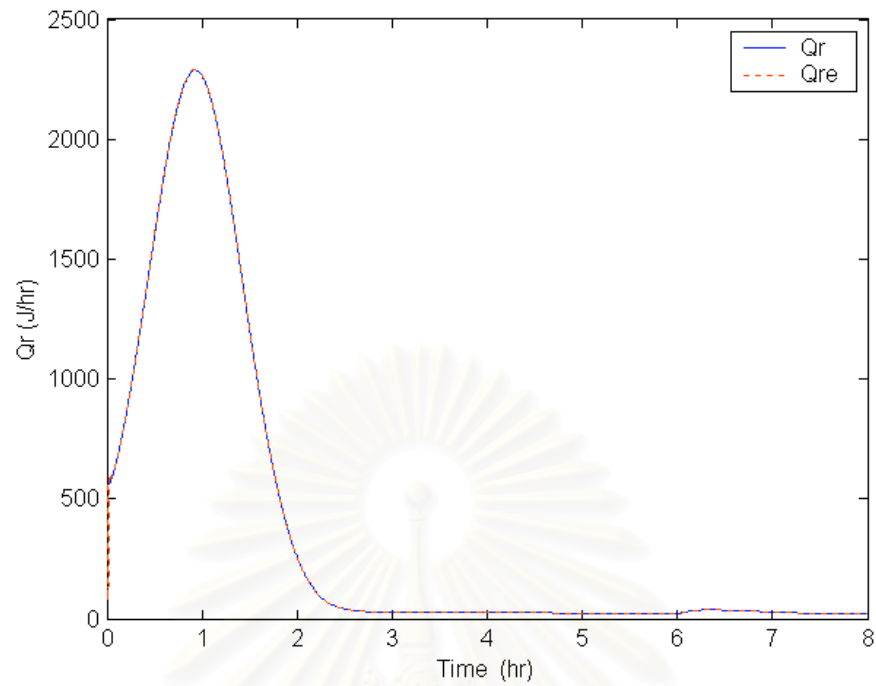(Case 2).

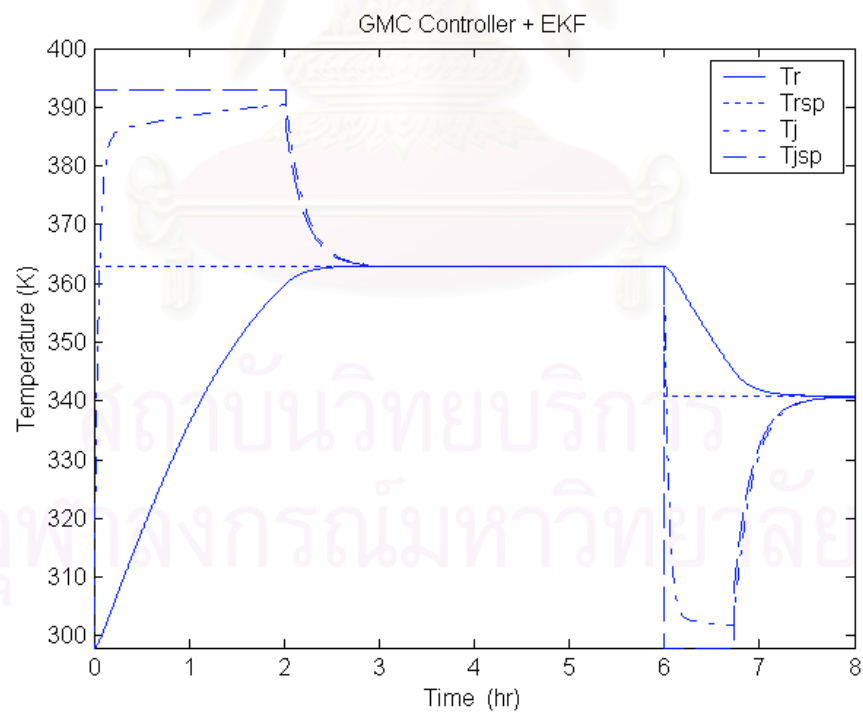**Figure 4.34** Estimates of heat released for -30% U change (Case 2).

Figure 4.35 Response of pervaporative membrane reactor for -30% U change (Case 2).
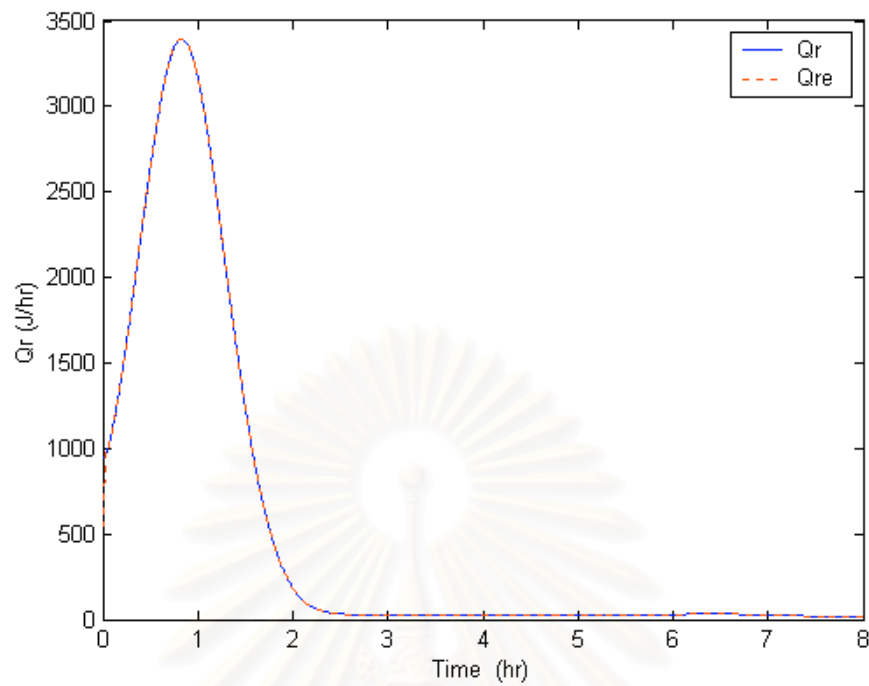
Figure 4.36 Estimates of heat released for $+30\%k_1$, $-30\%k_2$, $+30\%\Delta H$ and $-30\%U$ change (Case 2).
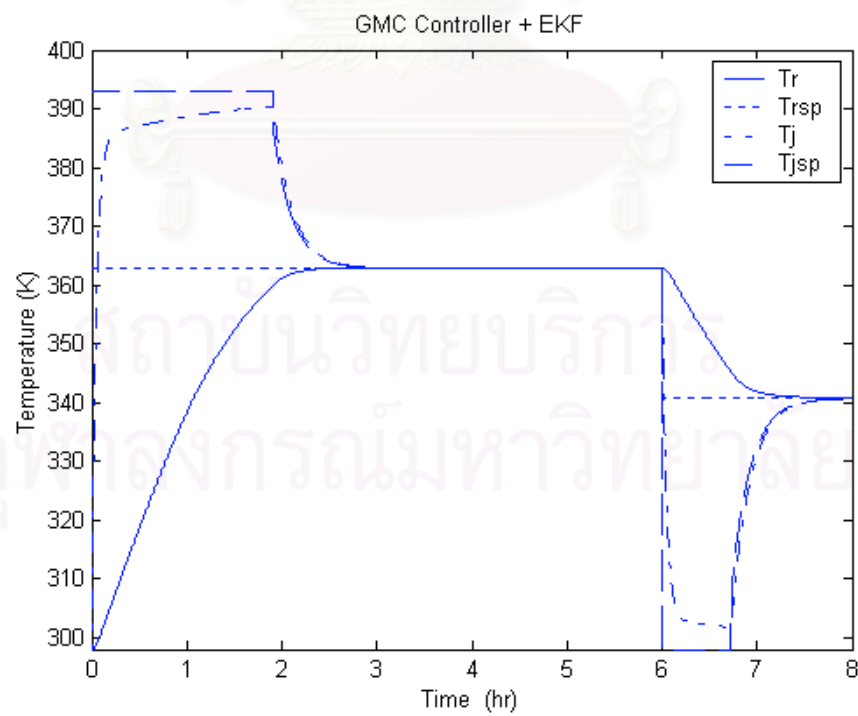

Figure 4.37 Response of pervaporative membrane reactor for $+30\%k_1$, $-30\%k_2$, $+30\%\Delta H$ and $-30\%U$ change (Case 2).

4.3.4 Discussion

Case 1: tracking an optimal temperature set point

- **Nominal case**

    Figure 4.10 and 4.11 show the heat released estimation and the response of the GMC controller in tracking an optimal temperature set point (T_r^{sp} = 363 K) of a pervaporative membrane reactor operating under a nominal case, respectively. It can be seen from figure 4.10 that the extended Kalman filter gives a reasonable estimate of the heat released. With this estimate of heat released, the GMC controller performs satisfactorily; the reactor temperature is delivered to the desired set point with no overshoot as shown in figure 4.11.

- **Rate constant change**

    In the cases of the rate constant changes, the results are given in figure 4.12-4.17. It can be seen that the estimation of the heat released by reaction is not sensitive to the rate constant changes. The GMC controller has still provided good control action similar to the nominal case.

- **Heat of reaction change**

    The results given in figure 4.18-4.19 show the heat released estimation and the responses of the GMC controller for the case of the heat of reaction change, respectively. In this case, the heat of reaction has been increased by 30%. Figure 4.18 illustrates that the extended Kalman filter has still provided a reasonable estimate. The GMC controller is still robust.

- **Heat transfer coefficient change**

    Figure 4.21 gives the response of the GMC controller in response to a heat transfer coefficient change. This change tests the performance of the controllers in light of a change in unmeasured parameters. It can be seen that the estimation of the heat released by reaction is sensitive to the heat transfer coefficient. Figure 4.20 shows the behavior of the estimator when the heat transfer coefficient decreases with 30% of the actual value. The performance of the extended Kalman filter has deteriorated when compared to that of the nominal case. However, the GMC

controller is able to provide adequate control but with more sluggish than in the nominal case.

- **Rate constants, heat of reaction, and heat transfer coefficient change**

    Figure 4.22 and 4.23 show the performances of the extended Kalman filter and the GMC controller for the case that combines the increase in the rate constants, k_1, and the heat of reaction and the decrease in the rate constants, k_2, and the heat transfer coefficient. Figure 4.22 illustrates that at the beginning, the estimate of the amount of heat released is poor. However, the GMC controller still gives reasonably good control, but more sluggish than in the nominal case due to the decrease of the heat transfer coefficient.

Case 2: tracking an optimal temperature profile

- **Nominal case**

    Figure 4.24 and 4.25 show the estimate of the amount of heat released by the reaction and the response of the GMC controller in tracking an optimal temperature profile of a pervaporative membrane reactor operating under a nominal case, respectively. It can be seen from figure 4.24 that the extended Kalman filter gives a reasonable estimation. As shown in figure 4.25, the GMC controller performs satisfactorily; the reactor temperature is delivered to the desired set point with no overshoot.

- **Rate constant change**

    The simulation results of the rate constant change are given in figure 4.26- 4.31. It can be seen that the estimation of the heat released by reaction is not sensitive to the rate constant changes. The GMC controller has still provided good control action similar to the nominal case.

- **Heat of reaction change**

    Figure 4.32 and 4.33 show the estimate of the amount of heat released by the reaction and the responses of the GMC controller for the case of the heat of reaction change, respectively. In this case, the heat of reaction has been increased by 30%. The

extended Kalman filter has still provided a reasonable estimate as illustrated in figure 4.32. Figure 4.33 shows that the GMC controller is still robust.

- **Heat transfer coefficient change**

    Figure 4.35 gives the response of the GMC controller in response to a heat transfer coefficient change. It can be seen that the estimation of the heat released by reaction as shown in figure 4.34 is sensitive to the heat transfer coefficient. The performance of the extended Kalman filter has deteriorated when compared to that of the nominal case. However, the GMC controller still gives reasonably good control action as shown in figure 4.35 but the response is more sluggish than in the nominal case.

- **Rate constants, heat of reaction, and heat transfer coefficient change**

    Figure 4.36 and 4.37 show the performances of the extended Kalman filter and the GMC controller for the case that combines the increase in the rate constants, k_1, and the heat of reaction and the decrease in the rate constants, k_2, and the heat transfer coefficient. Figure 4.36 illustrates that at the beginning, the estimate of the amount of heat released is poor. However, the GMC controller is able to provide adequate control.

    The GMC controller coupled with the extended Kalman filter is implemented to track either optimal temperature set point or optimal temperature profile of a pervaporative membrane reactor. The performance of GMC controller coupled with extended Kalman filter are simulated in nominal case, in which all model parameter used to simulate are specified correctly, and plant/model mismatch case, in which some parameters have changed from their nominal value. From simulation results, it can be observed that this controller is able to accommodate all the changes very well. The GMC controller with the extended Kalman filter has been found to be effective and robust in tracking either optimal temperature set point or optimal temperature profile of the pervaporative membrane reactor.

CHAPTER V

CONCLUSIONS AND RECCOMENDATIONS

In this work, the pervaporative membrane reactor has been studied. In summary, to achieve the desired successful control of batch processes, the system depends on the integration of three important ingredients: an optimal operating trajectory, a suitable control law, and a suitable design of the control configuration. Due to the significant of the operating temperature, the optimization framework is formulated to determine the optimal temperature. The obtained optimal temperature is used as the set point for the pervaporative membrane reactor in the control study.

5.1 Conclusions

The optimization goal is to determine an optimal operating temperature for the pervaporative membrane reactor to maximize a final concentration of ester at specified batch time. From the optimization study it can be concluded that:

- The optimization program written in Matlab is tested to determine an optimal temperature of the exothermic batch reactor studied by Aziz et al. (2000) as detailed in Appendix D. The optimization results show that this program is effective and applicable to determine an optimal temperature of this work.

- The combination of a pervaporation with a conventional esterification process can shift the thermodynamically or kinetically limited reactions by removing water from the reaction mixture and, therefore, increases the yield of the desired product.

- The use of an optimal temperature profile gives an increase in the concentration of the desired product rather than an optimal temperature set point.

A generic model control (GMC) coupled with an extended Kalman filter (EKF) is implemented to track the optimal operating temperature. Both optimal temperature set point and optimal temperature profile are used as set point in this study. From the control study it can be concluded that:

- For nominal case, in which all model parameter used to simulate are specified correctly, the GMC controller performs satisfactorily in tracking both optimal temperature set point and optimal temperature profile of the pervaporative membrane reactor. The extended Kalman filter gives a reasonable estimate of the heat released. With this estimate of heat released, the GMC controller performs satisfactorily; the reactor temperature is delivered to the desired set point with no overshoot

- The robustness of the controllers is evaluated by changing process parameters such as rate constant, heat of reaction, and heat transfer coefficient. It has been found that the estimation of the heat released by reaction is sensitive to the heat transfer coefficient. Although the performance of the extended Kalman filter has deteriorated when compared to that of the nominal case, the GMC controller still gives reasonably good control action. From control study, it can ensure that the GMC controller coupled with the extended Kalman filter has been found to be effective and robust in tracking both optimal temperature set point and optimal temperature profile of the pervaporative membrane reactor.

5.2 Recommendations

In this research, the optimization technique is formulated to determine the optimal operating temperature of the esterification in the pervaporative membrane reactor studied by Liu et al. (2001). In fact, the performance of the pervaporative membrane reactor depends not only upon the operating temperature but also upon the initial molar ratio, the ratio of membrane area to reactor volume, and the catalyst concentration. The researchers must take the effect of the above parameters into account in order to optimize design parameters and operating conditions.

Due to the variation of the models and parameters used to simulate, e.g. kinetic or physical parameters, the uncertainty in process design and operations has been an active research area. The optimization under process model uncertainty is considered necessary to ensure that the process design and operation are flexible to operate over a given range of parameter values.

REFERENCES

THAI

ไพศาล กิตติศุภกร. <u>เอกสารคำสอนวิชา 2105-619 การควบคุมกระบวนการอัตโนมัติขั้นสูง</u>. ภาควิชา
วิศวกรรมเคมี จุฬาลงกรณ์มหาวิทยาลัย, 2543.

มนัส สังวรศิลป์ และ วรรัตน์ ภัทรอมรกุล. <u>คู่มือการใช้งาน MATLAB ฉบับสมบูรณ์</u>.
กรุงเทพมหานคร: ศูนย์การพิมพ์พลชัย, 2543.

รัตนา จิระรัตนานนท์. <u>กระบวนการแยกด้วยเยื่อแผ่นสังเคราะห์</u>. พิมพ์ครั้งที่ 2. กรุงเทพมหานคร:

ENGLISH

Ahicai, Y.; Xianbao, C.; and Jing, G. Esterification-distillation of butanol and acetic
acid. <u>Chem. Eng. Sci</u>. 53 (1998): 2081-2088.

Ali, E. M.; Abasaeed, A. E.; and Al-Zahrani, S. M. Optimization and control of
industrial gas-phase ethylene polymerization reactors. <u>Ind. Eng. Chem. Res</u>.
37 (1998): 3414-3423.

Aziz, N.; Hussain, M. A.; and Mujtaba, I. M. Performance of different types of
controllers in tracking optimal temperature profiles in batch reactors. <u>Comp.
Chem. Eng</u>. 24 (2000): 1069-1075.

Baker, W. R. <u>Membrane Technology and Applications</u>. McGraw-Hill, 2000.

Barolo, M.; Guarise, G. B.; Rienzi, S.; and Trotta, A. On-line startup of a distillation
column using generic model control. <u>Comp. Chem. Eng</u>. 17 (1993): 349-354.

Becerra, V. M.; Roberts, P. D.; and Griffiths, G. W. Applying the extended Kalman
filter to systems described by nonlinear differential-algebraic equations.
<u>Control Engineering Practice</u> 9 (2001): 267-281.

Bequette, B. W. Nonlinear control of chemical processes: A review. <u>Ind. Eng. Chem.
Res</u>. 30 (1991): 1391-1413.

Bitterlich, S.; Meiβner, H.; and Hefner, W. Enhancement of the conversion of
esterification reactions by non-porous membranes. <u>Proceedings of the fifth
International Conference on Pervaporation Processes in the Chemical
Industry, Bakish Material Corporation</u> (1991): 273-281.

Cacik, F.; Dondo, R. G.; and Marques, D. Optimal control of a batch bioreactor for
the production of xanthan gum. <u>Comp. Chem. Eng</u>. 25 (2001): 409-418.

Carrasco, E. F., and Banga, J. R. Dynamic optimization of batch reactors using adaptive stochastic algorithms. Ind. Eng. Chem. Res. 36 (1997): 2252-2261.

Chang, J. S., and Hseih, W. Y. Optimization and control of semibatch reactors. Ind. Eng. Chem. Res. 34 (1995): 545-556.

Chang, J. S., and Huang, K. L. Performance study of control strategies for trajectory tracking problem of batch reactors. Can. J. Chem. Eng. 72 (1994): 906-919.

Chang, J. S., and Lai, J. L. Computation of optimal temperature policy for molecular weight control in a batch polymerization reactor. Ind. Eng. Chem. Res. 31 (1992): 861-868.

Chang, J. S.; Hsu, J. S.; and Sung, Y. T. Trajectory tracking of an optimizing path in a batch reactor: Experimental study. Ind. Eng. Chem. Res. 35 (1996): 2247-2260.

Costello, D. J. Evaluation of model-based control techniques for a buffered acid-base reaction system. Chem. Eng. Res. Des. 72 (1994): 47-54.

Cott, B., and Macchietto, S. Temperature control of exothermic batch reactors using generic model control. Ind. Eng. Chem. Res. 28 (1989): 1177-1184.

David, M. O.; Gref, R.; and Nguyen, Q. T. Pervaporation-esterification coupling, I. Basic kinetic model. Trans. Inst Chem. Eng. 69 (1991): 335-340.

Dean, A. J. LANGE' s Handbook of Chemistry. 3rd ed. New York: McGraw-Hill, 1985.

Douglas, P. L.; Fountain, P. S.; Sullivan, G. R.; and Zhou, W. Model based control of a high purity distillation column. Can. J. Chem. Eng. 72 (1994): 1055-1065.

Dunia, H. R. and Edgar, T. F. Improved generic model control algorithm for linear systems. Comp. Chem. Eng. 20 (1996): 1003-1016.

Edgar, T. F.; Himmelblau, D. M.; and Lasdon, L. S. Optimization of Chemical Processes. 2nd ed. New York: McGraw-Hill, 2001.

Faliks, A.; Yetter, R. A.; Floudas, C. A.; Hall, R.; and Rabitz, H. Optimal control of methane conversion to ethylene. J. Phys. Chem. 104 (2000): 10740-10746.

Farrell, R. J., and Tsai, Y. C. Nonlinear controller for batch crystallization: development and experimental demonstration. AIChE J. 41 (1995): 2318-2321.

Feng, X., and Huang, M. Liquid separation by membrane pervaporation: A review. Ind. Eng. Chem. Res. 36 (1997): 1048-1066.

Feng, X., and Huang, M. Studies of a membrane reactor: esterification facilitated by pervaporation. Chem. Eng. Sci. 51 (1996): 4673-4679.

Garcia, M.; Cabassud, M. V.; Lann, M. V. L.; Pibouleau, L.; and Casamatta G. Constrained optimization for fine chemical productions in batch reactors. Chem. Eng. J. 59 (1995): 229-241.

Gudi, R. D.; Shah, S. L.;and Gray, M. R. Adaptive multirate state and parameter estimation strategies with application to a bioreactor. AIChE J. 41 (1995): 2451-2464.

Guntern, C.; Keller, A. H.; and Hungerbuhler, K. Economic optimization of an industrial semibatch reactor applying dynamic programming. Ind. Eng. Chem. Res. 37 (1998): 4017-4022.

Henson, M. A., and Seborg, D. E. Nonlinear Process Control. New jersey: Prentice Hall, 1997.

Huang, R. Y. M. Pervaporation membrane separation processes. Netherlands: Elsvier Science, 1991.

Kershenbaum, L. S., and Kittisupakorn, P. The use of a partially simulated exothermic (PARSEX) reactor for experimental testing of control algorithms. Trans IChemE. 72 (1994): 55-63.

Keurentjes, J. T. F.; Janssen, G. H. R.; and Gorissen, J. J. The esterification of tartaric acid with ethanol: kinetics and shifting the equilibrium by means of pervaporation. Chem. Eng. Sci. 49 (1994): 4681-4689.

Khandalekar, P. D., and Riggs, J. B. Nonlinear process model based control and optimization of a model IV FCC unit. Comp. Chem. Eng. 19 (1995): 1153-1168.

Lee, P. L., and Sullivan, G. R. Generic model control (GMC). Comp. Chem. Eng. 12 (1988): 573-580.

Lee, P. L.; Zhou, W.; Cameron, I. T.; Newell, R. B.; and Sullivan, G. R. Constrained generic model control of a surge tank. Comp. Chem. Eng. 15 (1991): 191-195.

Lee, P. L; Nowell, R. B.; and Sullivan, G. R. Generic model control- a case study. Can. J. Chem. Eng. 67 (1989): 478-484.

Lipnizki, F.; Field, R. W.; and Ten, P. K. Pervaporation-based hybrid process: a review of process design, applications and economics. J. Memb. Sci. 153 (1999): 183-210.

Liptak, B. G. Controlling and optimizing chemical reactors. Chem. Eng. 26 (1986): 69-81.

Liu, Q.; Zhang, Z.; and Chen, H. Study on the coupling of esterification with pervaporation. J. Memb. Sci. 182 (2001): 173-181.

Luus, R, and Okongwu, O. N. Towards practical optimal control of batch reactors. Chem. Eng. J. 75 (1999): 1-9.

Matouq, M.; Tagawa, T.; and Goto, S. Combined process for production of methyl tert-butyl ether from tert-butyl alcohol and methanol. J. Chem. Eng. Jpn. 27 (1994): 302-306.

Mohan, K., and Govind, R. Effect of temperature on equilibrium shift in reactors with a permselective wall. Ind. Eng. Chem. Res. 27 (1988): 2064-2070.

Myers, M. A., and Luecke, R. H. Process control applications of an extended Kalman filter algorithm. Comp. Chem. Eng. 15 (1991): 853-857.

Nantana Siripun. Globally linearizing control for pH control of the wastewater treatment process. Master of Engineering Thesis, Department of Chemical Engineering, Faculty of Engineering, Chulalongkorn University, 2000.

Nussara Boonprasert. Generic model controller application for polyvinyl chloride polymerization reactor. Master of Engineering Thesis, Department of Chemical Engineering, Faculty of Engineering, Chulalongkorn University, 1999.

Okamoto, K. I.; Yamamoto, M.; Otoshi, Y.; Semoto, T.; Yano, M.; Tanaka, K.; and Kita, H. Pervaporation-aided esterification of oleic acid. J. Chem. Eng. Jpn. 26 (1993): 475-481.

Perry, H. R. PERRY' s Chemical Engineer' s Handbook. 6th ed. New York: McGraw-Hill, 1984.

Pijak Meethong. GMC for relative degree higher than one processes a case study: A concentration control of continuous stirred tank reactor with first-order exothermic reaction. Master of Engineering Thesis, Department of Chemical Engineering, Faculty of Engineering, Chulalongkorn University, 2002.

Riggs, J. B., and Rhinehart, R. R. Comparison between two nonlinear process-model based controllers. Comp. Chem. Eng. 14 (1990): 1075-1081.

Rojnuckarin, A., and Floudas, C. A. Methane conversion to ethylene and acetylene: optimal control with chlorine, oxygen, and heat flux. Ind. Eng. Chem. Res. 35 (1996): 683-696.

Russell, S. A.; Robertson, D. G.; Lee, J. H.; and Ogunnaike, B. A. Model-based quality monitoring of batch and semi-batch processes. <u>Journal of Process Control</u> 10 (2000): 317-332.

Sarawut Phupaichitkun. <u>Application of model predictive control on the matlab for control of a batch reactor with exothermic reactions</u>. Master of Engineering Thesis, Department of Chemical Engineering, Faculty of Engineering, Chulalongkorn University, 1998.

Scott, K. <u>Handbook of Industrial membranes</u>. 1st ed. Elsevier, 1995.

Serborg, D. E.; Edgar, T. F.; and Mellichamp, D. A. <u>Process dynamics and control</u>. New York: Wiley, 1989.

Signal, P. D., and Lee, P. L. Robust stability and performance analysis of generic model control (GMC). <u>Chem. Eng. Comm</u>. 124 (1993): 57-76.

Sirkar, K.; Shanbhag, V.; and Kovvali, A. Membrane in a reactor: A functional perspective. <u>Ind. Eng. Chem. Res</u>. 38 (1999): 3715-3737.

Soroush, M., and Kravaris, C. Optimal design and operation of batch reactors. 1. Theoretical framework. <u>Ind. Eng. Chem. Res</u>. 32 (1993): 866-881.

Strathmann, H. Membrane separation processes: Current relevance and future opportunities. <u>AIChE J</u>. 47 (2001): 1077-1087.

Tan, L.; Dowling, J.; McCorkell, C.; and McCabe, H. State estimation for optimal control of a nonlinear system. <u>IECON Proceedings (Industrial Electronics Conference)</u> 3 (1991): 2235-2240.

Tremblay, M. D., and Luus, R. Optimization of non-steady-state operation of reactors. <u>Can. J. Chem. Eng</u>. 67 (1989): 494-502.

Valappil, J., and Georgakis, C. Systematic tuning approach for the use of extended Kalman filters in batch processes. <u>Proceedings of the American Control Conference</u> 2 (1999): 1143-1147.

Veerayut Lersbamrungsuk. <u>Kalman filter algorithm software design and development for chemical processes</u>. Master of Engineering Thesis, Department of Chemical Engineering, Faculty of Engineering, Chulalongkorn University, 2000.

Vega, A.; Diez, F.; and Alvarez, J. M. Programmed cooling control of a batch crystallizer. <u>Comp. Chem. Eng</u>. 19 (1995): 471-476.

Waldburger, R. M., and Widmer, F. Membrane reactors in chemical production processes and the application to the pervaporation-assisted esterification. Chem. Eng. Technol. 19 (1996): 117-126.

Wang, Z. L.; Corriou, J. P.; and Pla, F. Nonlinear control of a batch polymerization reactor with on-line parameter and state estimations. Proceedings of the IEEE Conference on Decision and Control 4 (1993): 3858-3863.

Worapon Kiatkittipong. Synthesis of ethyl tertiary butyl ether from ethanol and tertiary butanol using beta zeolite catalyst in a pervaporative membrane reactor. Master of Engineering Thesis, Department of Chemical Engineering, Faculty of Engineering, Chulalongkorn University, 2001.

Xie, X. Q.; Zhou, D. H.; and Jin, Y. H. Strong tracking filter based adaptive generic model control. Journal of Process Control 9 (1999): 337-350.

Xuehui, L., and Lefu, W. Kinetic model for an esterification process coupled by pervaporation. J. Memb. Sci. 186 (2001): 19-24.

Yang, B., and Goto, S. Pervaporation with reactive distillation for the production of ethyl tert-butyl ether. Sep. Sci. Tech. 32 (1997): 971-981.

Zhao, H., and Kummel, M. State and parameter estimation for phosphorus removal in an alternating activated sludge process. Journal of Process Control 5 (1995): 341-351.

Zhu, Y.; Minet, R. G.; and Tsotsis, T. T. A continuous pervaporation membrane reactor for the study of esterification reactions using a composite polymeric/ceramic membrane. Chem. Eng. Sci. 51 (1996): 4103-4113.

APPENDICES

APPENDIX A

PERMEABILITY COEFFICIENT DETERMINATION

The relationship between the permeablility coefficient and operating temperature can be expressed by Arrhenius' equation

$$P = P_O \exp(-E_a/RT) \tag{A.1}$$

where P_O is the pre-exponential factor,

E_a is the activation energy of permeation,

R is the gas constant,

T is the absolute temperature.

Table A.1 shows the values of the permeability coefficient at different temperatures given by Liu et al. (2001). Consider an ideal case where the membrane permeates only water. A curve fitting method is employed to find the relationship between the permeability coefficient and operating temperature.

Table A.1 The permeability coefficient of water at different temperatures

T (^{o}C)	P_W
90	4.20
80	3.87
70	3.52
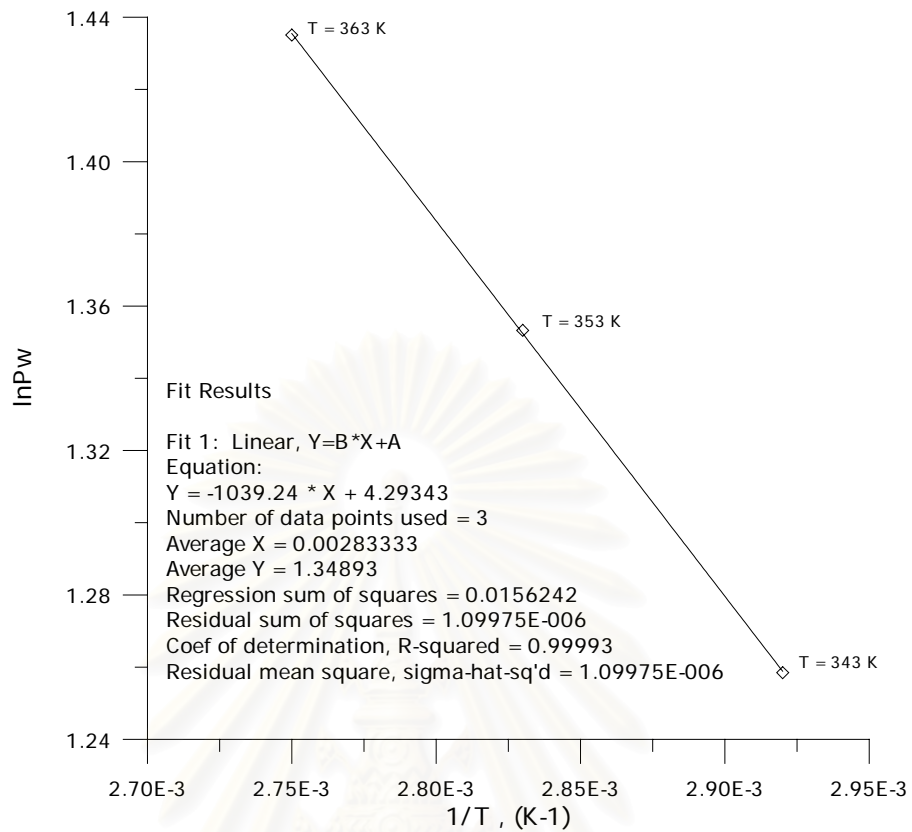
Figure A1 The variation of the permeation coefficient of water with temperature

Figure A1 shows the Arrhenius plot of the permeability coefficient, which can be expressed by the following equation:

$$\ln P_W = 4.2934 - \frac{1039.24}{T} \tag{A.2}$$

so that,

$$P_W = \exp\left(4.2934 - \frac{1039.24}{T}\right) \tag{A.3}$$

APPENDIX B

NUMERICAL METHOD

Any equation that expresses a relation between a function $y(t)$ and its derivatives is a differential equation; in particular, if the indicated relationship is nonlinear, it is a nonlinear differential equation. For example, the equation (B.1) is a first-order nonlinear differential equation if $f(t,y)$ is a nonlinear function of y.

$$\frac{dy}{dt} = f(t,y) \tag{B.1}$$

The general nonlinear nth-order differential equation may be represented as:

$$f\left(\frac{d^n y}{dt^n}; \frac{d^{n-1} y}{dt^{n-1}}; ...; \frac{dy}{dt}; y; t\right) = 0 \tag{B.2}$$

where $f(\cdot)$ is some nonlinear function of the indicated arguments.

There are no corresponding general procedures for generating solutions to all nonlinear equations. In fact, the determination of analytical solutions for nonlinear equations of any order is not always possible in general; only in a few very special cases are there some specialized methods for obtaining analytical solutions. In the vast majority of cases, one must resort to numerical techniques for constructing the approximate solutions

B.1 The Euler Method

In solving the nonlinear first-order equation shown in equation (B.1):

$$\frac{dy}{dt} = f(t,y)$$

given the initial condition $y(t_0) = y(0)$:

1. Letting $y(k)$ represent $y(t)$ at the point $t = t_k$ and replacing the continuous $f(t,y)$ with $f(t_k, y(k))$, and

2. Replacing the derivative with the finite difference approximation:

$$\frac{dy(t)}{dt} \approx \frac{y(t_{k+1}) - (t_k)}{\Delta t} \tag{B.3}$$

then the differential equation becomes:

$$\frac{y(t_{k+1}) - (t_k)}{\Delta t} = f(t_k, y(k)) \tag{B.4}$$

which is easily rearranged to give:

$$y(t_{k+1}) = y(t_k) + \Delta t f(t_k, y(k)) \tag{B.5}$$

or, simply:

$$y(k+1) = y(k) + \Delta t f(t_k, y(k)) \tag{B.6}$$

Observe now that starting with the initial value $y(0)$, equation (B.6) can be used recursively to generate the sequence $y(1)$, $y(2)$, $y(3)$, … as the required approximate solution to equation (B.1)

The formula in equation (B.4) is known as Euler's method; it represents one of the simplest schemes available for solving initial-value problems. It has the advantage that it is very straightforward to use, and very easy to program on the computer; its main disadvantage is that it is not very accurate.

B.2 The Runge-Kutta Method

The formula given in equation (B.7) is the formula for the (fourth-order) Runge-Kutta method; it is a very accurate and very popular method for obtaining numerical solutions to initial value problems (despite the fact that it is more complicated than the Euler methods).

$$y(k+1) = y(k) + \frac{\Delta t}{6}(c_1 + 2c_2 + 2c_3 + c_4) \tag{B.7}$$

where $\qquad c_1 = f(t_k, y(k))$ $\qquad\qquad\qquad\qquad$ (B.8a)

$$c_2 = f(t_k + \frac{1}{2}\Delta t; y(k) + \frac{1}{2}\Delta t c_1) \qquad\qquad \text{(B.8b)}$$

$$c_3 = f(t_k + \frac{1}{2}\Delta t; y(k) + \frac{1}{2}\Delta t c_2) \qquad\qquad \text{(B.8c)}$$

$$c_4 = f(t_k + \Delta t; y(k) + \Delta t c_3) \qquad\qquad \text{(B.8d)}$$

APPENDIX C

INTEGRAL ERROR CRITERIA

Integral error measures indicate the cumulative deviation of the controlled variable from its set point during the transient response. The following formulations of the integral can be proposed.
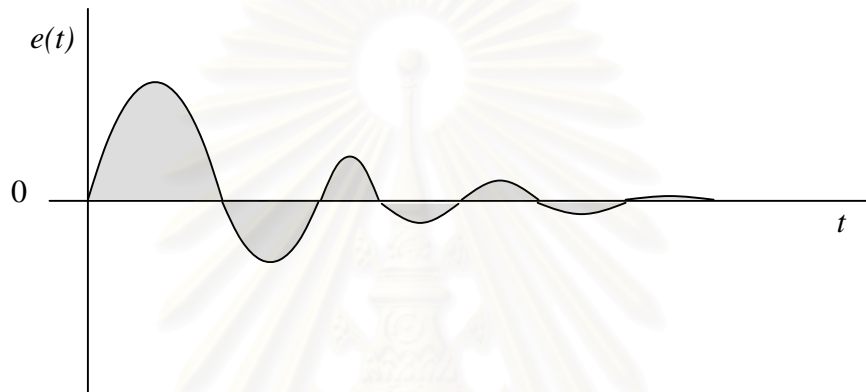

Figure C1 Definition of error integrals

Integral of the absolute value of error (IAE)

$$IAE = \int_0^\infty |e(t)| \, dt \qquad (C.1)$$

Integral of the square of error (ISE)

$$ISE = \int_0^\infty e^2(t) \, dt \qquad (C.2)$$

Integral of time-weighted absolute error (ISE)

$$ITAE = \int_0^\infty |e(t)| \, t \, dt \qquad (C.3)$$

where e is the usual error (i.e., set point – control variable).

Each of the three figures of merit given by equation (C.1), (C.2), and (C.3) have different purposes. The ISE will penalize (i.e., increase the value of ISE) the response that has large errors, which usually occur at the beginning of a response, because the error is squared. Th ITAE will penalize a response, which has errors that

persist for a long time. The IAE will be less severe in penalizing a response for large errors and treat all errors (large and small) in a uniform manner. The ISE figure of merit is often used in optimal control theory because it can be used more easily in mathematical operations (for example differentiation) than the figures of merit, which use the absolute value of error. In applying the tuning rules to be discussed in the next section, these figures of merit can be used in comparing responses that are obtained with different tuning rules.

APPENDIX D

INTROLDUCTION TO MATLAB

MATLAB, developed by Math Works Inc., is a technical environment for high performance numeric computation and visualization. The combination of analysis capabilities, flexibility, reliability, and powerful graphics makes MATLAB the premier software package for engineers. MATLAB provides extensive numerical resources. It contains over 200 reliable, accurate mathematical subprograms. These subprograms provide solutions to a broad range of mathematical problems including matrix algebra, complex arithmetic, linear systems, eigenvalues, differential equations, nonlinear systems, and many special functions

MATLAB also features a family of application-specific solutions- toolboxes-. Toolboxes are collections of MATLAB function (M-files) that extend the MATLAB environment in order to solve particular classes of problems. Areas in which toolboxes are available include optimization, signal processing, control design, dynamic systems simulation, and so on.

D.1 Optimization Toolbox

The Optimization Toolbox is a collection of functions that extend the capability of the MATLAB numeric-computing environment. The Optimization Toolbox consists of functions that perform minimization (or maximization) on general nonlinear functions. Functions for nonlinear equation solving and least squares (data-fitting) problems are also provided.

D.1.1 Problems Covered by the Toolbox

The table D.1 shows the functions available for minimization problem.

Table D.1 Minimization

Type	Notation	Function
Scalar Minimization	$\min_{a} f(a)$ such that $a_1 < a < a_2$	fminbnd
Unconstrained Minimization	$\min_{x} f(x)$	fminunc, fminsearch
Linear Programming	$\min_{x} f^T x$ such that $A \cdot x \leq b,\ Aeq \cdot x = beq,\ l \leq x \leq u$	linprog
Quadratic Programming	$\min_{x} \frac{1}{2} x^T H x + f^T x$ such that $A \cdot x \leq b,\ Aeq \cdot x = beq,\ l \leq x \leq u$	quadprog
Constrained Minimization	$\min_{x} f(x)$ such that $c(x) \leq 0,\ ceq(x) = 0$ $A \cdot x \leq b,\ Aeq \cdot x = beq,\ l \leq x \leq u$	fmincon
Goal Attainment	$\min_{x,\gamma} \gamma$ such that $F(x) - w\gamma \leq \text{goal}$ $c(x) \leq 0,\ ceq(x) = 0$ $A \cdot x \leq b,\ Aeq \cdot x = beq,\ l \leq x \leq u$	fgoalattain
Minimax	$\min_{x} \max_{\{F_i\}} \{F_i(x)\}$ such that $c(x) \leq 0,\ ceq(x) = 0$ $A \cdot x \leq b,\ Aeq \cdot x = beq,\ l \leq x \leq u$	fminimax
Semi-Infinite Minimization	$\min_{x} f(x)$ such that $K(x,w) \leq 0$ for all w $c(x) \leq 0,\ ceq(x) = 0$ $A \cdot x \leq b,\ Aeq \cdot x = beq,\ l \leq x \leq u$	fseminf

D.1.2 Using the Optimization Functions

Most of these optimization routines require the definition of an M-file containing the function to be minimized, i.e., the objective function. Alternatively, an inline object created from a MATLAB expression can be used. Maximization is achieved by supplying the routines with $-f$, where f is the function being optimized.

APPENDIX E

PROGRAM VERIFICATION

The purpose of this chapter is to verify a Matlab program written to optimize in this research. An optimization program written in Matlab is tested to illustrate that the program is reliable and can be applied to other processes. The case study considered here involves the batch reactor studied by Aziz et al. (2000).

E.1 Case Study

In this work, the exothermic batch reactor studied by Aziz et al. (2000) is used to be a case study for the testing of an optimization program. Aziz et al. used the reaction scheme considered by Cott and Macchietto (1989) to solve an off-line optimal control problem with fixed batch time to find the optimum temperature profile that maximizes the conversion of the desired product. A Matlab program is written to solve the optimization problem by using a successive quadratic programming (SQP) algorithm in Matlab Optimization Toolbox.

The reaction scheme considered here is a well-mixed, liquid-phase reaction system, which is:

$$A + B \longrightarrow C \tag{E.1}$$
$$A + C \longrightarrow D \tag{E.2}$$

where   A, B are the raw materials,

     C is the desired product,

     D is the waste product.

E.1.1 Mathematical Model

The model equations for the batch reactor can be written as:

$$\frac{dM_A}{dt} = -R_1 - R_2 \tag{E.3}$$

$$\frac{dM_B}{dt} = -R_1 \tag{E.4}$$

$$\frac{dM_C}{dt} = +R_1 - R_2 \tag{E.5}$$

$$\frac{dM_D}{dt} = +R_2 \tag{E.6}$$

where

$$R_1 = k_1 M_A M_B \tag{E.7}$$

$$R_2 = k_2 M_A M_C \tag{E.8}$$

$$k_1 = \exp\left(\frac{k_1^1 - k_1^2}{T_r + 273.15}\right) \tag{E.9}$$

$$k_2 = \exp\left(\frac{k_2^1 - k_2^2}{T_r + 273.15}\right) \tag{E.10}$$

All the parameters and constant values used in the model are given in Table E.1.

Table E.1 The constant parameter values of the model

Parameter	Name	Value	Unit
k_1^1	Rate constant 1 for reaction 1	20.9057	-
k_1^2	Rate constant 2 for reaction 1	10000	-
k_2^1	Rate constant 1 for reaction 2	38.9057	-
k_2^2	Rate constant 2 for reaction 2	17000	-
Initial Condition			
M_A	Number of moles of component A	12	kmol
M_B	Number of moles of component B	12	kmol
M_C	Number of moles of component C	0	kmol
M_D	Number of moles of component D	0	kmol

Two runs of off-line optimal control are carried out; run1 uses one control interval (time) and run2 uses three fixed control intervals. The batch time is 120 minutes.

The objective function is to maximize is the desired product 'C' (this will automatically minimize the by-product 'D') at the specified final time (t_f). The objective function can be written as:

$$f = M_C(t_f)$$

Subject to temperature constraints:

$$20\,^{\circ}\text{C} \leq T \leq 100\,^{\circ}\text{C}$$

The initial values of $[M_A, M_B, M_C, M_D]$ are [12, 12, 0, 0]. To solve the optimization problem, the function *fmincon*, a successive quadratic programming code in MATLAB, is employed in this work. The results (optimal temperature profiles) are shown in Table E.2 for both runs.

Table E.2 Simulation results

Run	From	Off-line optimum temperature ($^{\circ}$C)			M_C^*
		Switching time (min)			
		0	40	80	
1	This work	92.4612	-	-	6.5156
	Paper	92.46	-	-	6.5126
2	This work	92.83	91.20	93.40	6.5201
	Paper	92.83	91.17	93.41	6.5171

$*$ M_C is off-line product (kmol)

Table E.2 shows an agreement between the optimization results obtained in this work and obtained by Aziz et al. (2000). Therefor the written program is reliable and applicable to determine an optimal temperature of other processes.

APPENDIX F

TUNING OF GMC CONTROLLER

Lee and Sullivan (1988) outline a system for tuning GMC controllers based on choosing a target profile of the controlled variable, $y^*(t)$. This profile is characterized by two values, ξ and τ. Lee and Sullivan present a figure that outlines the relative control performances of different combinations of ξ and τ as shown in figure F1. The similar plots to the classical second-order response showing the normalized response of the system y/y^* vs. normalized time t/τ with ξ as a parameter can be produced.
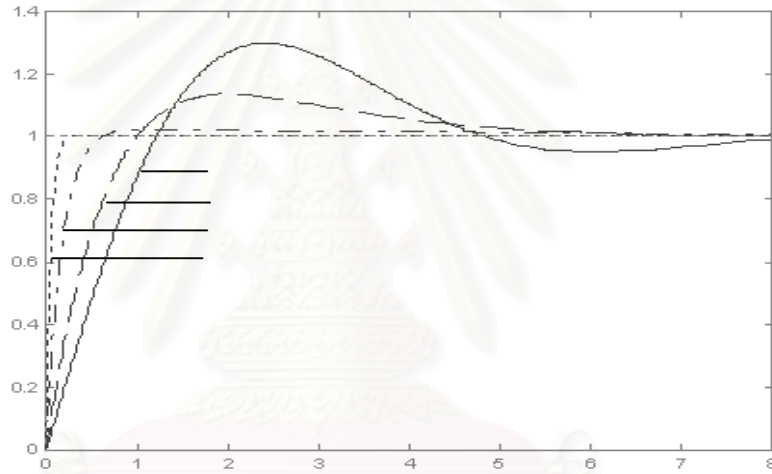
Figure F1 Generalized GMC profile specification

The general form of GMC control algorithm can be written as

$$\frac{dy}{dt} = K_1(y^{sp} - y) + K_2 \int (y^{sp} - y)dt \tag{F.1}$$

The value of the two tuning constants, K_1 and K_2, are obtained using the following relationships:

$$K_1 = \frac{2\xi}{\tau} \tag{F.2}$$

$$K_2 = \frac{1}{\tau^2} \tag{F.3}$$

In tuning the GMC controller, because overshoot is undesirable, ξ is set to 10. The value of τ is obtained by examining the tuning charts given by Lee and Sullivan and recognizing that, with $\xi = 10$, the controlled variable shall cross the set point at approximately 0.25τ.

- $t = 1$ hr. gives $\tau = \dfrac{1}{0.25} = 4$ hr, then

$$K_1 = \frac{2 \times 10}{4} = 5 \text{ hr}^{-1} \quad \text{and} \quad K_2 = \frac{1}{(4)^2} = 0.0625 \text{ hr}^{-2}$$
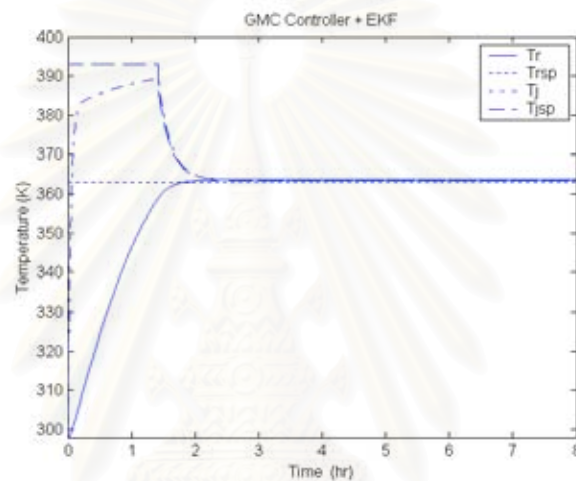
Figure F2 Response of GMC controller ($K_1 = 5$ hr^{-1}, $K_2 = 0.0625$ hr^{-2})

- $t = 2$ hr. gives $\tau = \dfrac{2}{0.25} = 8$ hr, then

$$K_1 = \frac{2 \times 10}{8} = 2.5 \text{ hr}^{-1} \quad \text{and} \quad K_2 = \frac{1}{(8)^2} = 1.5625 \times 10^{-2} \text{ hr}^{-2}$$
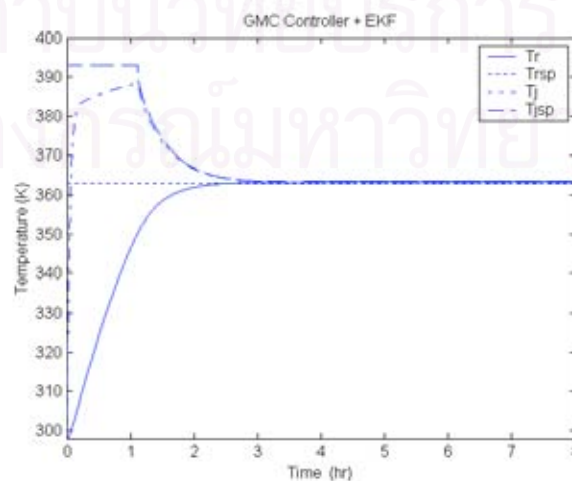
Figure F3 Response of GMC controller ($K_1 = 2.5$ hr^{-1}, $K_2 = 1.5625 \times 10^{-2}$ hr^{-2})

Figure F2 and F3 show the response of GMC controller using to track the reactor temperature with different tuning parameter. GMC controller is able to track the reactor temperature. However, the reactor temperature is operated with an offset. Offset can be described as a steady-state deviation of the controlled variable from set point, or simply as a steady-state error. From equation F.2, the first expression, $(K_1(y^{sp} - y))$, is to bring the process back to steady state due to change in dy/dt. The second expression, $(K_2 \int (y^{sp} - y)dt)$, is introduced in order to make the process have a zero offset. In this work, the appropriate values of the tuning parameters of GMC controller are $K_1 = 5$ hr^{-1} and $K_2 = 0.0008$ hr^{-2}. With these parameters, GMC controller is able to track the reactor temperature without offset.

For temperature control of a batch reactor, the energy balance on the reactor contents is given by the following equation:

$$\frac{dT_r(t)}{dt} = \frac{(-\Delta H)r(t)V(t) + UA(T_j(t) - T_r(t))}{M_r C_{pr}} \tag{F.1}$$

This equation is nonlinear, so the nonlinear term must first be linearized as the following equation.

$$f[x_1(t), x_2(t),...] \approx f(\overline{x}_1, \overline{x}_2,...) + \frac{\overline{\partial f}}{\partial x_1}[x_1(t) - \overline{x}_1] + \frac{\overline{\partial f}}{\partial x_2}[x_2(t) - \overline{x}_2] + ... \tag{F.2}$$

Defining the following deviation variables

$$C_A(t) = c_A(t) - \overline{c}_A \qquad C_B(t) = c_B(t) - \overline{c}_B \qquad C_E(t) = c_E(t) - \overline{c}_E$$

$$C_W(t) = c_W(t) - \overline{c}_W \qquad V(t) = v(t) - \overline{v} \qquad \Gamma(t) = T_r(t) - \overline{T}_r$$

$$\Gamma_j(t) = T_j(t) - \overline{T}_j$$

From equation (F.2), the transfer function is

$$\Gamma(s) = \frac{K_1}{\tau_1 s + 1}V(s) + \frac{K_2}{\tau_1 s + 1}C_A(s) + \frac{K_3}{\tau_1 s + 1}C_B(s) + \frac{K_4}{\tau_1 s + 1}C_E(s)$$

$$+ \frac{K_5}{\tau_1 s + 1}C_W(s) + \frac{K_6}{\tau_1 s + 1}\Gamma_j(s) \tag{F.3}$$

where

$$K_1 = \frac{\overline{\partial f}}{\partial V} \qquad\qquad K_2 = \frac{\overline{\partial f}}{\partial C_A} \qquad\qquad K_3 = \frac{\overline{\partial f}}{\partial C_B}$$

$$K_4 = \frac{\overline{\partial f}}{\partial C_E} \qquad\qquad K_5 = \frac{\overline{\partial f}}{\partial C_W} \qquad\qquad K_6 = \frac{\overline{\partial f}}{\partial T_j}$$

The following transfer function can be obtained.

$$\frac{\Gamma(s)}{\Gamma_j(s)} = \frac{K_6}{\tau_1 s + 1} \tag{F.4}$$

From equation (F.4), the dynamic response of the control system can be represented by first-order system while the close loop response of GMC controller represents by second-order system. This is the reason that why the reactor temperature controlled in this work by using the tuning chart given by Lee and Sullivan cannot give a reasonable response.

APPENDIX G

SIMULATION RESULT

This chapter shows the concentration profiles and the reaction rate of a normal batch reactor and a pervaporative membrane reactor. The simulation results of tracking an optimal temperature set point (Case 1) are shown in figure G3-G9 and the simulation results of tracking an optimal temperature profile (Case 2) are shown in figure G10-G16.
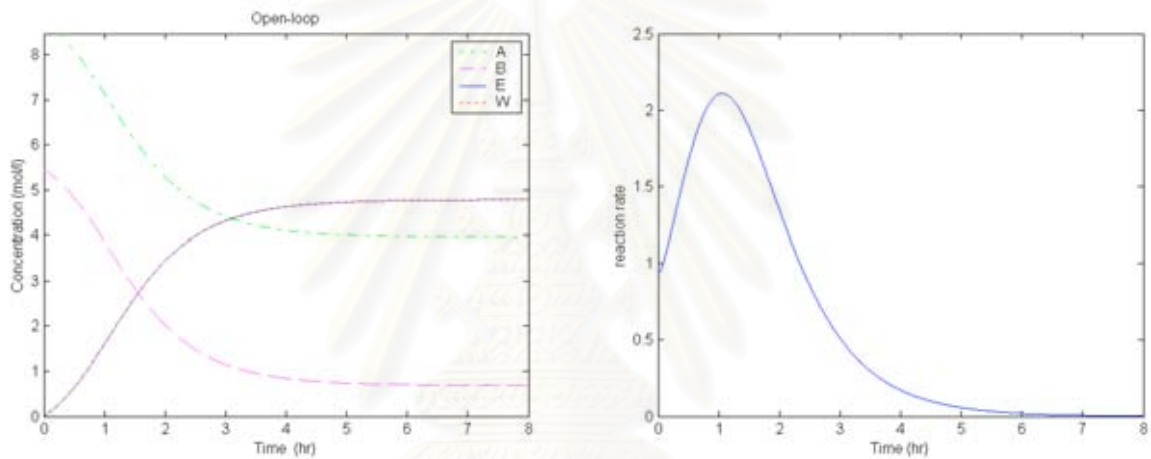
Fig.G1 The concentration profiles and the reaction rate of a normal batch reactor (Open-loop).
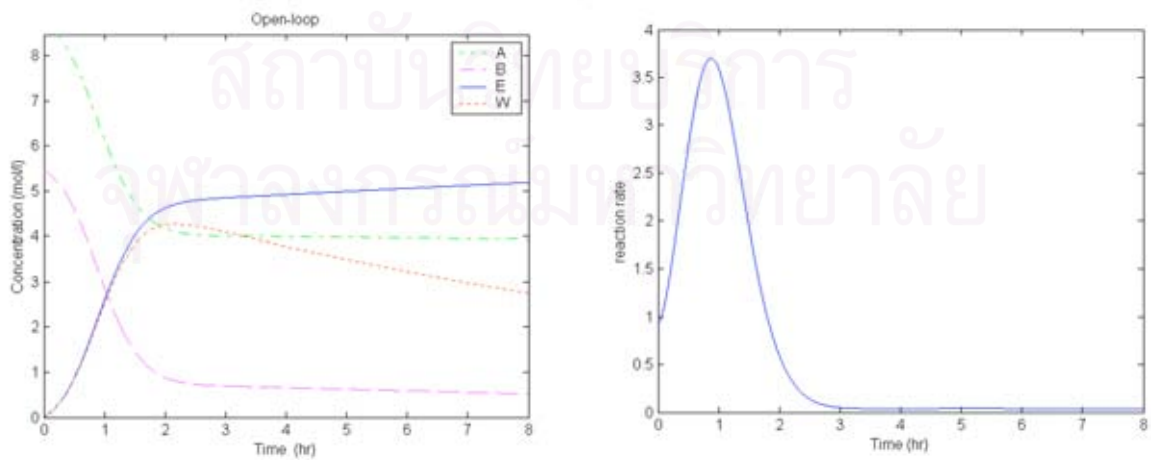
Fig.G2 The concentration profiles and the reaction rate of a pervaporative membrane reactor (Open-loop).
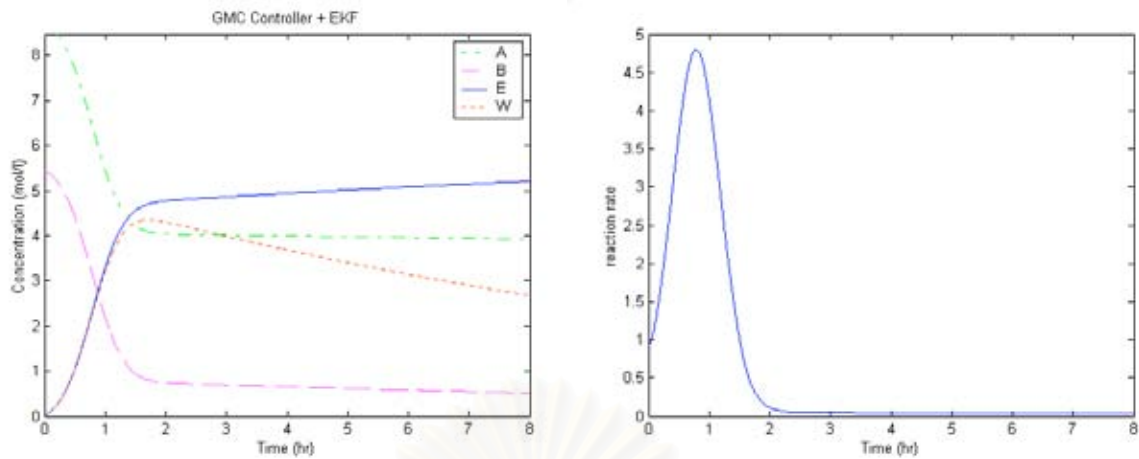
Fig.G3 The concentration profiles and the reaction rate of a pervaporative membrane reactor for nominal case (Case 1).
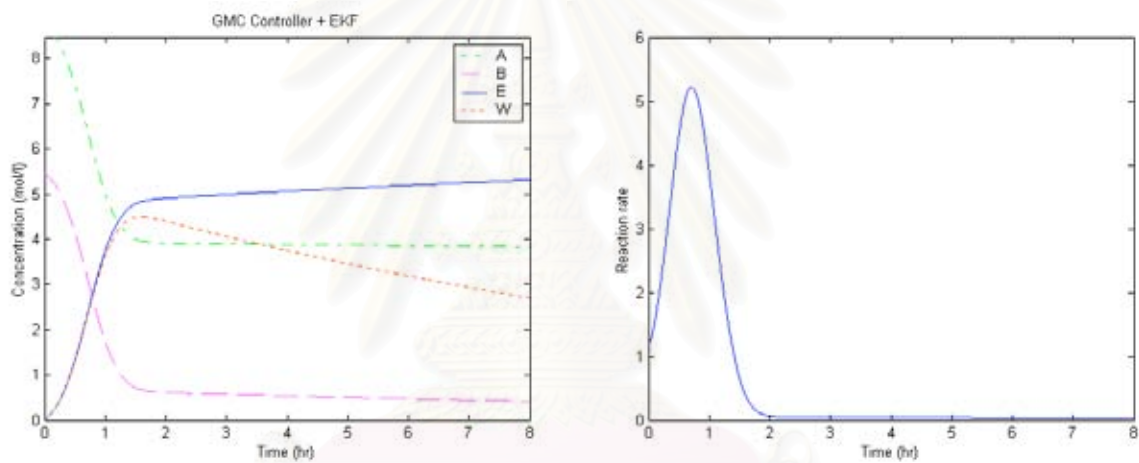
 Fig.G4 The concentration profiles and the reaction rate of a pervaporative membrane reactor for +30% k_1 change (Case 1).
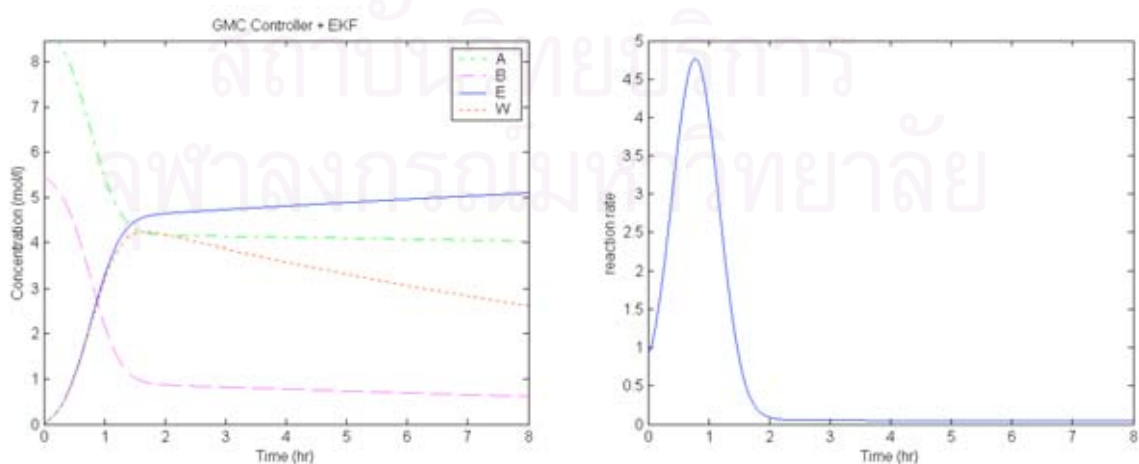
Fig.G5 The concentration profiles and the reaction rate of a pervaporative membrane reactor for -30% k_2 change (Case 1).
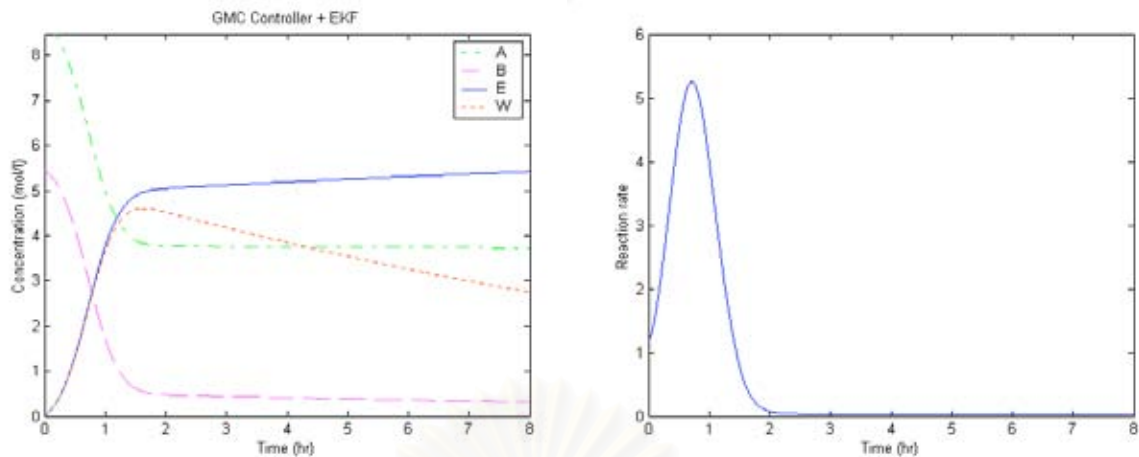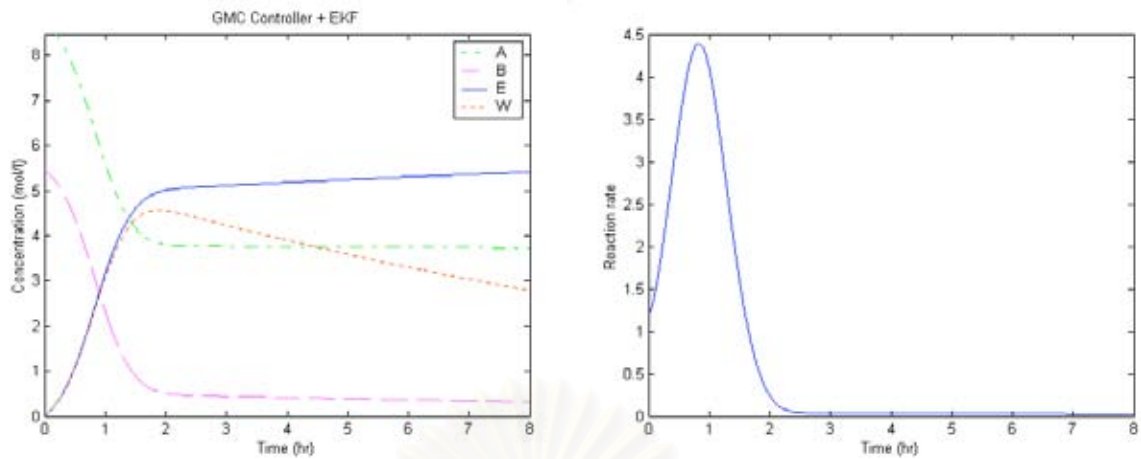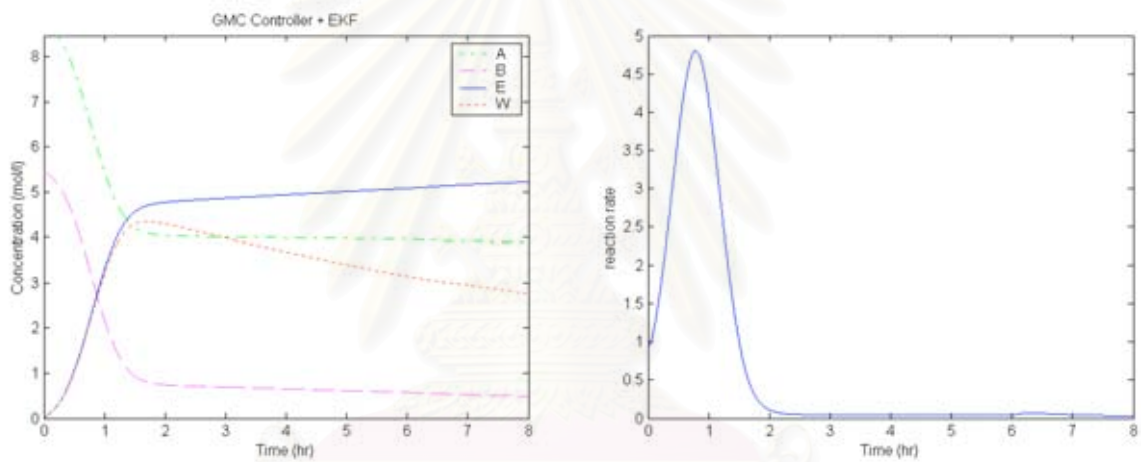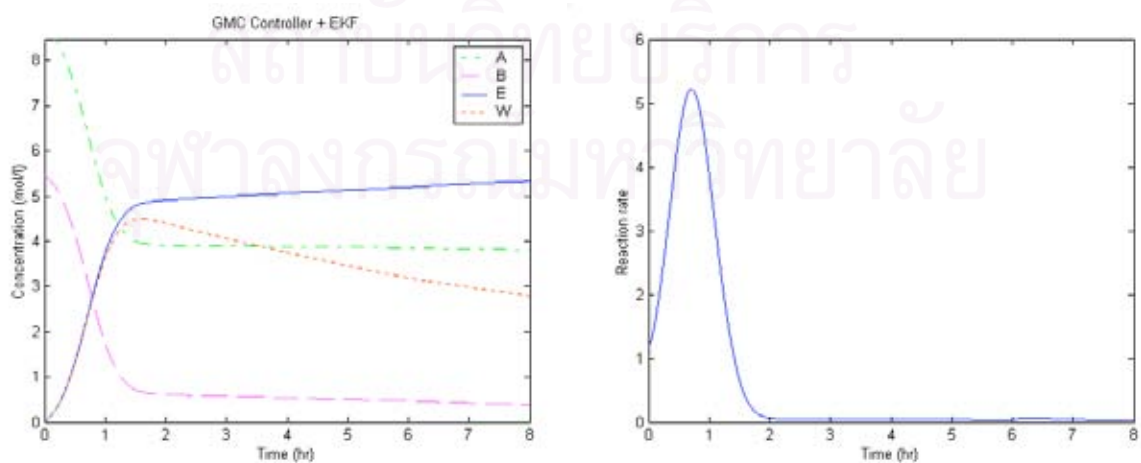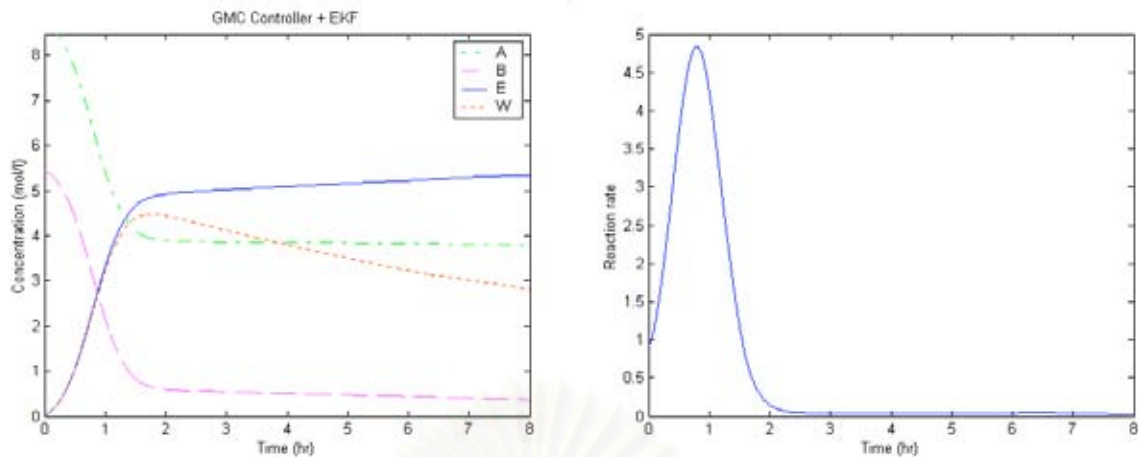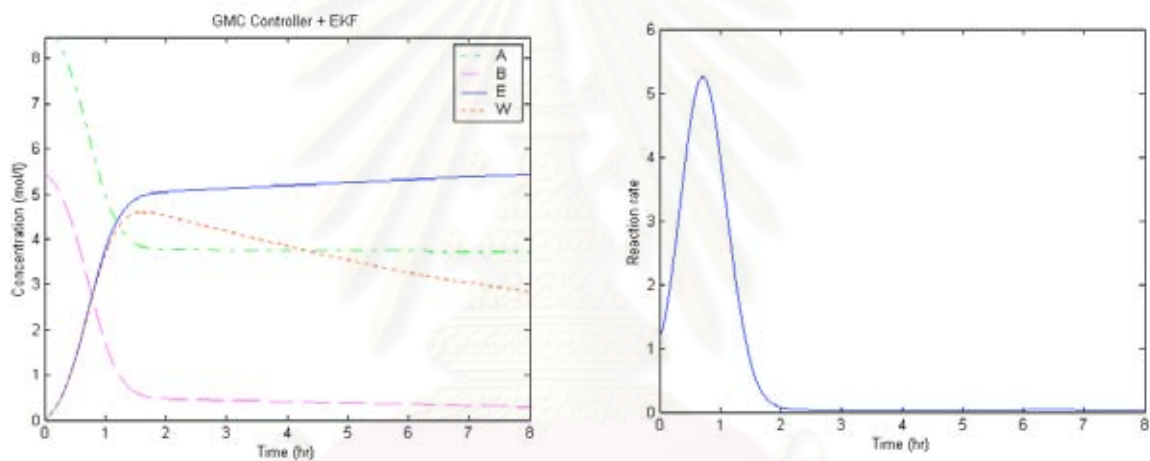
Fig.G6 The concentration profiles and the reaction rate of a pervaporative membrane reactor for +30%k_1 and -30%k_2 change (Case 1).
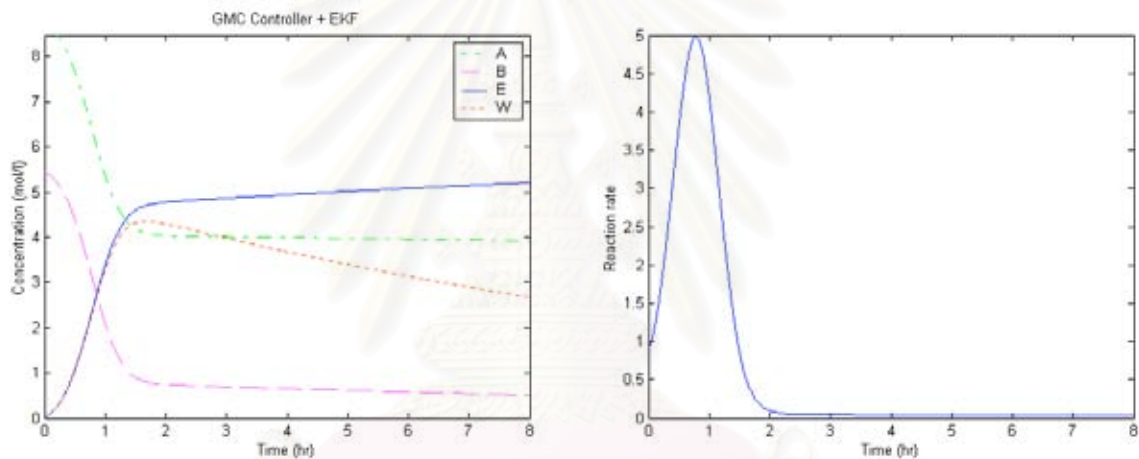
Fig.G7 The concentration profiles and the reaction rate of a pervaporative membrane reactor for +30% ΔH change (Case 1).
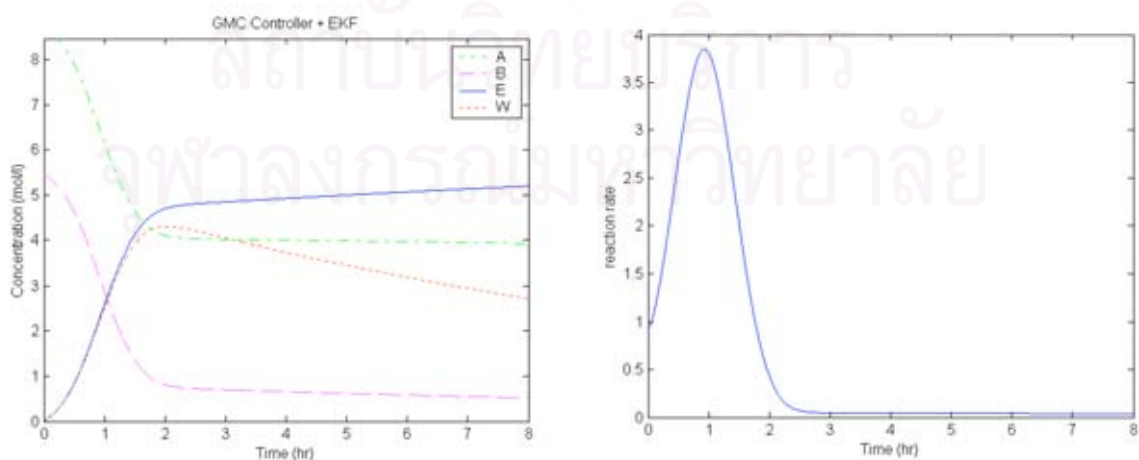
Fig.G8 The concentration profiles and the reaction rate of a pervaporative membrane reactor for -30% U change (Case 1).

Fig.G9 The concentration profiles and the reaction rate of a pervaporative membrane reactor for +30%k_1, -30%k_2, +30%ΔH and -30%U change (Case 1).

Fig.G10 The concentration profiles and the reaction rate of a pervaporative membrane reactor for nominal case (Case 2).

Fig.G11 The concentration profiles and the reaction rate of a pervaporative membrane reactor for +30% k_1 change (Case 2).

Fig.G12 The concentration profiles and the reaction rate of a pervaporative membrane reactor for -30% k_2 change (Case 2).

Fig.G13 The concentration profiles and the reaction rate of a pervaporative membrane reactor for +30% k_1 and -30% k_2 change (Case 2).
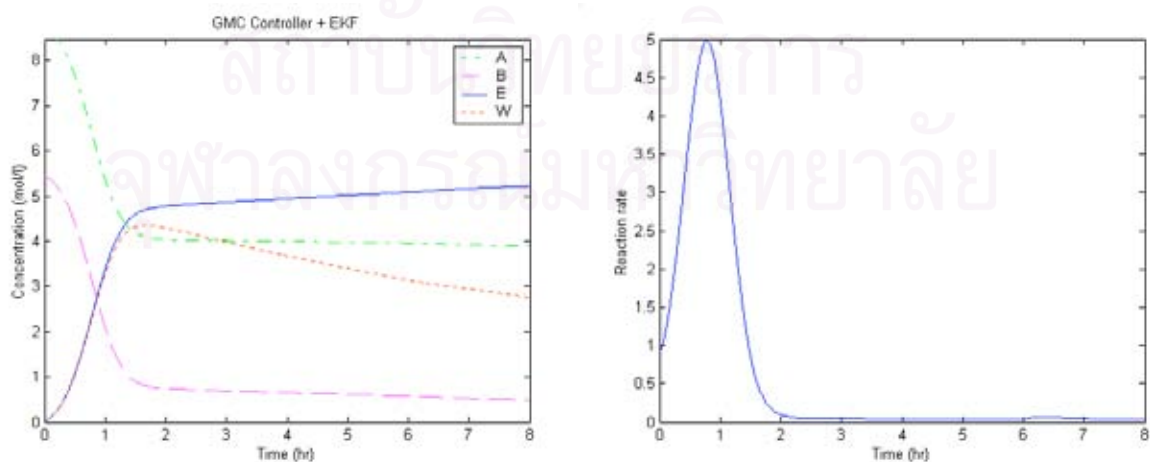

Fig.G14 The concentration profiles and the reaction rate of a pervaporative membrane reactor for +30% ΔH change (Case 2).
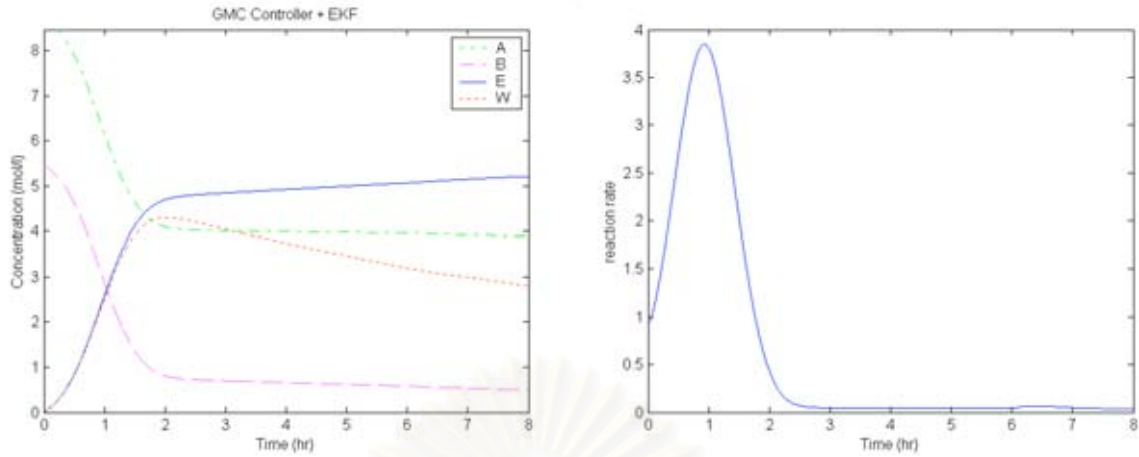
Fig.G15 The concentration profiles and the reaction rate of a pervaporative membrane reactor for -30% *U* change (Case 2).
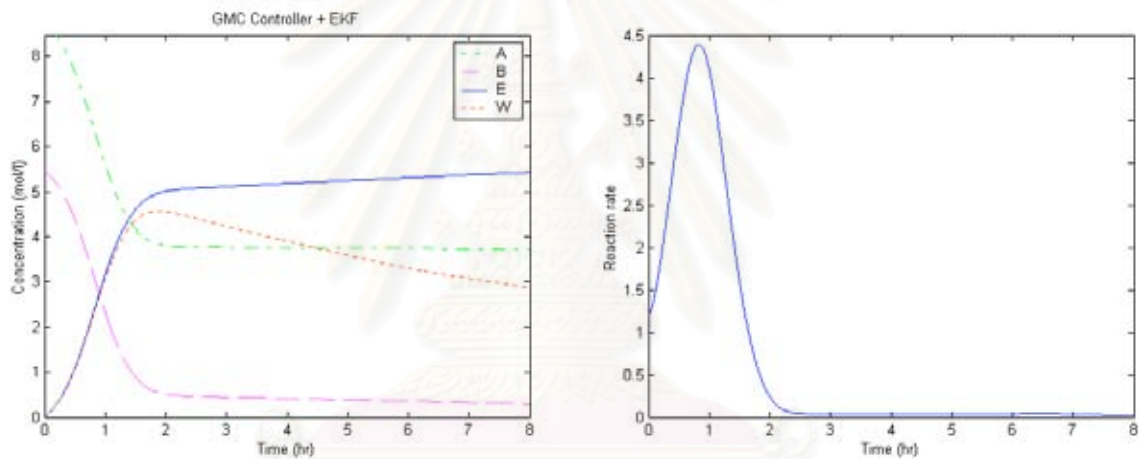

Fig.G16 The concentration profiles and the reaction rate of a pervaporative membrane reactor for +30%k_1, -30%k_2, +30%ΔH and -30%U change (Case 2).

VITA

Miss Orladda Moolasartsatorn was born in Surin on February 25, 1977. She graduated high school from Sirindhorn school, Surin Province, in 1995 and receive her Bachelor Degree in Chemical Engineering from Khon Kaen University in 1999. After that she studied for Master Degree in Chemical Engineering, Chulalongkorn University in 2000.